POLITECNICO DI TORINO

Master of Science Degree
in Automotive Engineering

Master's Thesis

Power loss analysis of a two-speed transmission for next-generation electric vehicles

Academic supervisor
Prof. Aldo Sorniotti
Company supervisor
Ing. Fabio Viotto

Candidate
Stefano Lovigu

Academic year 2023/2024

Abstract

The global transition towards a CO_2 emission reduction in the transportation sector forces the OEMs to rethink in a more efficient way how to convert and transmit the energy to produce motion for the vehicles. Recent years have seen an increasing transition to the electrified vehicles, both hybrid electric vehicles (HEVs) and battery electric vehicles (BEVs). To efficiently promote the adoption of electric vehicles (EVs), accurate energy consumption estimates and, consequently, the ability to evaluate drivetrain efficiency are essential requirements. A critical consideration for EVs is the selection between single-speed and multi-speed transmissions, as it significantly affects overall vehicle efficiency. This thesis provides a comprehensive review of recent research and technical progress present in literature related to the evaluation of efficiency and performance of the different types of transmission applications in EVs. The investigation of the power losses in the new Dana two-speed transmission for electric vehicles is addressed in this thesis through two simulation models: a transmission model and a vehicle model. The former calculates transmission power losses to obtain overall efficiency maps. An innovative approach is employed to break down the total power loss into individual components or the sources that generate them, by creating percentage maps. The latter is the vehicle model, where the transmission loss maps generated in the previous model are integrated. To investigate the realistic behavior of the transmission in terms of energy losses, three different driving cycles are simulated and their results are analyzed to provide a comprehensive understanding of the transmission's energy losses. The work proposes an innovative approach to accurately predicting transmission losses and efficiency. The detailed analysis of the three driving cycles provides valuable insights into the transmission's energy loss mechanisms, enabling better optimization and design improvements. This study underscores the potential of two-speed transmissions to enhance energy consumption performances in upcoming electric vehicles.

Introduction

A transmission is a mechanical system used to transfer power from an engine or an electric motor to the wheels or other driven components of a vehicle or machinery. It is an essential device in vehicles because it adjusts the input power's speed and torque to meet various operational needs by using a series of gears. By changing the gear ratios, a transmission can increase torque while reducing speed or increase speed while reducing torque, enabling efficient performance across different driving or operational conditions. Nowadays, multi-speed transmissions are exclusively adopted for internal combustion engine (ICE) vehicles, with only a few exceptions for their application in electric vehicles.

In literature, most studies on multi-speed transmissions for electric vehicles evaluate efficiency by focusing on motor operating points to maximize high-efficiency operation. They assess applicability by comparing simulation results of electric vehicle models with single-speed and multi-speed transmissions across different driving cycles. In the majority of these papers, only the motor's efficiency is considered, as in [**60**, **61**, **62**], and in some cases, as in [**63**], the inverter efficiency as well, while the loss contributions from the transmission are sometimes overlooked in these comparisons. However, to comprehensively enhance the whole efficiency of the automotive powertrain system, it is essential to account for all aspects of powertrain, includingh transmission power losses. There are only a limited number of studies that address the complete transmission's power losses, with most of them focusing primarily on manual transmission [**66**, **67**, **68**, **69**, **70**]. Some papers, on the other hand, as [**64**], incorporate efficiency data obtained from experimental bench tests. However, this assumes that the transmission already exists. For preliminary studies during the design phase, when it is not possible to obtain this data due to the absence of a physical model, power losses are estimated through theoretical models. This is precisely the focus of this thesis. In this work, the power losses within a two-speed transmission are discussed. To the author's knowledge, there is no study on power losses for a two-speed transmission specifically designed for electric vehicles with the same layout as the transmission analyzed in this thesis, apart from the analy-

sis in [**18**], where the efficiency of the first two-speed transmission model by Dana Graziano, formerly Oerlikon Graziano, is calculated using an efficiency model developed and experimentally validated by Oerlikon Graziano itself. However, no details are provided about this model. The only similar work is [**65**], which analyzes power losses in a DCT two-speed transmission for electric vehicles applying the ISO 14179-1 standard (American-derived version of the 14179 standard). In contrast to Xingxing and coworkers' study, this thesis analyzes power losses in a different transmission type for electric vehicles: an AMT two-speed transmission; moreover employing a different loss model, the ISO 14179-2 standard (German-derived version of the 14179 standard). The difference between the two standards lies in the evaluation of gear losses, particularly the load-dependent meshing losses, which require more detailed data for the German version, thereby enhancing its comprehensiveness.

The thesis' work extended beyond establishing the **overall efficiency of the transmission** at different operating points of the electric motor. It also involved creating percentage maps that **dissected the total efficiency into its distinct loss components**, thereby determining the impact of each type of loss on the efficiency of the entire system under varying operating conditions. Moreover, the analysis extended beyond categorizing losses by type to **analyze the physical components of the transmission that contributed to these losses**, utilizing percentage maps. Specifically, the thesis is structured as follows:

The first Chapter of this thesis justifies the use of a multi-speed transmission in electric vehicles by explaining the benefits, the types of multi-speed transmissions available, and the optimal number of gears to adopt, all while specifically referencing electric vehicles.

Chapter 2 introduces the solution of a 2-speed transmission developed by Dana, detailing its layout with components and power flows in both first and second gears.

As just explained, the transmission converts power from the electric motor to the wheels; however, this conversion is not free. In fact, the transmission exhibits a non-constant efficiency across different operating conditions. Chapter 3 addresses the topic of efficiency in transmissions in detail.

Chapter 4 delves into the detailed presentation of two models of the Dana 2-speed transmission developed within the *Matlab/Simulink* environment. These models are meticulously designed to accurately estimate power losses occurring within the transmission system.

Lastly, Chapter 5 analyzes and discusses the outcomes derived from the *Matlab/Simulink* models presented in Chapter 4, in order to obtain a comprehensive overview of the total efficiency of Dana 2-speed transmission solution and the various sources of power loss that contribute to inefficiencies.

Contents

List of Figures

Chapter 1

Electric drivetrain solutions

1.1 Overview

Today's available solutions for Battery Electric Vehicles (BEVs) layouts are mainly two: the centralized system configuration (single or multi-motor coupling powertrain) and the off board distributed system configuration (in-wheels motors).

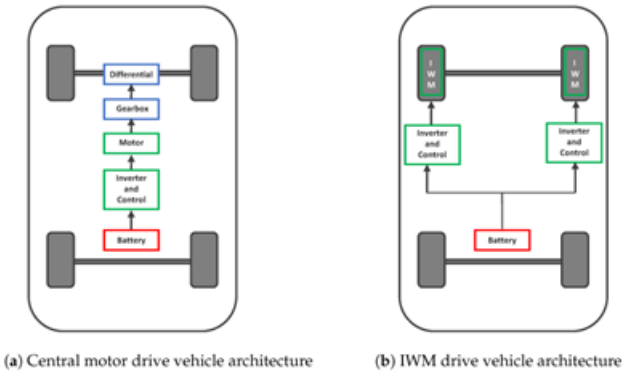

(a) Central motor drive vehicle architecture (b) IWM drive vehicle architecture

Figure 1.1: eDrivetrain solutions [**57**]

Despite no transmission system is needed for the off board distributed configuration, this solution affects the comfort and the safety of the vehicle because of the increase in the unsprung mass [**1**]. The centralized system consists of a motor and a single or multi-ratio gearbox; nevertheless, multi-motor driving systems can be used to better manage energy utilization together with an improvement in performances, by means the implementation of various driving modes [**2**]. In order to minimize mass, volume,

losses and costs of the drivetrain, the single motor powertrain configuration is the most suitable solution [**3**, **4**, **5**].

1.2 Single-speed vs multi-speed transmission

A great part of single motor powertrain solutions adopts a single reduction gear to sufficiently match the torque and the speed requirements of the vehicle for various road conditions by choosing an adequate motor and reduction gear combination [**6**]. This is possible because the electric motor produces consistent torque in its entire speed range, in addition, above its base speed, the motor power output is constant, so no need for more gears to control the wheels is requested.
However, a multi-speed transmission can be used to further improve vehicle's performance (top speed, increase in acceleration, gradeability) and fuel consumption (optimization of the motor/inverter operating points, overall mass and volume reduction) for the single motor centralized layout. To properly implement these kinds of transmissions, a control for the gearbox and a shift strategy study are needed [**7**]; disadvantages in adopting this solution may be the raise in the manufacturing cost for the EV and a lower gearbox efficiency than a single-speed gearbox.

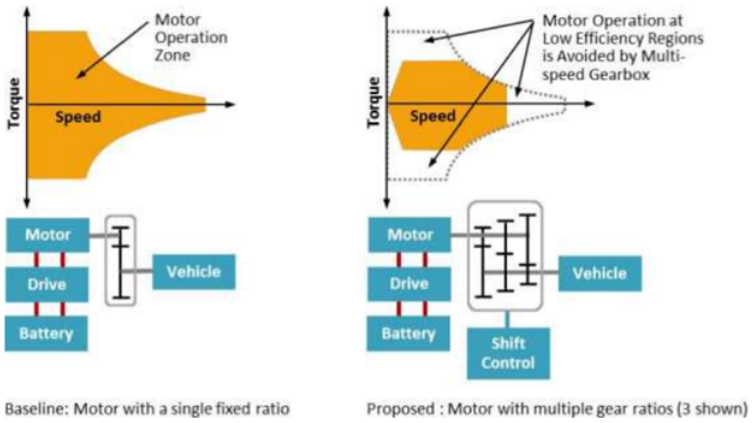

Figure 1.2: Single reductor vs multi-speed gearbox [**58**]

The main performance indexes to consider while evaluating a multi-speed gearbox for EVs applications are production coast, energy consumption, dynamic performances and driving comfort. Basing on the specific application, a different weight could be assigned to each of them.

1.3 Multi-speed gearbox overview

The main types of multi-speed gearboxes used in the automotive field can be classified into the following categories: manual transmission (MT), automated manual transmission (AMT), dual clutch transmission (DCT), automatic transmission (AT) and continuous variable transmission (CVT). There are other types of less conventional architectures researchers focused on: infinitely variable transmission (IVT), inverse-automated manual transmission (I-AMT) and magnetic gear transmission (MGT).
The gearset of an AT is usually composed by a set of planetary gears properly controlled to achieve various gear ratios. To enable the engine connection to the driveline during gearshifts, a torque converter is used.
The MT is the simpler gearbox solution, the gearshift is performed manually by the driver by disconnecting the engine by means of a shift lever connected to a clutch. AMTs are based on the MT but they use a transmission control unit (TCU) to automatically control the shift. The I-AMT is similar to the AMT, rather than a synchronizer it includes a clutch for the connection of the second gear, while the first gear is engaged by the synchronizer. DCT is a solution that uses two shafts, one for the even gears and one for the odd gears. The two shafts are both connected to the motor by two independent clutches, by controlling the two clutches simultaneously it is possible to achieve a seamless gearshift. Differently from the previous cases, the CVT enable the gear ratio to vary in a continuous way within a defined ratio range thanks the use of taper discs and a belt. IVT is based on the same concept of the CVT but a fixed ratio and a planetary gearset are added to reduce the minimum ratio, even to negative values [**8**]. In the MGT a magnetic field is used to transmit force instead of gears. The gear ratio is determined by the ratio of magnetic pole pairs on the inner and the outer rotors in the case of a coaxial magnetic gear, or by the planetary gear ratios for the planetary magnetic gear.

1.4 Multi-speed gearbox for electric vehicles

In order to be competitive in the automotive industry, the transmission system of a Battery Electric Vehicle (BEV) must meet high efficiency targets and a seamless gearshift behavior. Focus on efficiency is crucial, because it directly impacts the vehicle's overall performance, energy consumption and range.
Additionally, seamless gearshifting enhances driving experience by improving the comfort and gearshift quality, significant factors for the satisfaction of an electric vehicle consumer.

Ensuring that, the transmission operates with minimal energy loss and with smooth and imperceptible gears transition. A multi-speed transmission for BEVs can continuously varies the gear (CVT) or utilize a discrete gearbox, which shifts between predetermined gears.

Although the adoption of a Continuously Variable Transmission (CVT) system maximizes the working points distribution of the motor/inverter system, its adoption presents drawbacks in efficiency [**9**, **10**, **11**] and in speed of response at launch [**12**]. As result, a discrete multi-speed transmission seems to be the most cost effective solution for controlling the operating conditions of the motor for an assigned driver power demand.

The efficiency of a manual transmission (MT) can reach 97% [**13**] but because in an electric vehicle, changing gears is not intuitive for users due to the motor's quiet operation, they are practically not used in EVs applications; also the automated manual transmission (AMT) efficiency is comparable to the MT's one, but AMTs are affected by torque gap during gearshift due to the disengagement of the clutch to allow the synchronization; so they cannot guarantee a seamless gearshift behavior. The I-AMT was introduced to overcome the driving comfort limitations of a traditional AMT, by reducing its traction interruption during gearshift [**14**]. ATs instead, allow a seamless gearshift but have no longer efficiency than MTs (up to 86% according [**13**]), mainly because of viscous shear losses in the torque converter, due to that they are not suitable for EVs. DCT permits to have a higher efficiency than an AT system with torque converter and the capability to fill in the torque gap during gearshift, allowing seamless longitudinal accelerations. Anyway DCTs, when coupled with engines able to generate considerable torque, need wet clutches. Wet clutches are used to dissipate the big amount of heat produced during power-on gearshift. As a result, DCT efficiency is reduced by churning and ancillary power dissipation associated with the wet clutch pack. The adoption of MGT could be attractive due its benefits deriving from the contactless mechanism, anyway its efficiency is low, and the production cost is prohibitive (because the large number of magnets used) for the application in the automotive field. Research literature shows that among the various solutions, AMTs and DCTs are the most promising ones. Although I-AMT, IVT and MGT have been studied, they have not yet real applications. In [**15**] a complete analysis between the abovementioned transmission layouts is done. Latest designs and real application gearboxes are examined and compared. Authors inspected the relative cost and the relative mass of the various gearbox topologies respect to the MT solution, taken as a reference (factor=1). The

best performance, after the MT reference one, for both cost and mass is achieved by the AMT and the I-AMT (factor=1.09), followed by the DCT (1.32). The worst value is for the IVT (1,88). No values are reported for the MGT since it is still at the research stage, so no sufficient data is available. The qualitative study conducted by Machado and coworkers also shows that the DCT is ranked highest for potential dynamic performance, due to its benefit in reducing the torque gap. While the highest potential drivetrain efficiency index is shared among DCT, AMT and I-AMT, the maximum gearbox efficiency index is for the MT. Overall, they concluded that clutch-less AMTs and DCTs are the most common and promising technologies.

1.5 Gears number for an electric vehicle gearbox

Besides the investigation on the most suitable type of gearbox, the academic literature also investigated the most convenient number of gears to be adopted for an EV to achieve a compromise between performances, costs and efficiency. In particular, Ruan et al. [**16**] compared alternative multi-speed powertrains (two-, three-, four-speed DCT) in a hybrid cycle application that combines FTP75 for the city cycle and HWFET for the highway cycle. The results demonstrate that the two-speed DCT, among the three proposed, shows the best energy utilization rate improvement with respect to the reference single-speed transmission (+16.4% for the B-class case study, + 9.6% for the E-class case). [**17**] investigated motor efficiency among three types of multi-speed transmissions in pure electric vehicles (BEVs) driving on an urban and a highway driving cycle. The results indicate that an increasing number of gears could make the motor work in a steady efficient driving status. Fang and coworkers stressed that the obtained rate improvement in motor efficiency depends on the driving routes, this fact, combined with the increasing cost of a transmission with more gears, led them to finally state a two-speed transmission is enough for an EV driving mostly on non-complex routes. Lastly, [**18**] and [**19**] assert two-speed transmission system represents the best compromise between the benefits derived from a multi-speed transmission and the simplicity of a compact and lightweight drivetrain.

Chapter 2

The novel Dana 2-speed transmission

The necessity of high efficiency also for high performance applications together with the need of a seamless gearshift to emulate the behavior of the single reduction gear solution typical of an EV, combined with constrains in costs, led the company Oerlikon Graziano together with Sorniotti and co. [**18**, **20**] to investigate a new type of transmission suitable for EV that could represent an alternative to the DCT and overcomes its drawbacks. A novel 2-speed transmission has been developed from the Oerlikon Graziano single-speed unit. A transmission layout including a dual stage reduction and a single dry clutch, able to combine the high mechanical efficiency typical of an AMTs and with a torque fill capability to allow seamless gearshifts, was presented. The main benefit of this new solution is to reduce the production costs respect to the DCT's ones, by granting similar performances, even in high power operational conditions, and lower power dissipation. A seamless gearshift control system [**21**] has been also specially developed for the transmission to ensure an optimal gear change.

2.1 The transmission layout

The transmission studied in [**18**] and [**20**] is the first version of the Dana 2-speed transmission, which was later followed by a new version that is the subject of this study. The first version presents a layout as depicted in Figure 2.1. Specifically, the transmission comprises a dual stage reduction; the first gear is achieved through a device known as *Selectable One Way Clutch* (SOWC), while the second gear is attained via a friction clutch. It includes three shafts: the motorshaft, where the

friction clutch is mounted; the layshaft 1 where the SOWC is mounted, and a third shaft, the differential shaft, where the differential gear is keyed on, serving as the final reduction stage that transmits motion to the half shafts, and subsequently to the wheels.
The key component of this transmission is the *One Way Clutch* (OWC), a device consisting of two main parts that automatically engages or disengages basing on the relative speeds of the two parts. The second clutch is a traditional friction clutch that can be engaged or disengage with a pressure command.

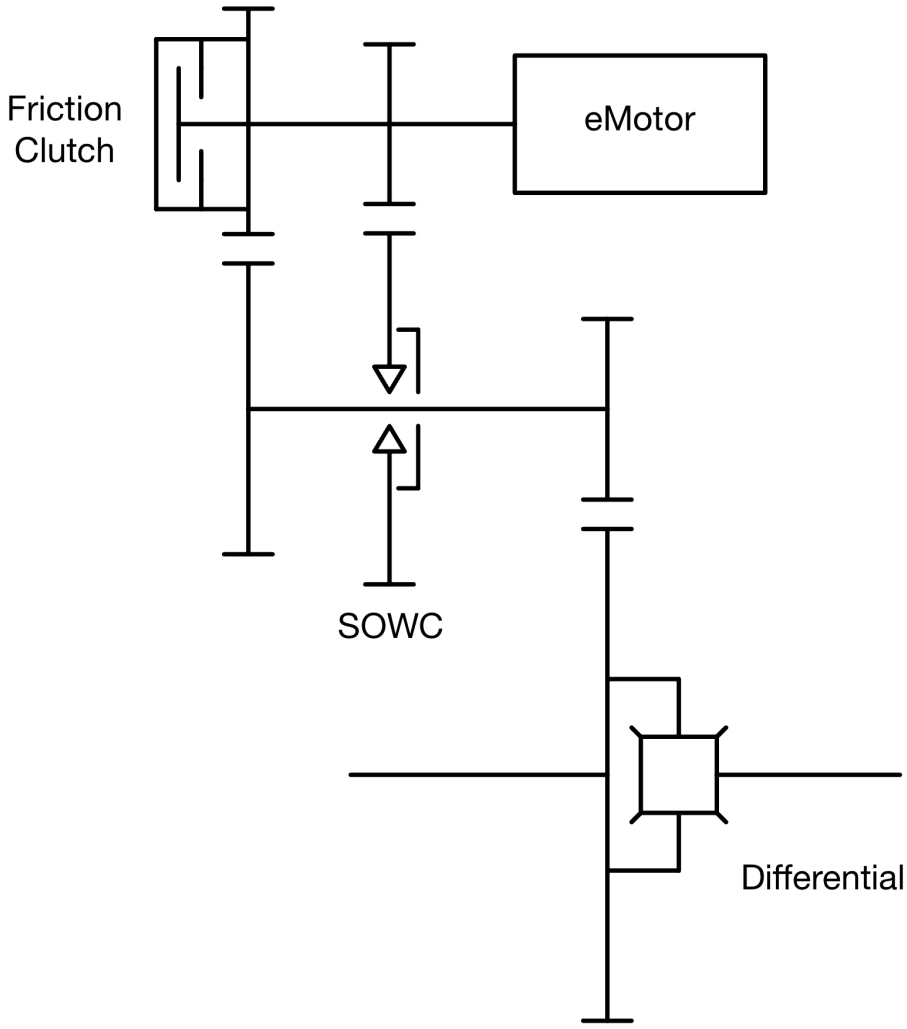

Figure 2.1: Transmission layout: first version

The selectable one way clutch SOWC

The OWC is an unidirectional motion device, also known as freewheel or overrunning clutch. It can be seen as a mechanism composed of two discs: the driving disc and the driven disc, represented in Figure 2.2 as the blue and the green parts respectively. The clutch is actively engaged and transmits power when the driving component rotates faster than the driven component. Conversely, when the driven part starts rotating faster than the driving part, the clutch disengages so that the driven component, usually a shaft, can keep spin faster and freely without the upstream components of the system controlling it. This is the overrunning condition, from which the overrunning clutch device also derives its name.

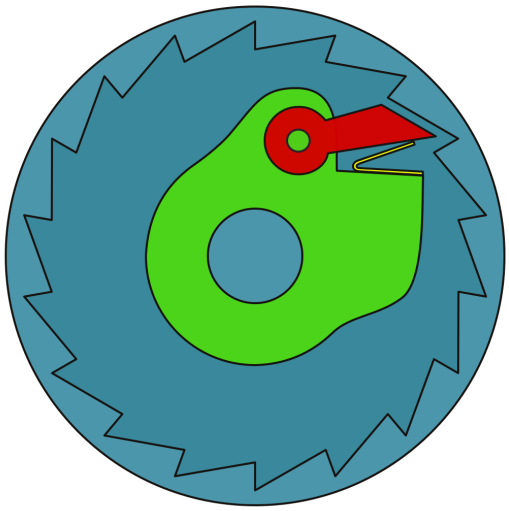

Figure 2.2: One Way Clutch [**22**]

As we will see in the following sections, the OWC does not allow energy recovery during braking when the first gear is engaged, because, in such a condition, it would be in overrunning condition. To perform regenerative braking in first gear, it is necessary to prevent the clutch from disengaging when the driven component rotates faster than the driving component. To achieve this, the OWC has been replaced with an evolved version of it, called *Selectable One Way Clutch* (SOWC). Unlike the OWC, the SOWC, when properly activated, allows torque transfer in both directions of rotation.
Specifically, the SOWC has two operating modes: it can be activated (ON mode) or deactivated (OFF mode). Contrary to the standard OWC, the ON mode of the SOWC prevents the driven part from moving freely under no circumstances, thanks

to a mechanism that, if properly activated, rigidly couples the two discs in both the directions. This allows to transfer power from the motor to the wheels and from the wheels to the motor, allowing both traction and regeneration.

The new Dana two-speed transmission design

Unlike the original version, the new version of the Dana 2-speed transmission comprises a three-stage reduction with four shafts. The first reduction occurs between the motor shaft and layshaft 1, the first or second gear reductions between layshaft 1 and layshaft 2, and the final reduction between layshaft 2 and the differential shaft. Its layout is shown in Figure 2.3. As for the first version, the first and second gear selections are performed using a selectable one-way clutch (SOWC) and a traditional clutch, respectively.

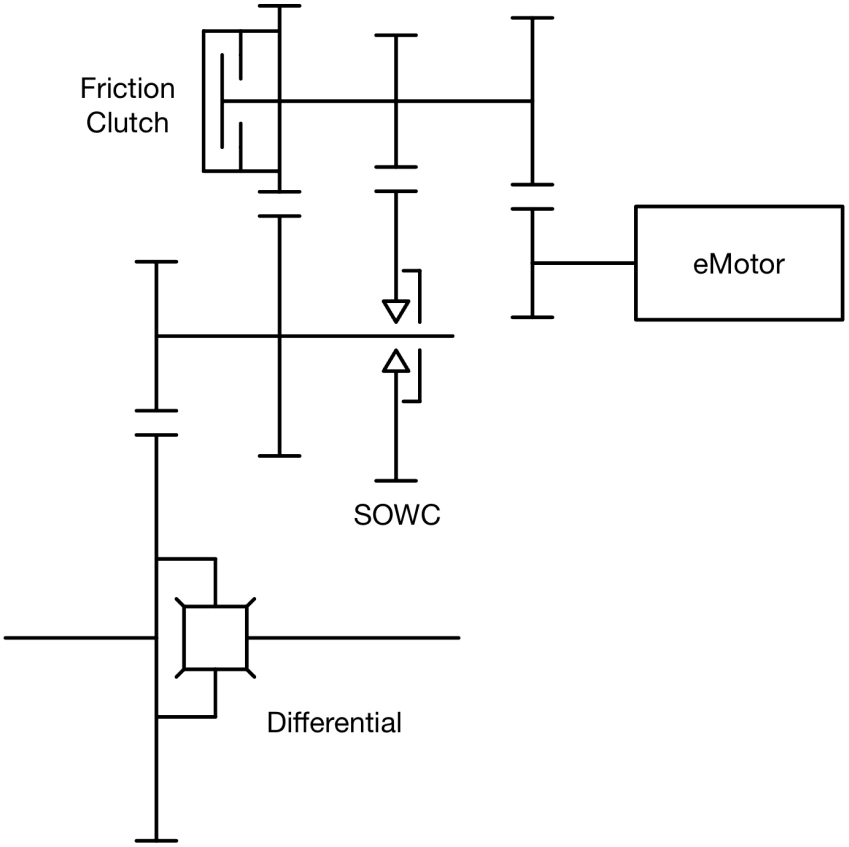

Figure 2.3: Transmission layout: new version [**22**]

2.2 Transmission power flow

The power flow in a battery electric vehicle, in driving condition, is considered positive from the electric motor to the wheels. In such instance, the electric motor generates power, converting electrical energy from the battery into mechanical energy, typically in rotational motion of a rotating shaft (the motor shaft). This shaft transfers the power into the gearbox. Then, a set of reduction stages, modifies the power by increasing torque and reducing speed. A final gear reduction, the differential, finally distributes the mechanical power to drive the vehicle's wheels by splitting it between the left and right wheels.
In contrast, the transmission power flow for an electric vehicle is considered negative when it flows from the wheels to the motor; this case is the regenerative condition (hereafter shortened as regen).

2.2.1 Power flow in first gear

In Figure 2.4 the power flow, in driving condition in first gear, is showed for the last version of the product. The transmission presents three reduction stages: the power generated in the electric motor, encounters a first reduction stage (from motor shaft to layshaft 1), a second stage, which varies according to the gear engaged, and the final ratio (the differential ratio). When the first gear is engaged, power flows across the first stage, then passes in the second stage through the SOWC, and finally in the differential stage. First gear reduction is achieved through the SOWC: during driving conditions, the friction clutch is disengaged, allowing the power flow to pass solely through the one-way clutch (OWC). During regeneration (Figure 2.7), the SOWC is set to ON mode to allow the power to flow through it, thereby preventing overrunning.

Motoring

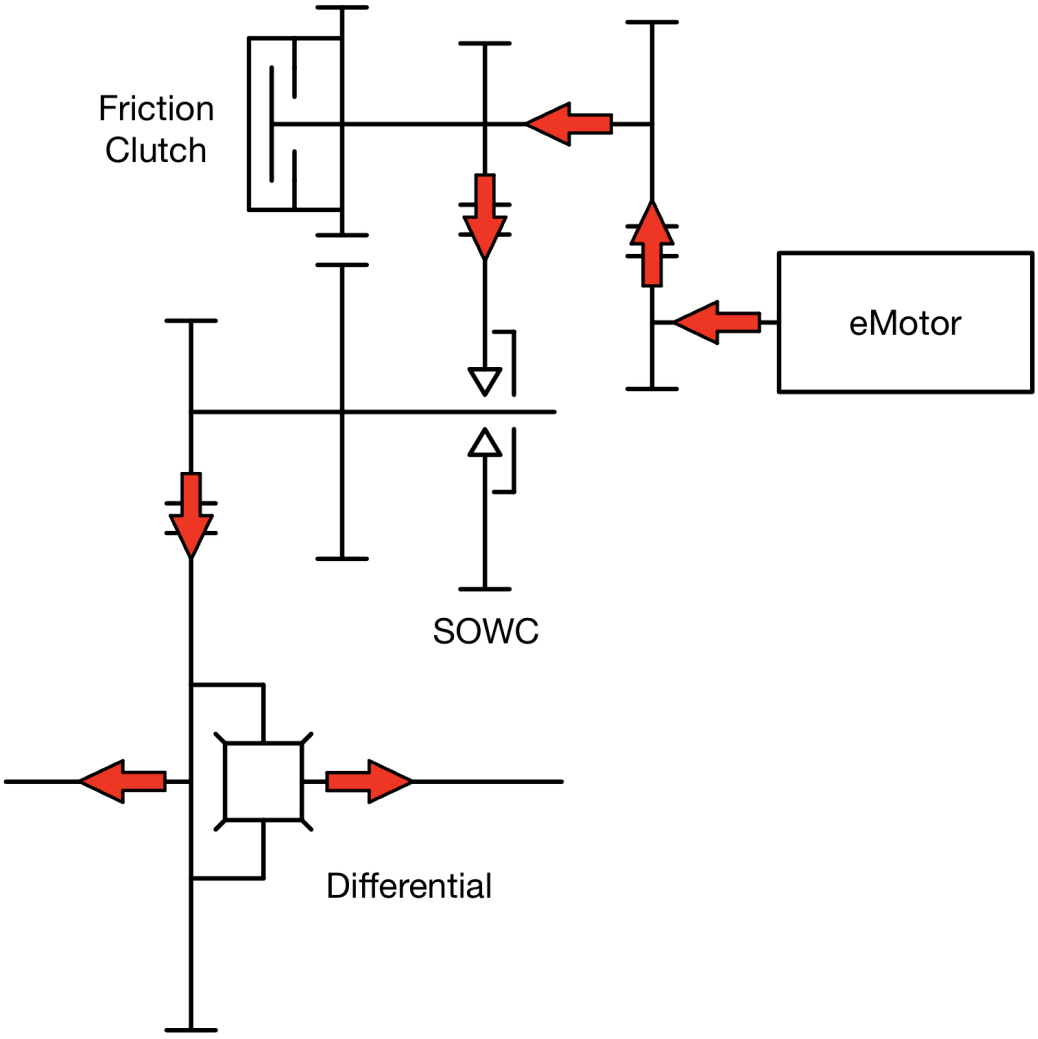

Figure 2.4: Transmission power flow in 1st gear - Drive

Regen

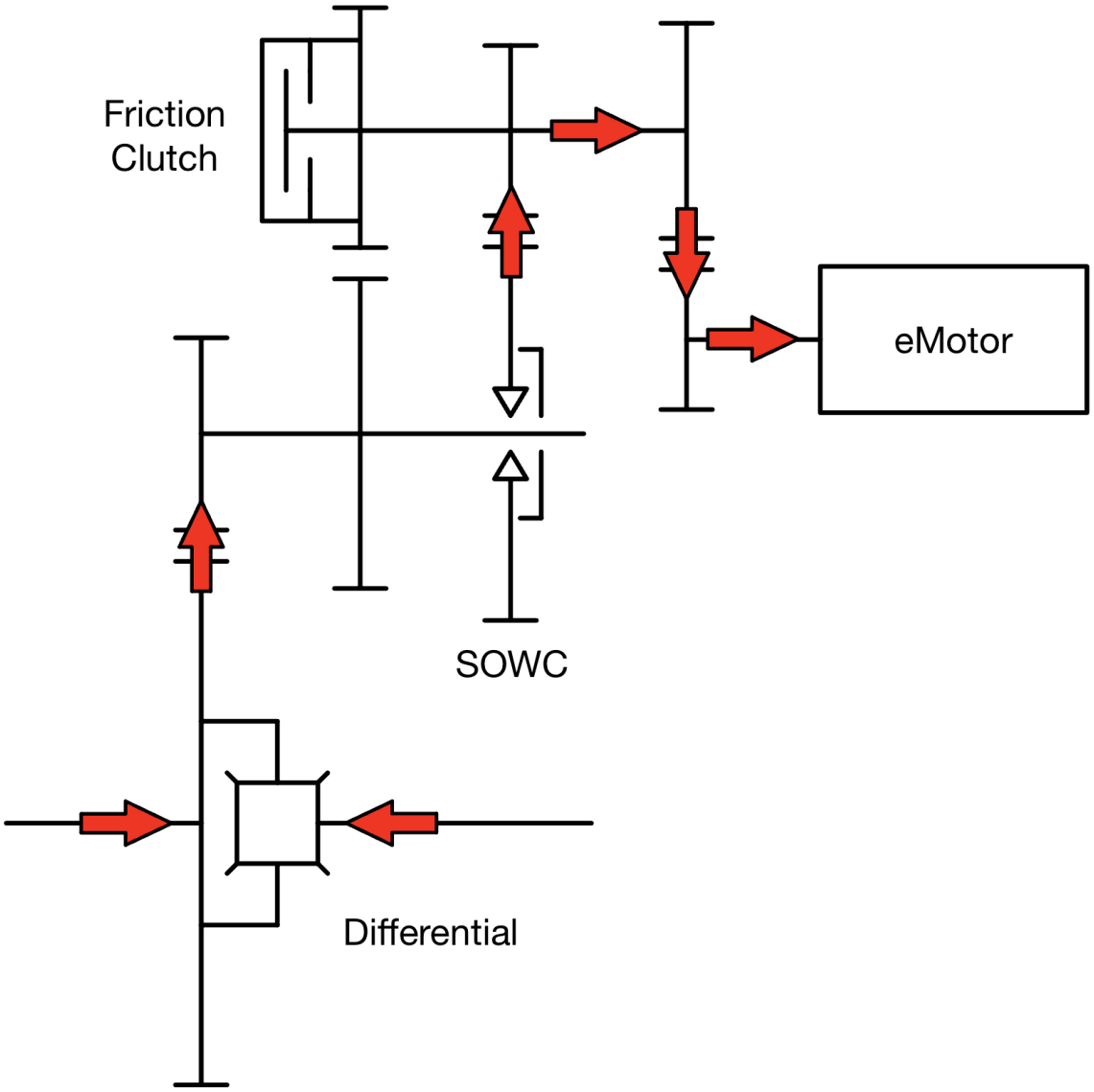

Figure 2.5: Transmission power flow in 1st gear - Regen

2.2.2 Power flow in second gear

When in second gear, the power is transmitted to the layshaft 2 through the friction clutch. From here, power is then transferred to the third shaft via the differential, which splits the power flow into the two halfshafts connected to the wheels.
As seen before in Figure 2.4, in first gear the electric motor delivers torque that passes through the SOWC, which is set to ON mode to enable regenerative braking. Instead, in second gear (Figure 2.6 and 2.7), the hydraulic system operates the friction clutch, while the SOWC is set to OFF mode, working as a standard OWC. Under these circumstances, the speed imposed by the second gear to the layshaft 2 is higher than the speed that the first gear imposes on the driving component of the OWC. Consequently, the driven part, integral with the layshaft 2, rotates at a higher speed, and thus not allowing the SOWC to transmit torque to the layshaft 2. Resulting in all the power flow passing through the friction clutch.

Motoring

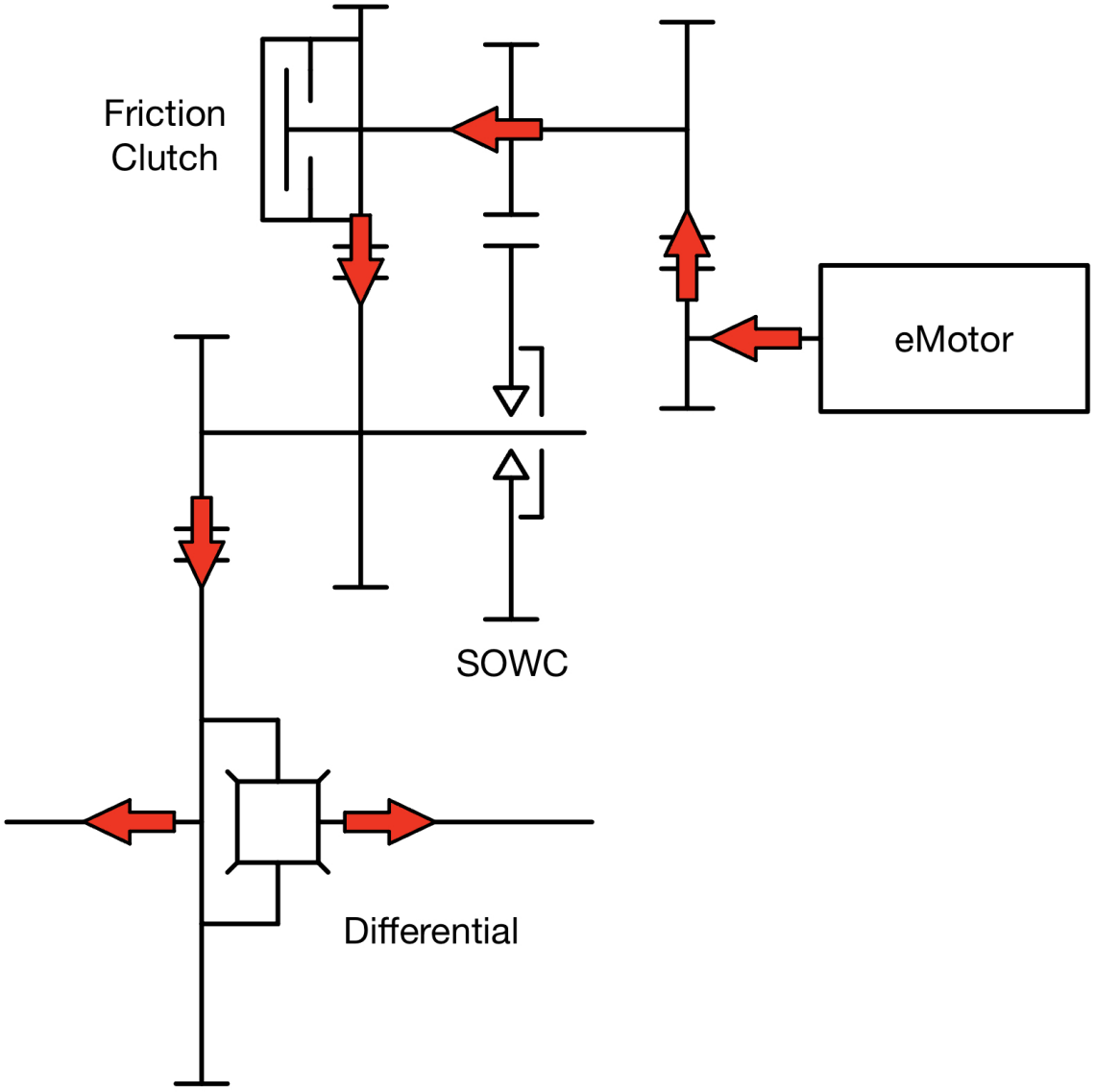

Figure 2.6: Transmission power flow in 2nd gear - Drive

Regen

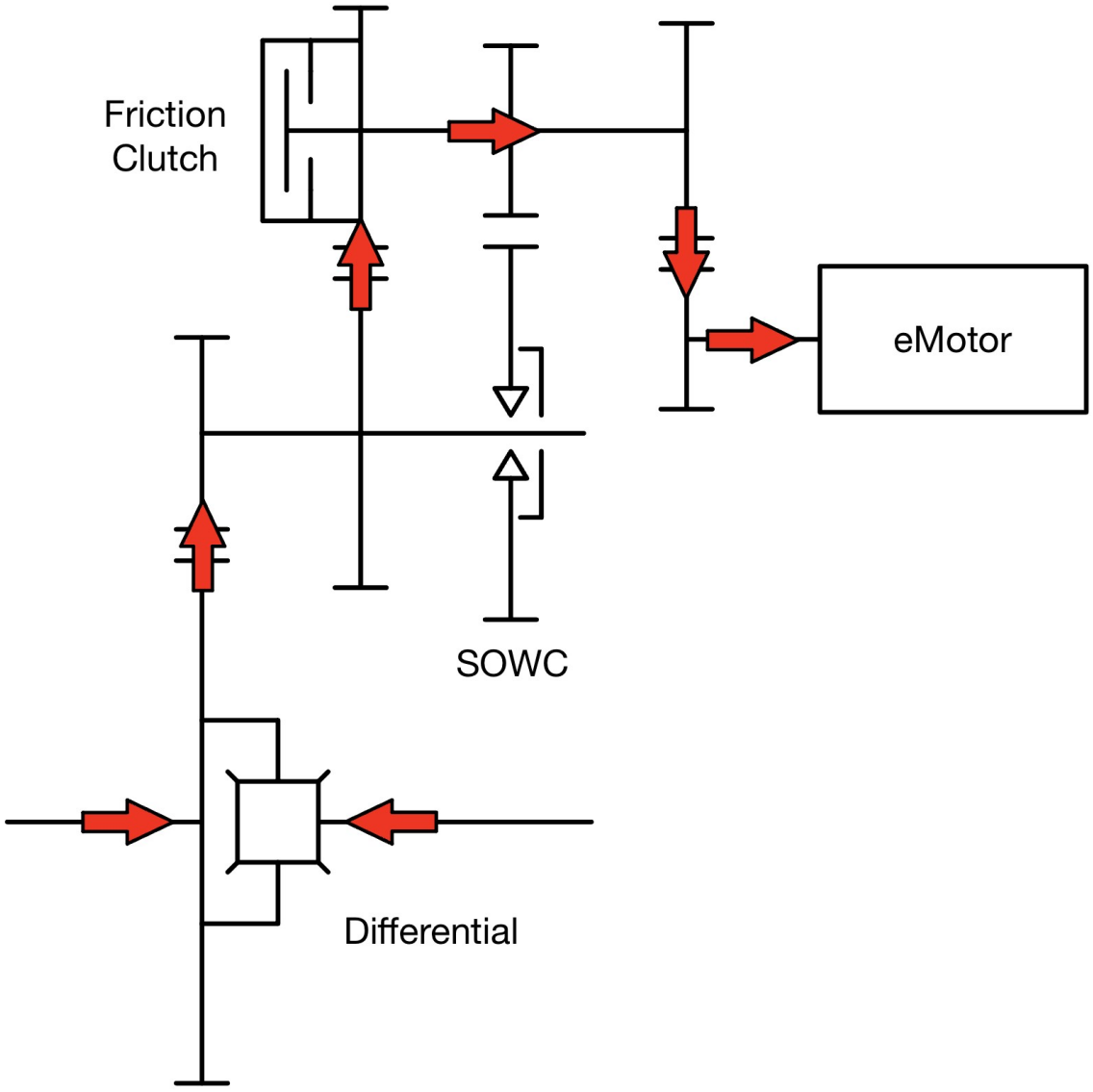

Figure 2.7: Transmission power flow in 2nd gear - Regen

Chapter 3

Power losses in a transmission

Recent legislation, particularly in California and the EU, portends more stringent requirements for road transport CO_2 emissions across the globe. Additionally, reducing energy consumption and conserving resources, are becoming increasingly important areas of interest for consumers. This drives vehicle manufacturers to enhance the efficiency of their products. To achieve these targets, optimizing the efficiency of the powertrain is essential. Since transmissions are one of the main components in a vehicle powertrain, their powerlosses cannot be considered negligible in the total powertrain losses [**23**].

Transmission power losses are inefficiencies that result in the loss of energy as it is transmitted from the engine (or electric motor) to the wheels of a vehicle, or vice versa during regenerative braking (EVs only). They can significantly affect the overall efficiency and performance of a vehicle. These losses occur due to a variety of factors, including mechanical inefficiencies, thermal effects, and dynamic interactions within the transmission system. Understanding and addressing these power losses is crucial for optimizing vehicle performance and energy efficiency. Especially, for internal combustion engine (ICE) vehicles, this means improving fuel economy and reducing emissions, while, for electric vehicles (EVs), it means enhancing battery range. Optimizing transmission efficiency is thus a critical area of focus, especially as electric vehicles become more widespread. Researchers have spent lot of effort to build models able to estimate transmission power losses. These models are essential for understanding how different factors, such as friction, lubrication, and mechanical design, impact the overall efficiency of the transmission. By using these models, engineers can identify areas for improvement and implement design changes or new technologies to reduce losses and enhance the performance of the entire powertrain. Therefore, summing up, the importance of transmission efficiency is crucial in auto-

motive field for improving fuel economy and satisfying the growing consumer demand for more efficient and environmentally friendly vehicles.

3.1 Power loss sources

This section presents a detailed overview of the different types of power losses that can occur within a transmission: losses in a gearbox are originated from gears P_{VZ}, bearings P_{VL}, seals P_{VD}, and auxiliary elements P_{VX} [**24**]. Consequently, the total power loss P_V is the sum of these power losses contributions, considering all the elements comprising the transmission.

$$P_V = P_{VZ} + P_{VL} + P_{VD} + P_{VX}$$

Literature [**25**] divides gearbox losses in load independent (subscription 0) and load dependent losses (subscription P).

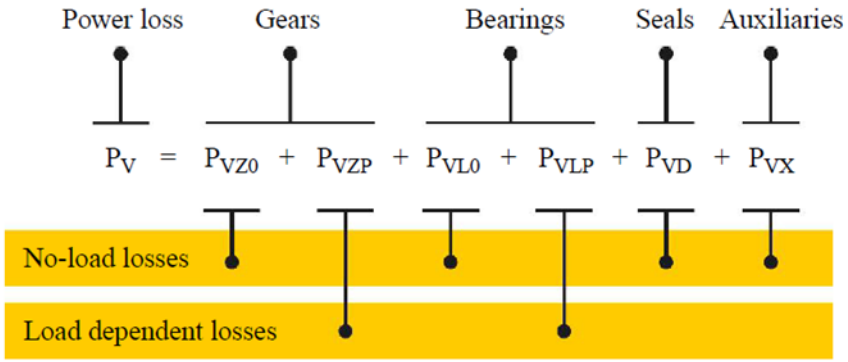

Figure 3.1: Transmission power losses sources [**46**]

Load dependent power losses occur when torque is transferred while independent power losses occur regardless of whether torque is being transmitted. In fact, gears and bearings produce losses even when no load is transmitted, due to the rotation of shafts, which causes them to be dragged in the lubricant. More specifically, it is possible to distinguish the following loss components:

- **Gear Power Losses -** composed by a load dependent component P_{VZP} and a load independent component P_{VZ0}

- **Bearing Power Losses -** composed by a load dependent component P_{VLP} and a load independent component P_{VL0}.
- **Shaft Seal Power Losses**
- **Auxiliaries Power Losses**

3.1.1 Gear Power Losses

Gear power losses P_{VZ} refer to the total energy dissipation resulting from the interaction and operation of gears within a transmission system. P_{VZ} can include a load-dependent component P_{VZP} and another component P_{VZ0} that is independent of the load .

Load dependent component

Gear load depending losses refer to energy losses, within a transmission, that is generated because of load is transmitted through to the gears. They mainly result from the frictional force generated at the contact points between gear teeth (known as meshing friction). Ohlendorf [**26**] was the first introducing a theoretical approach to calculate the load dependent losses in gears. This approach is still today used in the ISO-14179-2.

$$M_{VZ,P} = M_{IN}\mu_m H_V$$

$M_{VZ,P}$ Gear load dependent resistant torque

M_{IN} Input torque

μ_m Constant friction coefficient

H_V Gear loss factor

Load independent component

Gear load independent losses, also known as *Churning Losses*, are the component of gear losses which occur regardless of whether torque is being transmitted or not. Churning losses are due to swash and squeeze effects in splash lubrication, resulting from gears turning in a fluid, which can be either lubricant oil or an oil-air mixture, or they are due to oil impulses in spray lubrication. Load independent gear losses can be seen as formed by the following contributions:

- Splash lubricated gears case:

$$M_{VZ,0} = M_{VZ,Q} + M_{VZ,PI} + M_{VZ,V}$$

- Spray lubrication case:

$$M_{VZ,0} = M_{VZ,Q} + M_{VZ,I} + M_{VZ,V}$$

Where:

$M_{VZ,0}$ Gear load independent resistant torque

$M_{VZ,Q}$ Contribution due to the displacement of the oil in the contact area between the teeth (negligible if oil stream meets the regressing contact area)

$M_{VZ,PI}$ Resistance torque of the gear wheel when rotating in an oil bath

$M_{VZ,I}$ Impulse loss torque caused by the oil stream in spray lubrication

$M_{VZ,V}$ Air drag due to air or oil mist, composed of the loss of the gear wheel itself MVZ_{VZ} and the loss in the contact area between the teeth MVZ_{VE}

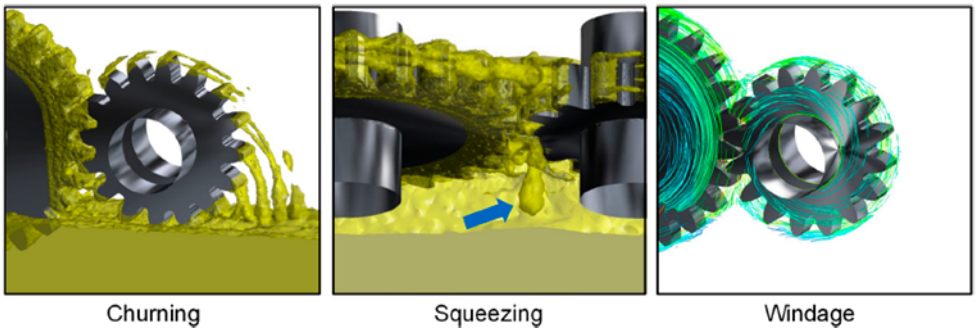

Figure 3.2: Transmission Churning losses [**27**]

Most power losses models of spinning gears present in literature are based on dimensional analysis, because of the difficulty of the phenomenon. Mauz [**28**] investigated various influencing factors experimentally, resulting in the formulation of an equation where spinning direction, oil viscosity, oil volume, and housing effect were taken into consideration. Since many parameters are required in the Mauz's equations, and also

its validity range is limited, another model for the oil churning losses prediction is derived and currently employed in the ISO 14179-2 [**24**].

$$T_H = C_{SP} \cdot C_1 \cdot e^{C_2 \frac{V_T}{V_{T0}}}$$

The parameters C_{SP}, C_1 and C_2 depend on the immersion depth and on the gears dimensions.

3.1.2 Bearing Power Losses

The main contribution for bearing power losses P_{VL}, arise from rolling and sliding friction, lubrication losses and seal losses. In vehicle gearboxes, rolling contact bearings are predominantly used. For these types of bearings, six distinct loss contributions can be identified, as illustrated in Figure 3.3: Friction from rolling and sliding interactions between the rolling elements and bearing rings (contribution 1 and 2), sliding friction deriving from interactions between the cage bar and the bearing rings (contribution 3), sliding friction occurring between cage and rolling element front surface (contribution 4), friction from sliding between rolling element and outer ring (contribution 5), and friction from interactions between cage and rolling element (contribution 6).

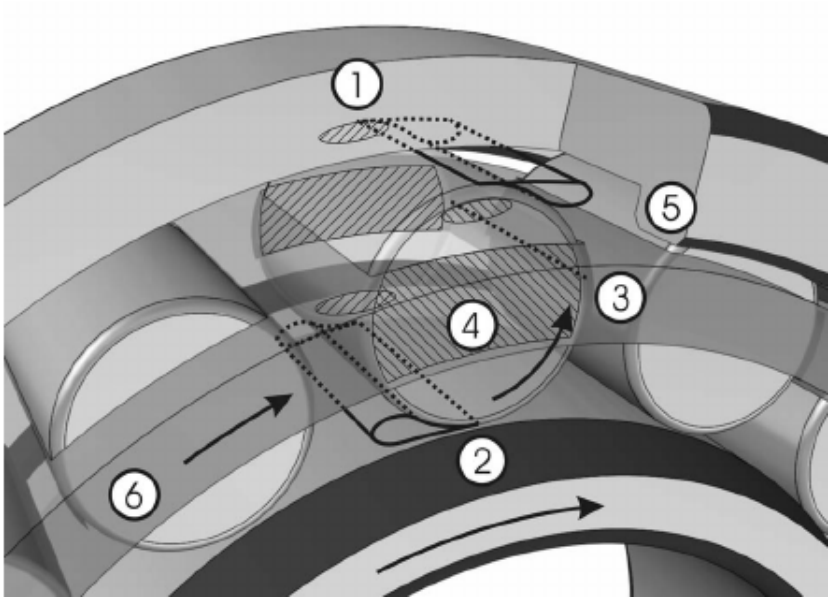

Figure 3.3: Bearing losses types [**29**]

As previously observed, one of the factors influencing power loss in bearings is their type. Due to the wide variety of bearings available on the market, manufacturers provide empirical models to estimate the drag torque. Two main approaches are present in literature:

1. The Palmgren approach that splits the drag into a torque dependent and a torque independent part
2. The SKF approach that investigates where each loss is generated

Palmgren approach

The Palmgren approach, used by INA/FAG [**30**] and also included in the ISO 14179-2 [**24**], consists in splitting the total resistant torque into a load dependent torque $M_{VL,P}$ and load independent torque $M_{VL,0}$ contribution. This formulation was published by Palmgren [**31**] and represented the first comprehensive approach to calculating drag torque in rolling contact bearings.

$$M_{VL} = M_{VL,0} + M_{VL,P}$$

Where:

$M_{VL,0}$ Bearing load independent resistant torque

$M_{VL,P}$ Bearing load dependent resistant torque

SKF approach

SKF investigate a more detailed model [**32**] for calculating the frictional moment of a bearing, assigning each type of loss to its specific location within a bearing.

$$M_{VL} = M_{rr} + M_{sl} + M_{seal} + M_{drag}$$

Where:

M_{rr} Rolling frictional moment

M_{sl} Sliding frictional moment

M_{seals} Frictional moment of seals

M_{drag} Frictional moment of drag losses, churning, splashing etc.

3.1.3 Shaft Seal Power Losses

Radial shaft seals losses P_{VD} are attributable to the loss torque generated by the friction between the sealing lip and the rotating shaft. A simple formulation to estimate shaft seals losses is provided by Linke [**33**].

$$M_{VD} = [145 - 1.6 \cdot \theta + 350 \cdot log(log(\nu_{40} + 0.8))] \cdot 10^{-7} \cdot d_w^2 \cdot \frac{30}{\pi}$$

Where:

d_w Shaft diameter

θ Oil temperature

ν_{40} Kinematic viscosity of oil at 40 °C

3.1.4 Auxiliaries Power Losses

Auxiliaries losses P_{VX} in a transmission system refer to the general power losses that occur due to components other than gears, bearings, and seals. Examples of auxiliary power losses include those caused by clutches and synchronizers. These losses can be expressed as:

$$P_{VX} = P_{VDDF} + P_{VS} + P_{VK} + P_{VNA}$$

Where:

P_{VDDF} Rotary union loss

P_{VS} Synchronization loss

P_{VK} Clutch loss

P_{VNA} Oil pump loss

Rotary union loss

Rotary unions loss P_{VDDF} is due to the friction between the lateral surfaces and depends on oil pressure and shear flow in the pressure chamber. According to Gronitzki [**34**] the loss torque in a rotary union can be described as the sum of three main loss sources:

$$M_{VDDF} = 2M_I + 2M_{II} + M_{III}$$

Where:

M_I Friction torque due to the oil leakage

M_{II} Friction torque between the groove and the seal ring

M_{III} Friction torque due to shear flow between the outer and the inner shaft, in a pressurized chamber

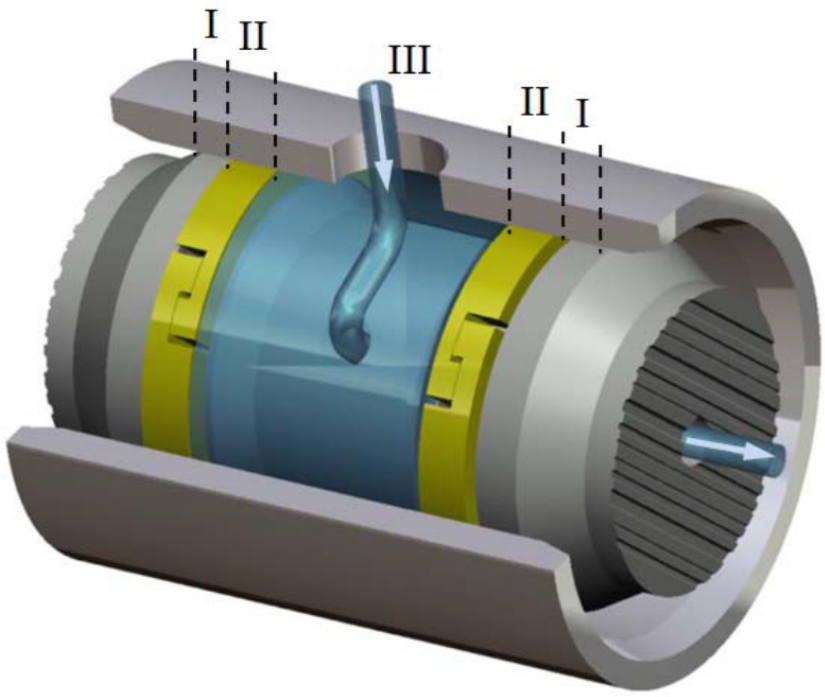

Figure 3.4: Rotary union losses areas [**29**]

Synchronization loss

Synchronization losses P_{VS} are due to the fluid drag between synchronizer and friction cone.

Use drag data based on measurements provided by the manufacturer.

Clutch loss

Clutch losses P_{VK} are due to the fluid drag between disc of wet multi-disc clutches.

Use drag data based on measurements provided by the manufacturer.

Oil pump loss

Oil pump losses P_{VNA} depend on system pressure, temperature and oil viscosity.

Use drag data based on measurements provided by the manufacturer.

3.2 Power losses modelling

A complete model to estimate transmission losses can be built by choosing from literature the proper sub-models for each loss contribution. The grade of complexity and the available transmission's data can drive the choice of a model over another. In [**35**] a comparison between a model built by using ISO 14179-2 sub-models and a model, referred to as *joint overall model*, built by the combination of various sub-models taken from the literature (integration model for the mesh gearing losses, Changenet model for oil churning and the SKF model for bearing losses) is carried out on a two-speed transmission. Results show that the joint overall model predicts a higher efficiency than the ISO 14179-2 methods and it gives a better overall efficiency prediction for the analyzed transmission. The joint overall model is also used in [**36**], where authors proposed a novel method to improve power losses estimation in a transmission by eliminating the deviation between simulation results obtained with joint overall model and the experimentally measured data from test bench. The methodology is based on identifying some parameters that can reduce the efficiency deviation between the simulation results and measurements by using a sensitivity analysis. The two transmissions study cases both show that the methodology is reliable.
Since this work aims to estimate the losses of a transmission that is still under study and has not yet entered production, it is not possible to compare the results obtained

through a prediction model with experimental measurements. For this reason, a loss prediction model that employs sub-models from the well-established ISO 14179-2 standards has been chosen.

3.2.1 The ISO approaches

The *International Organization for Standardization* (ISO) is a global federation comprising national standards bodies from various countries. Its primary mission is to develop and publish international standards that promote quality, safety, efficiency, and interoperability across various industrial and commercial sectors. These standards are developed by ISO technical committees, where member bodies and relevant international organizations collaborate to define best practices and common requirements.
The ISO 14179 is a thermal rating method that utilizes an analytical model, based on heat balance, to calculate the thermal transmittable power for a single or multiple stage gear drive that are lubricated with mineral oil. Two proposals exist for this standard, the American proposal ISO 14179-1 and the German proposal ISO 14179-2.
Below is the official definitions directly derived from the standard [**37**]:

ISO 14179-1

*The procedure ISO 14179-1 is based on the calculation method presented in AGMA (American Gear Manufacturers Association) Technical Paper 96FTM9 [**38**]. The bearing losses are calculated from catalogue information supplied by bearing manufacturers, which in turn can be traced to the work of Palmgren. The gear windage and churning loss formulations originally appeared in work presented by Dudley, and have been modified to account for the effects of changes in lubricant viscosity and amount of gear submergence. The gear load losses are derived from the early investigators of rolling and sliding friction who approximated gear tooth action by means of disk testers. The coefficients in the load loss equation were then developed from a multiple parameter regression analysis of experimental data from a large population of tests in typical industrial gear drives. These gear drives were subjected to testing which varied operating conditions over a wide range. Operating condition parameters in the test matrix included speed, power, direction of rotation and amount of lubricant. The formulation has been verified by cross checking predicted results to experimental data for various gear drive configurations from several manufacturers.*

ISO 14179-2

The procedure ISO/TR 14179-2 is based on a German proposal whereby the thermal equilibrium between power loss and dissipated heat is calculated. From this equilibrium, the expected gear oil sump temperature for a given transmitted power, as well as the maximum transmittable power for a given maximum oil sump temperature, can be calculated. For spray lubrication, it is also possible to calculate the amount of external cooling necessary for maintaining a given oil inlet temperature. The calculation is an iterative method.

3.3 Influence factors on transmission power losses

3.3.1 Gear losses - load independent

The addition of lubricant in a gearbox is crucial for reducing friction and wear of the gears by forming a lubricating film between their flanks. This film minimizes direct metal-to-metal contact and helps dissipate the heat generated during operation. The cooling effect provided by the lubricant is essential to maintain the structural integrity of the gears, preventing a loss in their mechanical strength. However, the introduction of lubricant also has negative consequences, such as increased energy losses and a decrease in overall transmission efficiency.

Gear speed and direction of rotation

The dependance between load independent gear losses and increasing rotational speed was reported by Seetharaman and coworkers [**39**]. As the rotational speed increases, the lubricant oil is splashed around more intensively, thus generating more churning losses. This phenomenon is visible in Figure 3.5, where a FZG gear test was carried out at different rotational speeds [**40**].

Figure 3.5: Lubricant splashing at different velocities (from the left: wheel rotating at 145 rpm, 290 rpm, 580 rpm) [**41**]

In the work done by Seetharaman et al. [**39**] it is also reported that the sense of rotation of the gears have an influence on the gear churning losses: standard rotational direction (Figure 3.6) of gears gives lower gear churning losses respect to the opposite direction. In this scenario, greater attention must be given to the scuffing phenomenon because the centrifugal force causes most of the oil to be hurl off the gear teeth before they engage again.

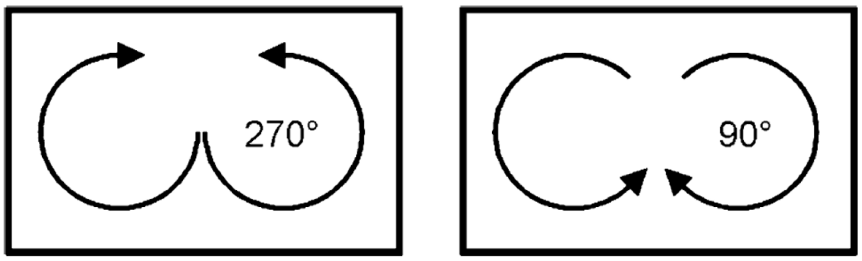

Figure 3.6: Standard (left) and changed (right) rotational direction for FZG test rig

Immersion depth

Otto [**42**] investigated the oil immersion depth influence in a sump lubricated gearbox. Three different oil depth configurations (3·module at pinion, 3·module at gear, 1·module at gear) were tested and the respective oil churning to the oil at shaft center configuration compared. It was observed that reducing the immersion depth leads to a corresponding decrease in churning losses (more than 50% reduction was found when immersion depth is reduced from center line to 3 times module of the gear). One significant drawback of reducing the immersion depth is the potential compromise of the cooling performance. When the gears are not sufficiently immersed, the lubricant cannot effectively dissipate the heat generated during operation. This issue becomes particularly critical at high speeds and under heavy loads, where the heat generated can be substantial. In the worst-case scenario, the pinion bulk may reach temperatures high enough to cause the material to temper, leading to a loss of its mechanical properties and potentially resulting in failure.

Oil viscosity

Terekhov [**43**], Michaelis [**44**] and Mauz [**28**] investigated the influence of oil viscosity on churning losses. Terekhov and Michaelis documented that increasing oil viscosity led to an elevation in churning losses. Terekhov specifically noted this trend with high viscosity oils, whereas Michaelis observed it irrespective of the oil type. Additionally,

Mauz highlighted a correlation with operating speed: at lower speeds, higher viscosity oils amplified churning losses, whereas at higher speeds, an increase in oil viscosity actually reduced churning losses. In order to optimize lubrication and efficiency, the *Computational Fluid Dynamics* (CFD) method can be employed during the initial phases of transmission design, this approach allows for the visualization and analysis of oil flow within a gearbox in a more flexible way compared to traditional methods involving transparent gearbox designs and direct measurements. In this specific context, it is noteworthy to discuss the research carried out by Liu and colleagues [**27**], who examined the no-load power losses in the FZG rig using a CFD model based on the finite volume method. Their study focused on investigating how oil viscosity and circumferential speed impact the oil flow characteristics of different lubricants (specifically FVA2, FVA3, and FVA4) during a FZG test. They compared the results from their CFD simulations with high-speed camera recordings of real-world FZG tests (Figure 3.7). This comparative analysis provided insights into the accuracy and reliability of using CFD simulations to predict and analyze oil flow behaviors within gearbox testing environments.

Housing dimension

The research conducted by Changenet and Velex [**45**] indicated that gear churning losses in dip-lubricated gearboxes are significantly influenced by the dimensions of the housing. They introduced flanges and deflectors around the gears in both axial and radial directions to mitigate these losses (Figure 3.8). It was found that adjusting the oil volume while maintaining a constant immersion depth can effectively reduce gear churning losses. Specifically, at higher speeds, reducing the lubricant volume tends to increase churning losses, although this behaviour is no longer visible at lower speeds, as declared by the authors. Nevertheless, it is important to emphasize that in practical applications, within a fixed transmission design context, variations in oil volume influences variation in immersion depth. Consequently, contrary to initial expectations, decreasing lubricant volume does not necessarily result in increased churning losses due to these interrelated factors.
They also conducted an analysis of both the influence of axial clearance between the gear face and the gearbox wall, and the effect of radial clearance between the gear tip radius and a deflector. These components were specifically introduced for the purpose of the experiments.
Differently from Figure 3.8, the test was carried out with a single pinion. For this particular configuration, it was observed that a reduction in axial clearance led to a decrease in gear churning losses, highlights the importance of minimizing the distance

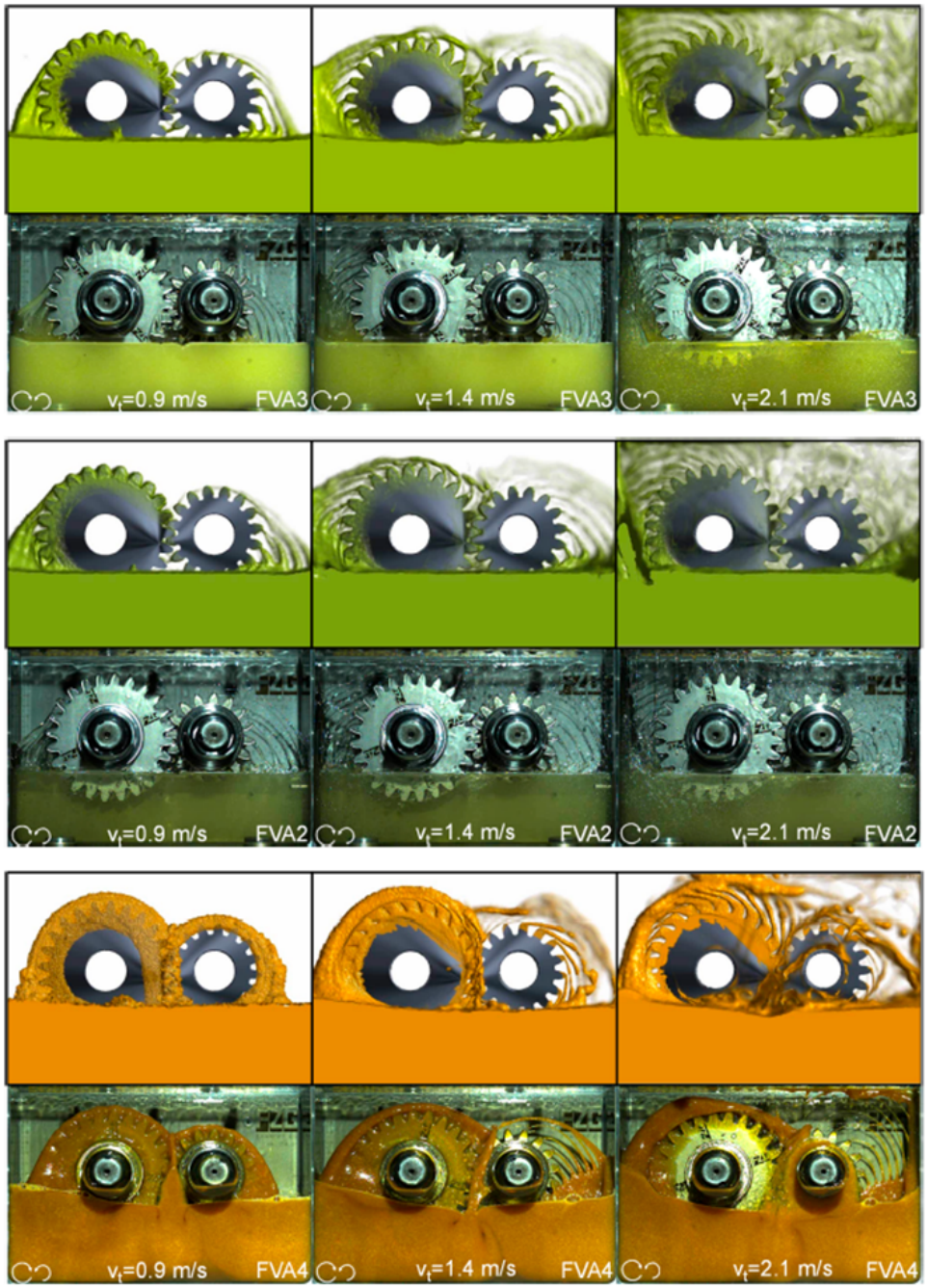

Figure 3.7: Comparison between simulated oil distribution and high speed camera recordings for FVA3, FVA2 and FVA4 at oil temperature of 40°C and for different circumferential speeds of 0.9; 1.4; 2.1 m/s. [**27**]

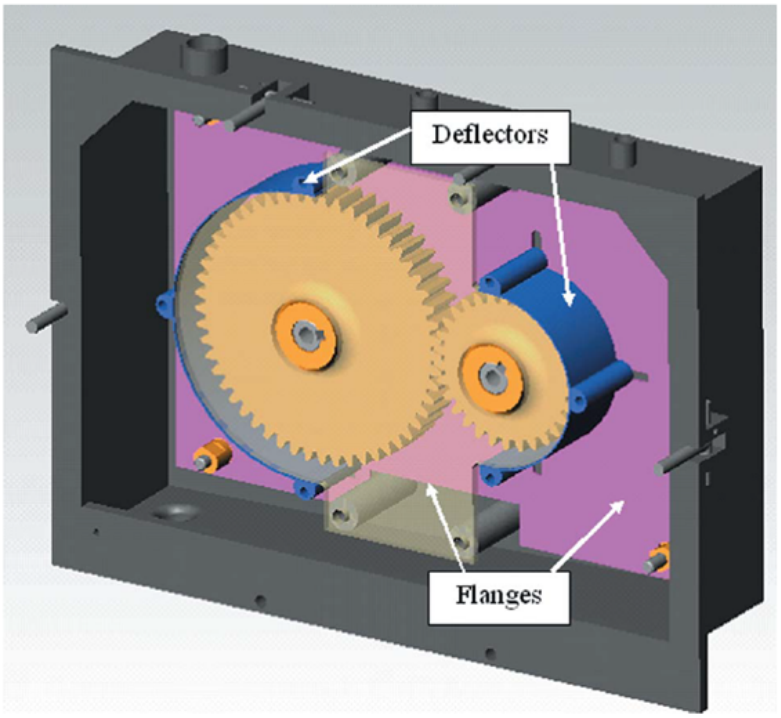

Figure 3.8: Housing shape modifications [**45**]

between the gear face and the gearbox wall to enhance efficiency. On the other hand, the introduction of radial deflectors, which were intended to guide the lubricant flow around the gear tip radius, had a negligible effect on reducing churning losses. This suggests that while axial clearance is a critical factor, radial deflectors do not contribute substantially to mitigating losses in this setup.

3.3.2 Gear losses - load dependent

Load gear losses result from sliding and rolling of the tooth flanks, of the wheel and the pinion, against each other on the path of contact (Figure 3.9).

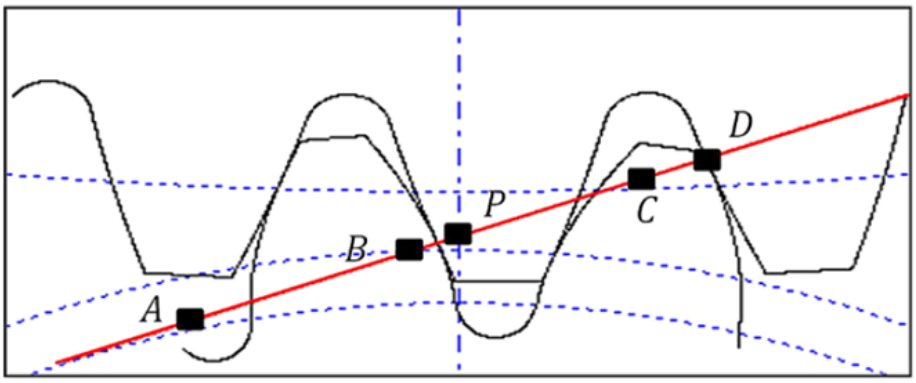

Figure 3.9: Path of contact [**35**]

Power losses resulting from gear meshing P_{VZP} are calculated as follows:

$$P_{VZP} = F_R(x) \cdot V_{rel}(x)$$

Where x is a generic point along the path of contact.

The friction force $F_R(x)$ can be expressed as the product F_N multiplied by $\mu(x)$:

$$P_{VZP} = F_N(x) \cdot \mu(x) \cdot V_{rel}(x)$$

By multiplying $\frac{F_N(x)}{F_{Nmax}} \cdot \frac{V}{V} = 1$ with the previous equation, it becomes:

$$P_{VZP} = F_{Nmax} \cdot \frac{F_N(x)}{F_{Nmax}} \cdot \mu(x) \cdot V \cdot \frac{V_g(x)}{V}$$

Where $V_g(x)$ is the sliding velocity and V the pitch line velocity.

Figure 3.10 shows the trend of $\frac{F_N(x)}{F_{Nmax}}$, $\mu(x)$ and $\frac{V_g(x)}{V}$, factors characterizing the load dependent gear losses, along the path of contact of Figure 3.9.

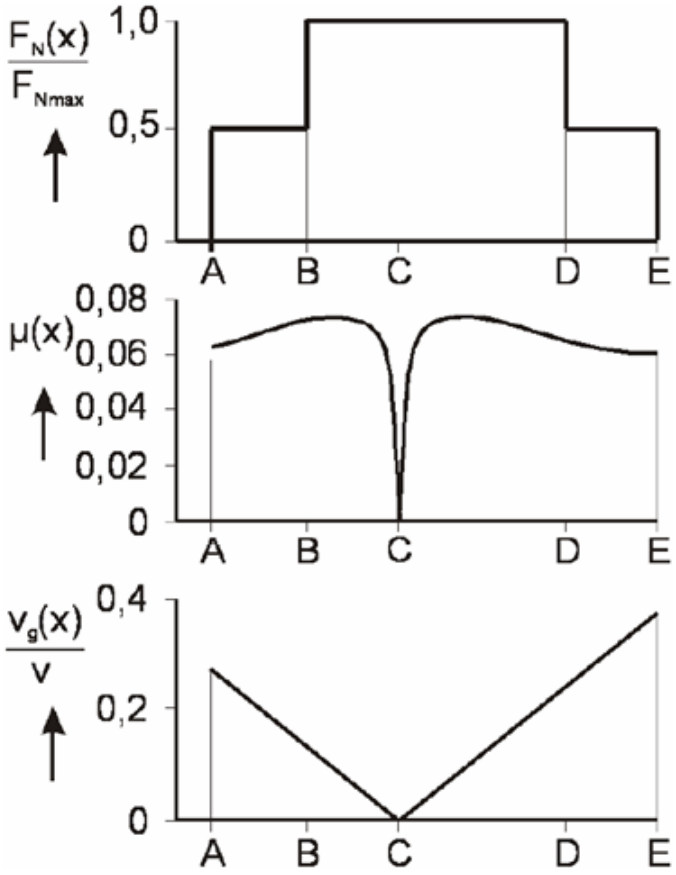

Figure 3.10: Load, friction coefficient and sliding speed along path of contact [**46**].

Gear geometry

One of the factors influencing the load gear losses is the relative velocity of teeth in mesh: a reduction of the sliding velocity contact path, concentrated around the pitch point with zero sliding (visible in Figure 3.10), reduces the mesh losses. Hoehn et al. [**47**] compared standard FZG type C gears and low loss gears, with minimum sliding speed (Figure 3.11), at different operating conditions. The tests demonstrate a reduction in total gearbox power losses ranging from 75%, at low speeds, to 35%, at high speeds, when employing alternative low-loss gear designs, featuring smaller module sizes and transverse contact ratios compared to standard designs. Additionally, they noted decreased energy losses associated with the use of an increased pressure angle. The same conclusion is present in [**48**], where authors, following

a comparison of various gear geometries, observed reduced energy losses associated with smaller module sizes and shorter gear teeth geometries.

Figure 3.11: Geometry of standard C type gears (left) and lowloss gears (right) [**46**].

Surface roughness

The benefits of superfinishing on frictional losses were discussed in [**49**]. Britton et al. investigated the impact of surface finishing on frictional losses, revealing a reduction of approximately 31% (at the highest loads and speeds) with superfinished gear teeth, with a roughness average (Ra) of 0.05 µm compared to ground gear teeth with Ra=0.4 µm. The advantages of superfinishing become particularly pronounced at elevated oil temperatures. Furthermore, they noted a decrease in tooth temperature across the entire operating range.

Coatings

While literature focuses on fine surfaces and the use of low-viscosity lubricants as a way to enhance gearbox efficiency and minimize churning losses, Sjöberg [**50**] proposed an alternative approach. He noticed that the employment of a manganese phosphate coating to gear surfaces can lead to reducing the coefficient of friction during sliding. This coating not only lowers the risk of scuffing but also, according to [**51**], allows for a substantial reduction in gearbox lubricant requirements. Thus,

coatings adoption on gears offer the dual benefit of improving frictional characteristics and optimizing lubrication management within the gearbox system.

Oil type and additives

As previously seen, a critical factor influencing load-dependent gear losses is the coefficient of friction between the gears, which directly impacts gearbox efficiency. In the field of boundary lubrication the use of additives can be beneficial. According to the tests conducted by Doleschel [**52**], a reduction in the boundary friction coefficient was observed under conditions of low speeds, high temperatures, and high pressures when utilizing soluble molybdenum-thio-phosphate additives. Conversely, under mixed and elastohydrodynamic (EHL) lubricationoperating conditions, significant variability based on the type of base oil used was found [**53**]. Various base oil types with different viscosity grades were evaluated in a FZG-FVA efficiency test. A potential reduction of friction in gear mesh is observed compared to lubrication with a mineral oil case, approximately 10-20% with a polyalphaolefin plus ester type base oil, around 20-30% with a polyglycol type base oil, and up to 50% when using a polyether type base oil.

3.3.3 Bearing losses - load independent and dependent

Several factors influence no-load and load dependent bearing losses, among the various factors, no-load losses depend on the bearing type, size, arrangement, lubricant viscosity, and supply characteristics. On the other hand, load-dependent bearing losses are influenced by factors such as bearing type, size, lubricant type, applied load, and sliding conditions. These variables collectively determine the efficiency and performance of bearings within mechanical systems, emphasizing the importance of selecting appropriate bearings and optimizing lubrication to minimize energy losses across varying operational conditions.

Bearing type

In [**54**] a no-load dependent bearing losses comparison among different types of bearings with the same load capacity (C=20kN) and the same utilization ratio (P0/C=0,1) is carried out, the results are visible in Figure 3.12. Cylindrical roller bearings exhibit the minimal power loss compared to other types of radial bearings. Similarly, taper roller bearings also show low power losses, however, this advantage is observed in unloaded bearing arrangements. In practical applications involving

cross-loading configurations, such as those requiring axial preloading, taper roller bearings experience significantly increased no-load losses.

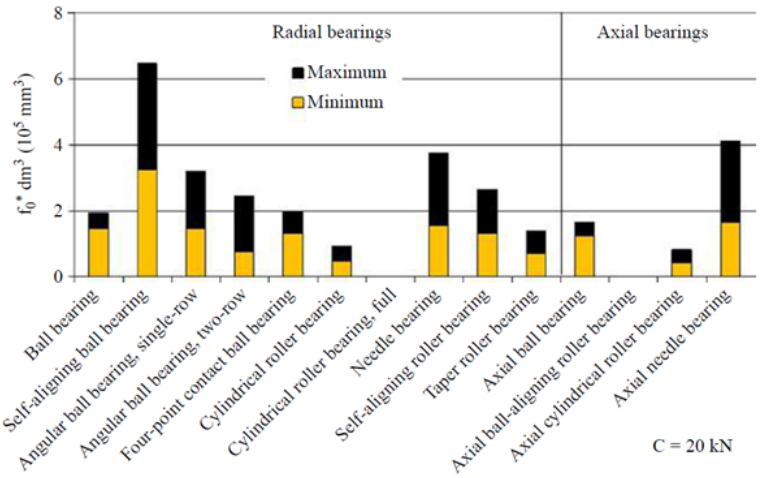

Figure 3.12: Influence of bearing type on no-load losses [**54**].

A similar comparison can be made for load-dependent losses 3.13. In this case cylindrical roller bearings consistently exhibit the lowest radial power losses among radial bearing types. Taper roller bearings also demonstrate low power losses under load conditions, primarily attributed to their small diameter. This comparative analysis underscores the advantageous performance characteristics of both cylindrical and taper roller bearings in different load scenarios, emphasizing their suitability for various mechanical applications where minimizing power losses is critical.

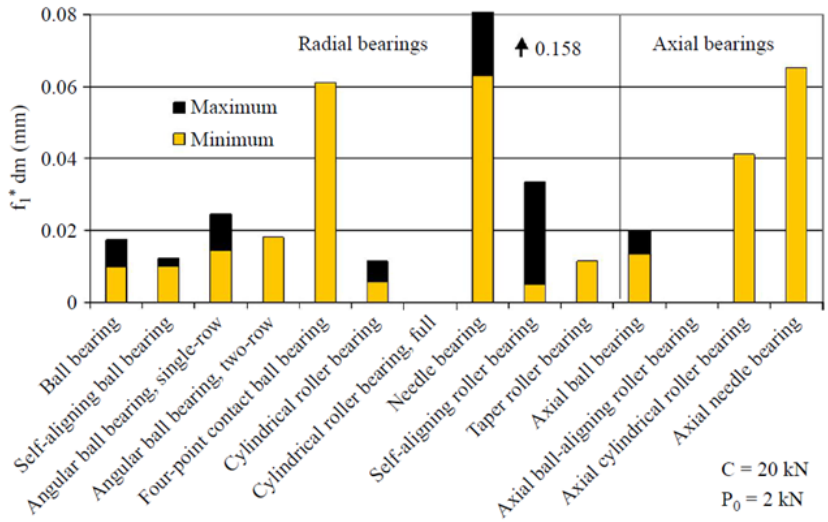

Figure 3.13: Influence of bearing type on load losses [**54**].

Arrangement

Another factor influencing bearing power losses is the arrangement of bearings within the transmission system. Regarding this topic, it is noteworthy to mention the work done by Hoehn et al. [**46**], who proposed an alternative bearing solution for a manual transmission. Preloaded cross locating taper bearings of the original design are substituted with locating four-point contact ball bearings and non-locating cylindrical roller bearings, on the gearbox shafts, and cross locating angular contact ball bearings of the final drive wheel for the alternative proposed design (Figure 3.14). Bearing losses were calculated according the SKF approach: for medium load and medium speed conditions at 40°C oil temperature, a reduction of the bearing losses of more than 50% was found for the alternative design. At high gear oil temperature (90°C) the improvement is reduced at around 20% because the preload is reduced almost to zero.

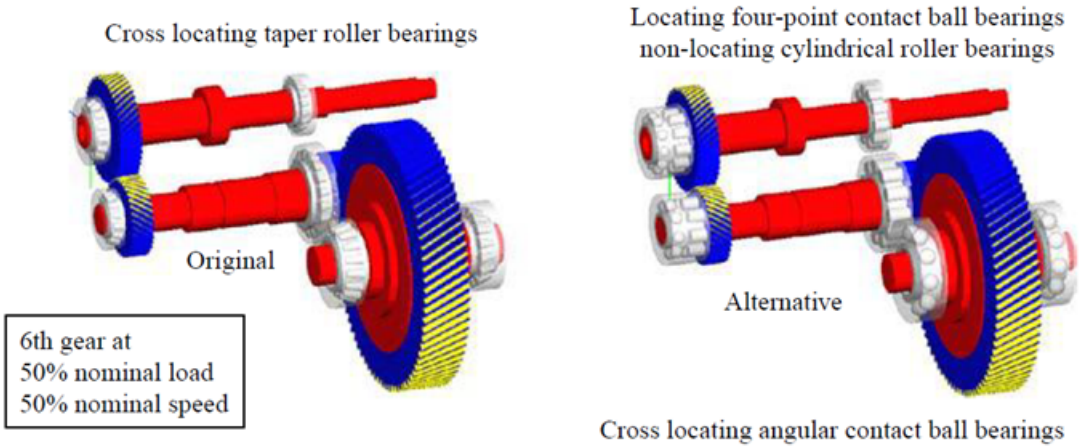

Figure 3.14: Alternative bearing design in a manual transmission [**55**].

Real measurements were conducted by von Petery [**56**] to compare bearing losses in two different designs of a BMW rear axle. The study examined both the original bearing design, which featured a cross-locating taper roller bearings arrangement, and an alternative solution employing a cross-locating arrangement of double- and single-row angular ball bearings (Figure 3.15).

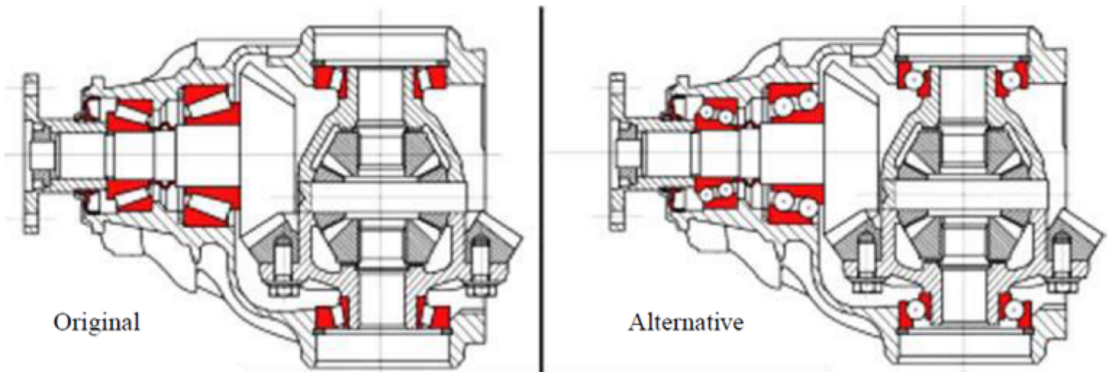

Figure 3.15: Bearing designs for a BMW rear axle [**56**].

Chapter 4

Methodology

In this Chapter, a detailed description of the methodologies and tools employed in the execution of this research is provided. The objective of this thesis is to perform a predictive analysis to calculate the power losses within the innovative 2-speed transmission by Dana, which will be used in electric vehicles. At the time this thesis was written, the transmission under study had not yet entered production and was in the final stages of its development. The analysis is conducted on a model that utilizes the formulas specified in the ISO 14179-2 standard for all contributions to power loss, with the exception of the friction clutch loss data, which was supplied directly by the manufacturer of the component.
The entirety of this research was conducted using the Matlab/Simulink/Simscape environment. The use of Matlab proved to be indispensable for the implementation of the equations and control mechanisms, as well as for the post-processing of the resulting data. The integrated Simulink/Simscape environment facilitated the modeling of the entire transmission system model and a corresponding vehicle model through the use of predefined blocks, including the management of gear shift.
Two distinct Simulink/Simscape models have been developed as part of this research.

The first model is designed to represent the architecture of the transmission system, serving as a crucial tool for deriving detailed information concerning the transmission's efficiency under various operating conditions. This model plays a fundamental role in understanding how different factors influence the overall performance and efficiency of the transmission.

The second model has been created with the specific purpose of performing comprehensive vehicle simulations across various driving cycles. It is an evolution of the one previously utilized in [**59**], offering enhanced capabilities in the evaluation of vehicle performance, in terms of efficiency analysis, over diverse driving scenarios.

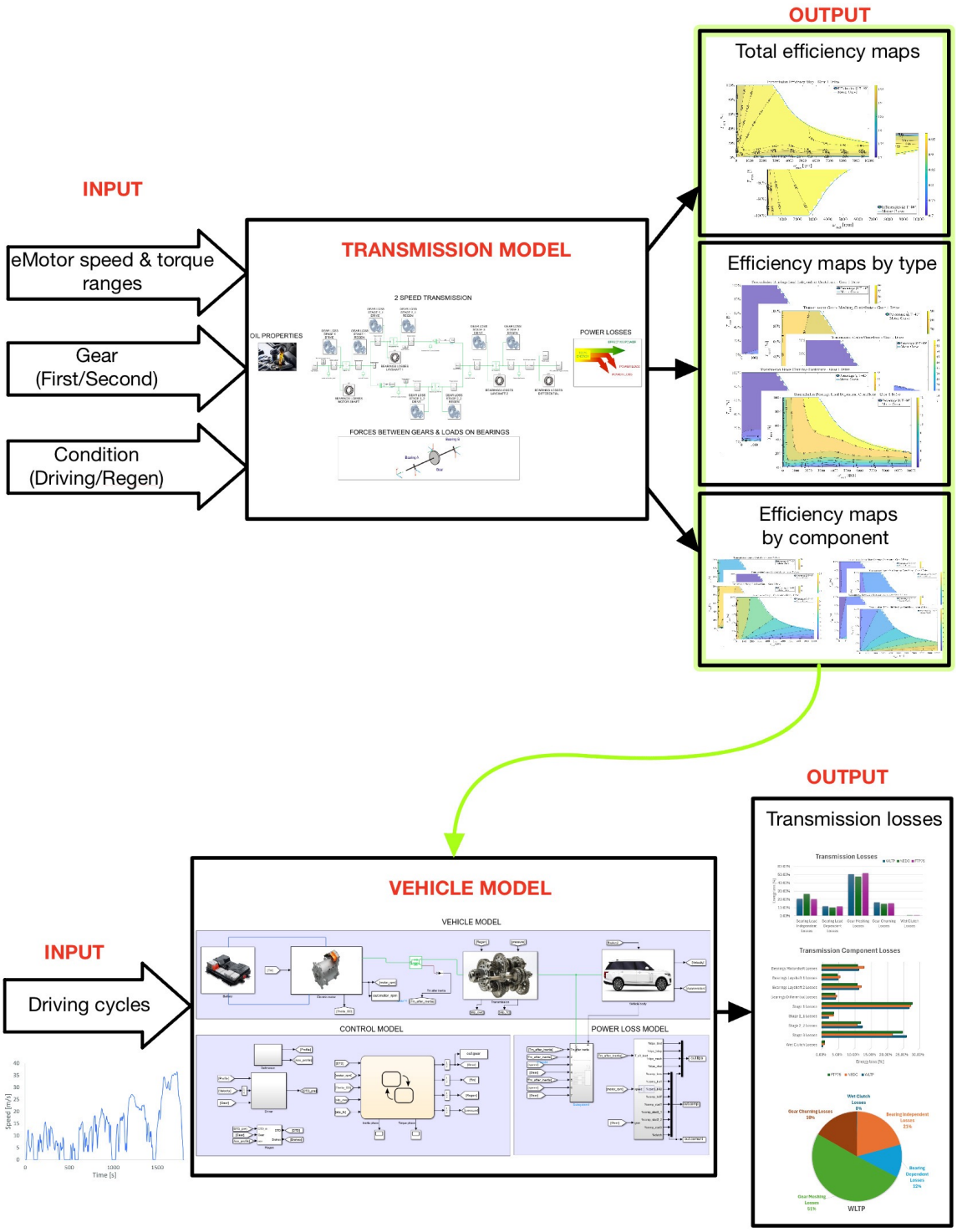

Figure 4.1: Transmission and vehicle models

In the following sections, each of these models will be presented in greater detail, aiming to offer a clear understanding of their roles and contributions to the final objectives of this research.

4.1 Transmission model

As an initial step, a model representing the Dana 2-speed transmission system (Figure 4.2) was created within the Simulink/Simscape environment. The main purpose of this model is to generate efficiency maps, both overall efficiency maps and efficiency maps which express the percentage contribution of each type of loss relative to the total transmission loss, as functions of motor torque and speed. Since the maps are intended to be obtained at constant gear, this transmission model is designed to operate exclusively in either first or second gear, without considering the dynamics of gear shifting. This approach has allowed for a simplified modeling process for certain components that would otherwise require more detailed attention due to their contributions during gear changes.

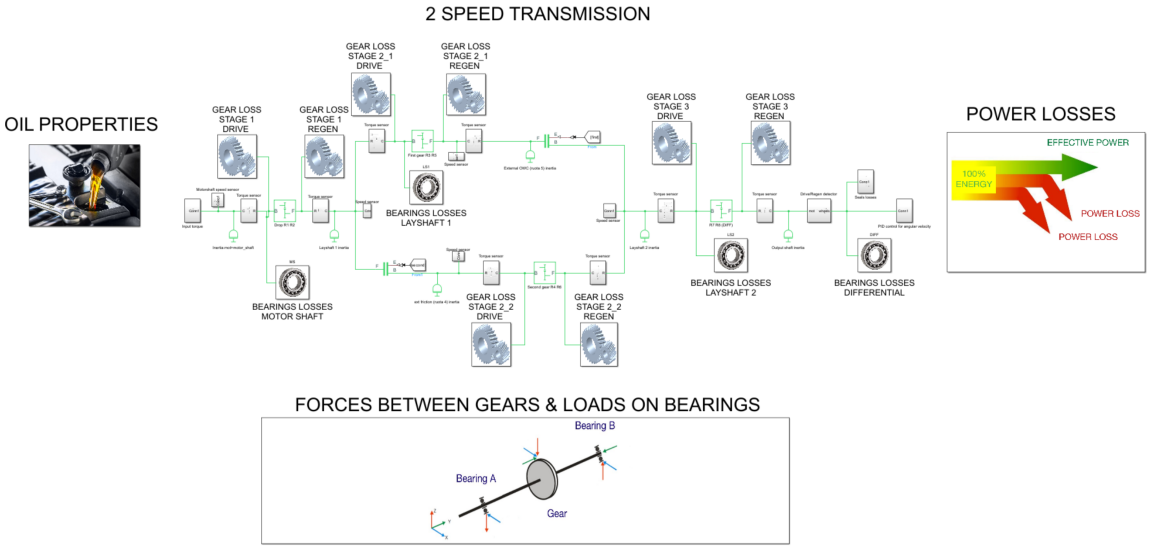

Figure 4.2: Transmission complete model

The operating logic of the transmission model is illustrated in the flowchart in Figure 4.3. The purpose of the model is to create transmission efficiency maps, which will subsequently be implemented in the second model, the vehicle model, to conduct simulations on driving cycles. The transmission model operates based on a Matlab script, within which the model parameters are set. The Matlab script also defines the main simulation parameters, such as the engaged gear, the transmission operating condition (drive or regen) and, through a *for loop*, it provides the input torques and speeds for the transmission model created in Simulink.

Transmission model flowchart

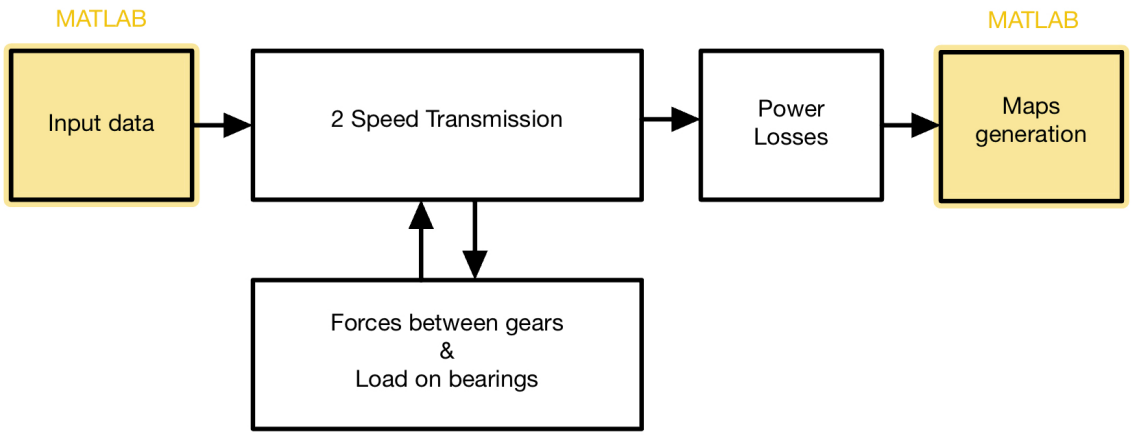

Figure 4.3: Flowchart of the Transmission model

The Simulink model operates the transmission in steady state at the torque and speed values determined by the Matlab script. The torque values are imposed on the transmission model via a block called *Ideal Torque Source*, positioned upstream of the transmission system (Figure 4.4).

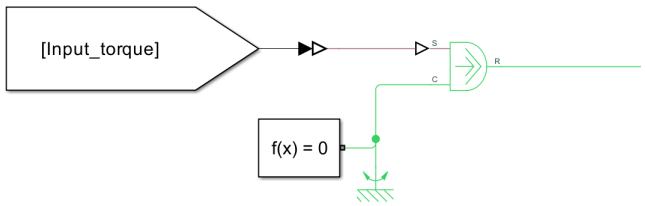

Figure 4.4: Torque input

The speed values, on the other hand, are controlled through a PID controller that takes as input the difference between the angular speed set by the Matlab script and the speed measured through the *Ideal Rotational Motion Sensor* block. The output value is then provided to the transmission model via a block called *Ideal Angular Velocity Source*, shown in Figure 4.5.

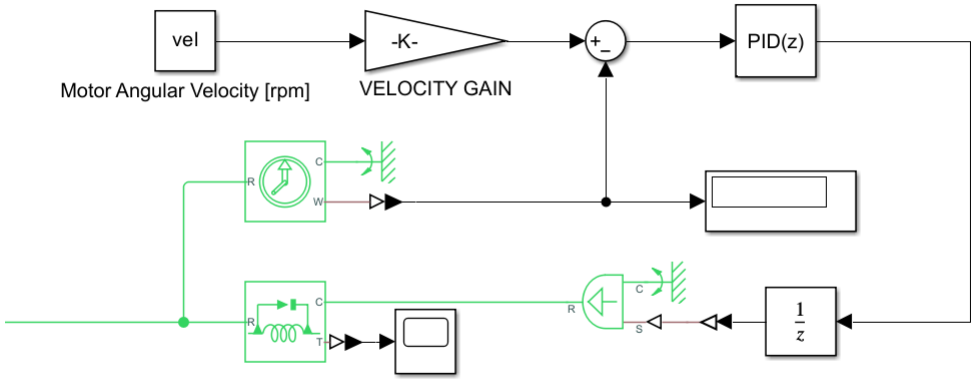

Figure 4.5: Speed input

These blocks are included in the "2 Speed Transmission" submodel. Within it, *Ideal Torque Sensors* are positioned, they communicate with the "Forces between gears & Load on bearings" submodel. The measured torque is used to calculate the forces exchanged between the gears in the three spatial directions and to calculate the forces acting on the bearings. These forces are fed back into the "2 Speed Transmission" submodel, where specific blocks calculate the system's power losses. These losses are

introduced into the model as resistant torques, reducing the output power compared to that initially received from the motor. Subsequently, the losses values are sent to the "Power Losses" block, where the total transmission losses are calculated for each input torque and speed value. Additionally, this submodel splits the total losses based on the type or based on the components generating them.

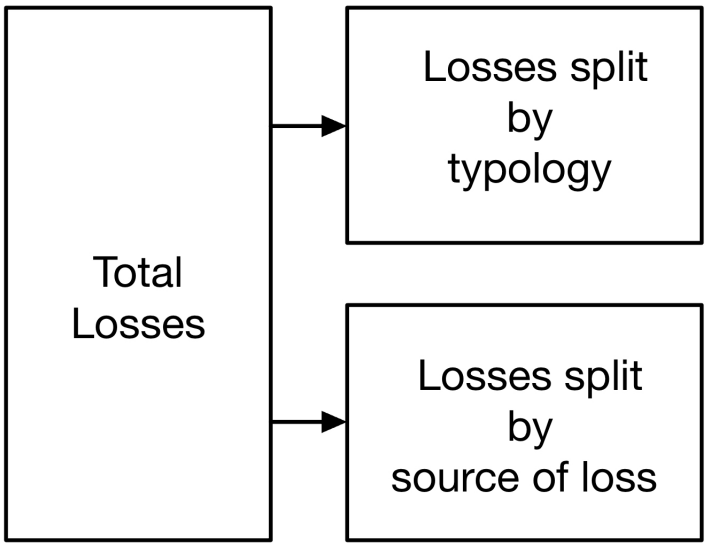

Figure 4.6: Power Losses submodel logic

For each pair of motor speed and torque values, the computed losses are sent back to the Matlab script, which stores them in a matrix before proceeding to the next step of the *for loop* with new torque and speed values, in order to complete the range of torques and speeds that the motor can provide.
Finally, the Matlab file post-processes the obtained matrices to generate the transmission efficiency maps, which will then be analyzed in the Results Chapter (Chapter 5). This step involves refining and organizing the data to ensure accuracy and clarity in the efficiency maps. These maps are crucial as they provide a visual representation of the transmission's efficiency performance across different operating conditions, highlighting areas of optimal efficiency.

It has been identified that the main submodel is the "2 Speed Transmission" submodel, and alongside this submodel, several "satellite environments" were created to support the main model by calculating the necessary factors for determining power losses.

Specifically, these submodels are:

- The submodel dedicated to calculating the loads acting on the transmission bearings and loads exchanged between the different gear stages of the transmission, which is essential for determining load-dependent losses
- The submodel for calculating the properties of the lubricant
- The submodel focused on calculating the actual losses themselves

In the following paragraphs, the aforementioned models will be analyzed.

4.1.1 Transmission submodel

The Dana 2-speed transmission was modeled using blocks from the Simulink/Simscape library. Two possible power flows are clearly visible in Figure 4.7. The upper branch represents the power flow path when the transmission operates in first gear, while the lower branch represents the path for second gear. The model aims to create efficiency maps given a specific gear, therefore it does not need to perform gear shifts as it operates either in first or second gear exclusively. Gear selection is controlled by a dedicated flag signal. When set to 1, it allows power flow only through the upper branch. When set to 2, the flag signal engages the friction clutch, allowing power flow solely through the lower branch.
The loss contributions from gears and bearings are accounted for in dedicated blocks. The "Gear loss" blocks calculate the power losses that occur in the gears whereas the "Bearing loss" blocks account for the losses that occur in the bearings. Within these blocks, the equations from the ISO 14179-2 standard are implemented to calculate both load-dependent and load-independent power losses for the gears and bearings. The inputs for these blocks include data related to the geometry of the gears and bearings, lubricant properties such as density and viscosity, oil level for the gears, and information signals originated in the subsystem "forces between gears & loads on bearings", which is analyzed below.
The model also includes angular speed and torque sensors, which are useful for blocks responsible for calculating losses and for the "Forces between gears & Loads on bearings" subsystem. The loss contributions calculated by the dedicated blocks are then fed into the model as torque signals. The resisting torque accounts for the operating conditions of the transmission (driving or regeneration) by adjusting the sign of the torque signal accordingly.

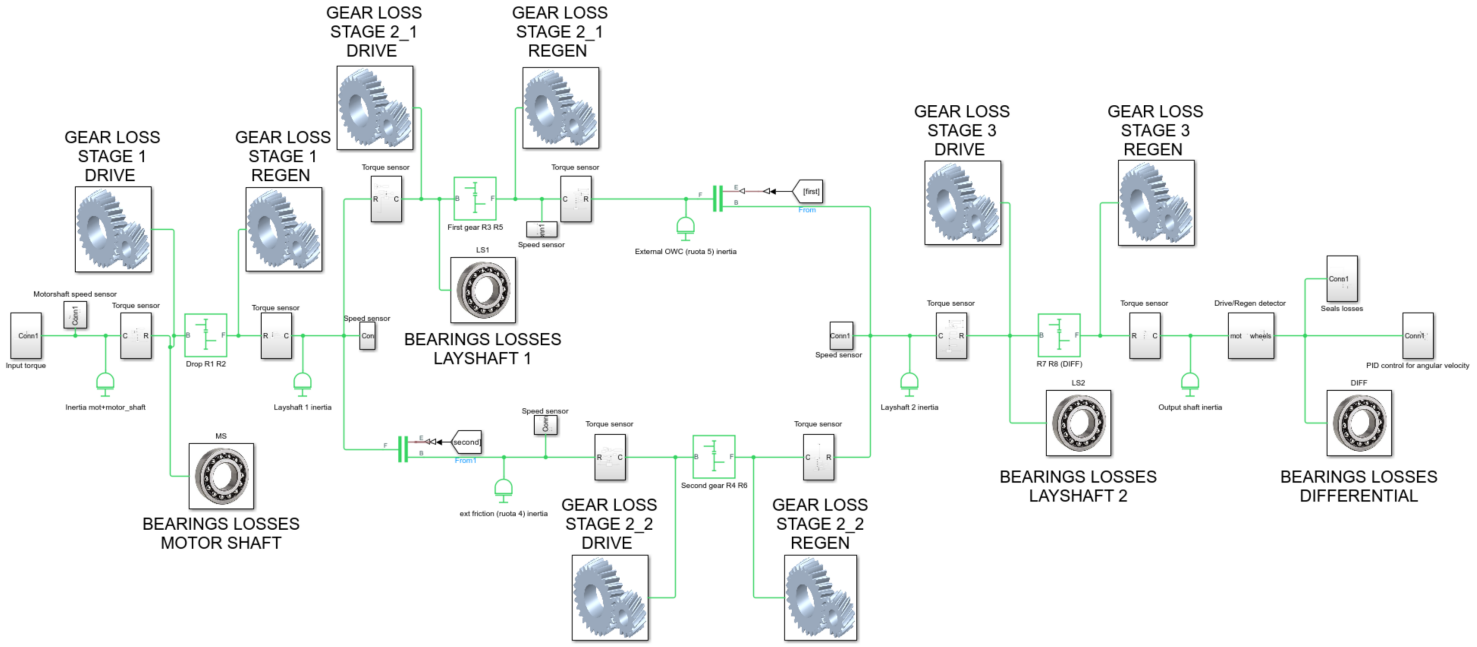

Figure 4.7: Transmission submodel

4.1.2 Forces between gears & Loads on bearings submodel

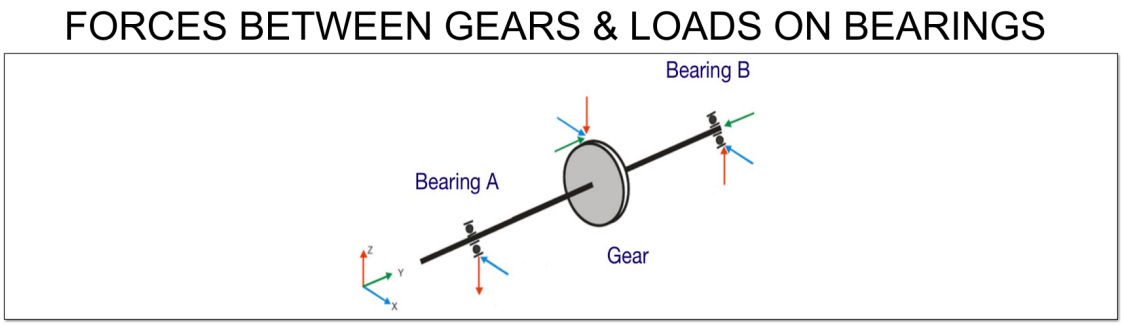

Figure 4.8: Forces between gears & Load on bearings submodel

The "Forces between gears & Loads on bearings" submodel, visible in Figure 4.9, represents the foundational starting point for enabling the comprehensive transmission system model to execute all necessary calculations required for generating transmission efficiency maps. Its purpose is to calculate the forces exchanged between the various reduction stages of the transmission, as well as to determine the loads acting on the bearings, as the motor input torque and angular velocity conditions vary.

The initial step in this process was to conduct a thorough study of the transmission's geometry. Given that not all the transmission shafts are aligned on the same plane, it was necessary to reference the local forces, which were obtained through free-body diagrams, to a global coordinate system, through the use of rotation matrices. The translation to a global reference frame ensured that forces and moments of different shafts were calculated using equilibrium equations referenced to the same global coordinate system. However, to ensure data confidentiality, the specific layout of the transmission, including the precise inclination angles between the various shafts, cannot be disclosed in this document.
As shown in Figure 4.9, the "Forces between gears & Load on bearings" submodel is composed of four additional submodels, each of which accounts for the corresponding transmission shaft and calculates the interactions associated with it. The submodels, presented below, are named according to the shaft they reference: motor shaft, layshaft 1, layshaft 2, and differential shaft.

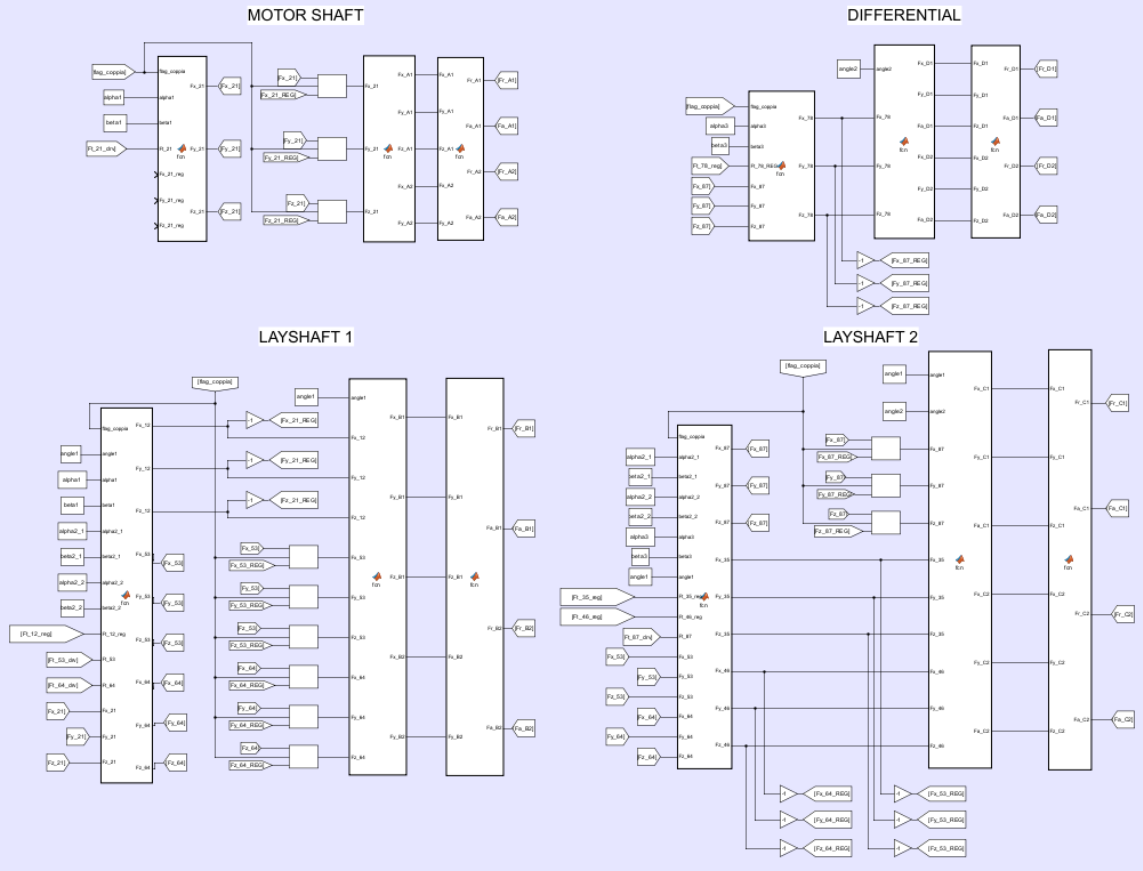

Figure 4.9: Forces between gears & Load on bearings submodel

Motor shaft

This submodel is dedicated to calculating the forces and moments of components interacting with the motor shaft. It is of fundamental importance since, under drive conditions (when the power from the motor to the wheels is positive), it is the starting point for determining all the forces and moments acting on the rest of the transmission system. Among the input signals are those concerning the geometric characteristics of the transmission, which are crucial for calculating the force components in the global coordinate system. Additionally, a torque flag signal is an input to this model too, and it is used to determine whether the transmission is in drive condition (positive power from the motor to the wheels) or regen condition (positive power from the wheels to the motor) at any given moment.

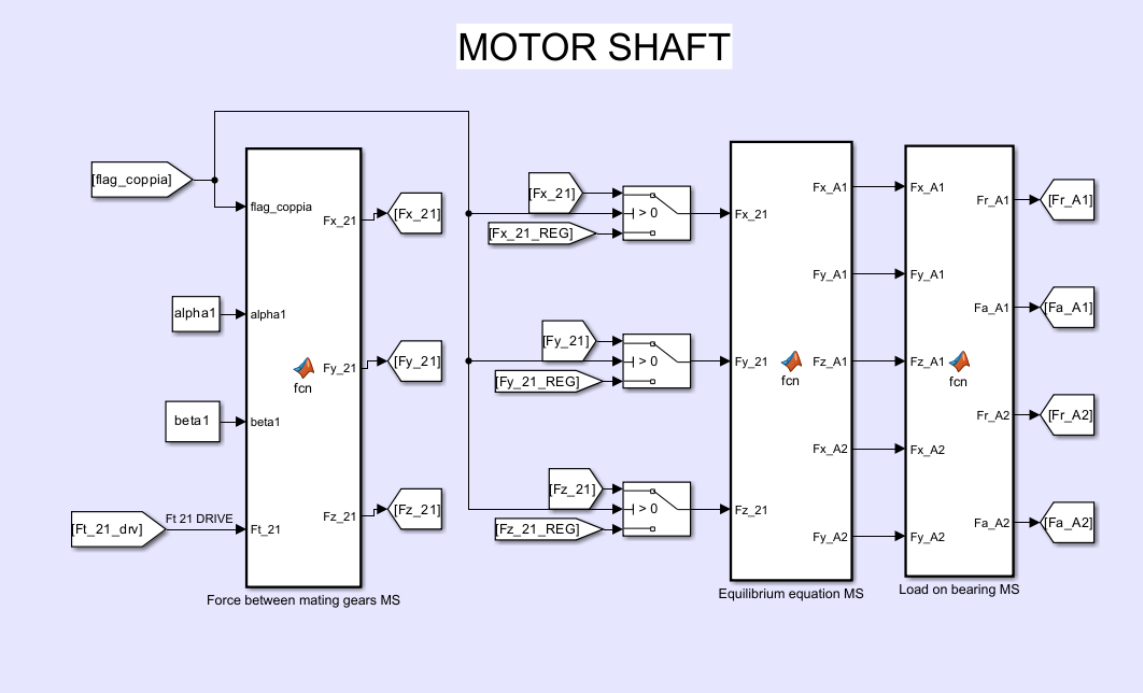

Figure 4.10: Motor shaft computation

Starting with the torque generated by the motor and acting on the rotor, which is fixed to the motor shaft, it is possible to establish the force exchanged in the first stage by knowing the geometry data of the gears. This force is then decomposed into its axial, radial, and tangential components, relative to the local coordinate system. The Matlab first block in Figure 4.10 includes both the equation for calculating the exchanged forces and rotation matrices that allow the axial, radial, and tangential components (referred to the local coordinate system of the motor shaft) to be expressed in the global coordinate system of the transmission. The following block contains the equilibrium equations. It takes as input the forces exchanged between the gears from the previous block and computes the reaction forces. The output from this block is utilized by the subsequent block, tasked with calculating the loads acting on the bearings. This block incorporates equations provided by the bearing manufacturers, which vary based on the type and size of the bearings used, whose specifications cannot be disclosed due to confidentiality reasons.

Layshaft 1

Similarly to what was seen for the motor shaft submodel, the submodel used for the layshaft 1 (Figure 4.11) also contains three main blocks. However, unlike the motor shaft, layshaft 1 exchanges forces with two shafts through three gears. As a result, the blocks in this model involve more variables compared to the previous model. In the first block, the forces exchanged between the gears and the two shafts (motor shaft and layshaft 1) are projected onto the global coordinate system. The second block uses the equilibrium equations to calculate the reaction forces, which are then taken as input by the subsequent block to determine the loads on the bearings.

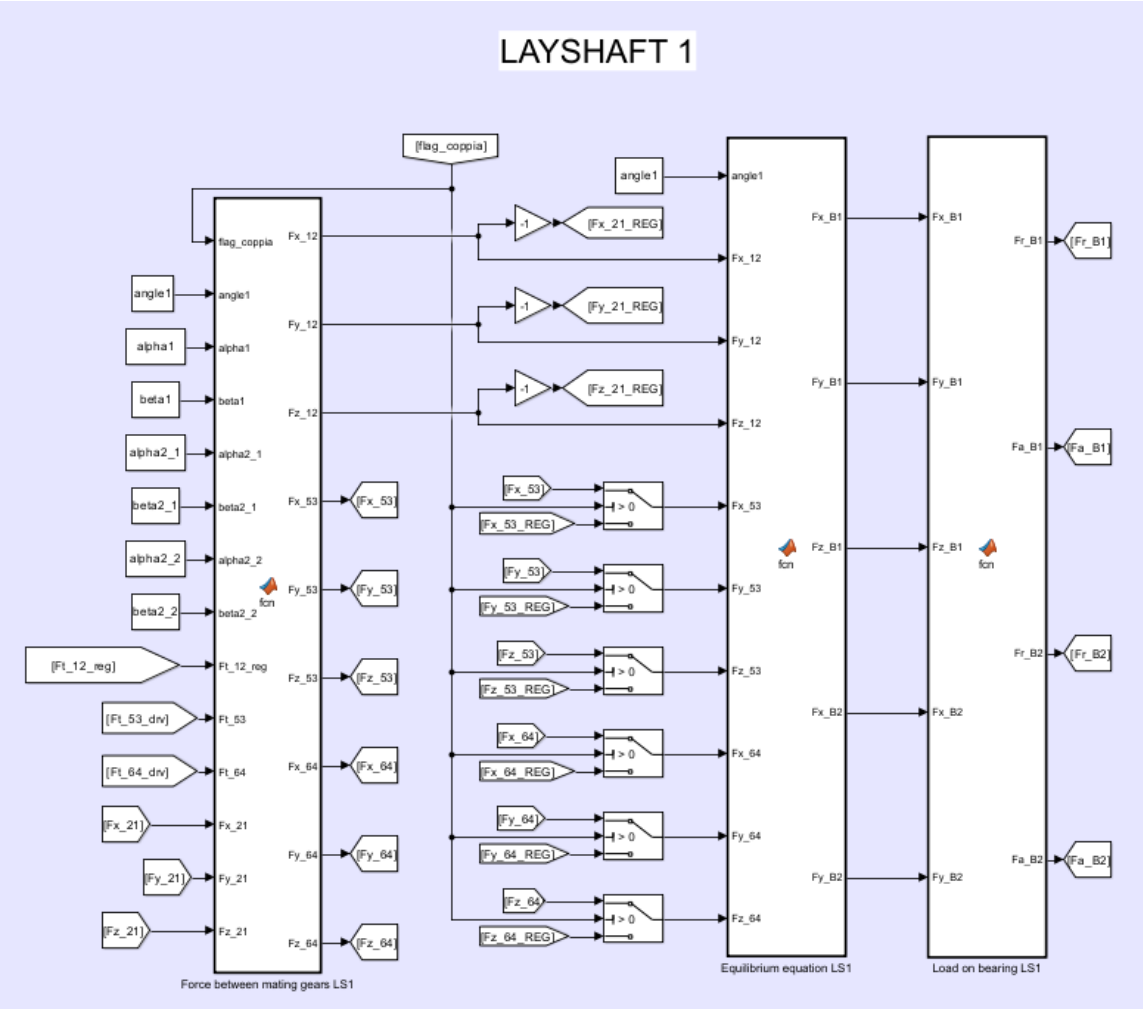

Figure 4.11: Layshaft 1 computation

Layshaft 2

The layshaft 2 submodel operates using the same procedure as the layshaft 1 submodel, as shown below.

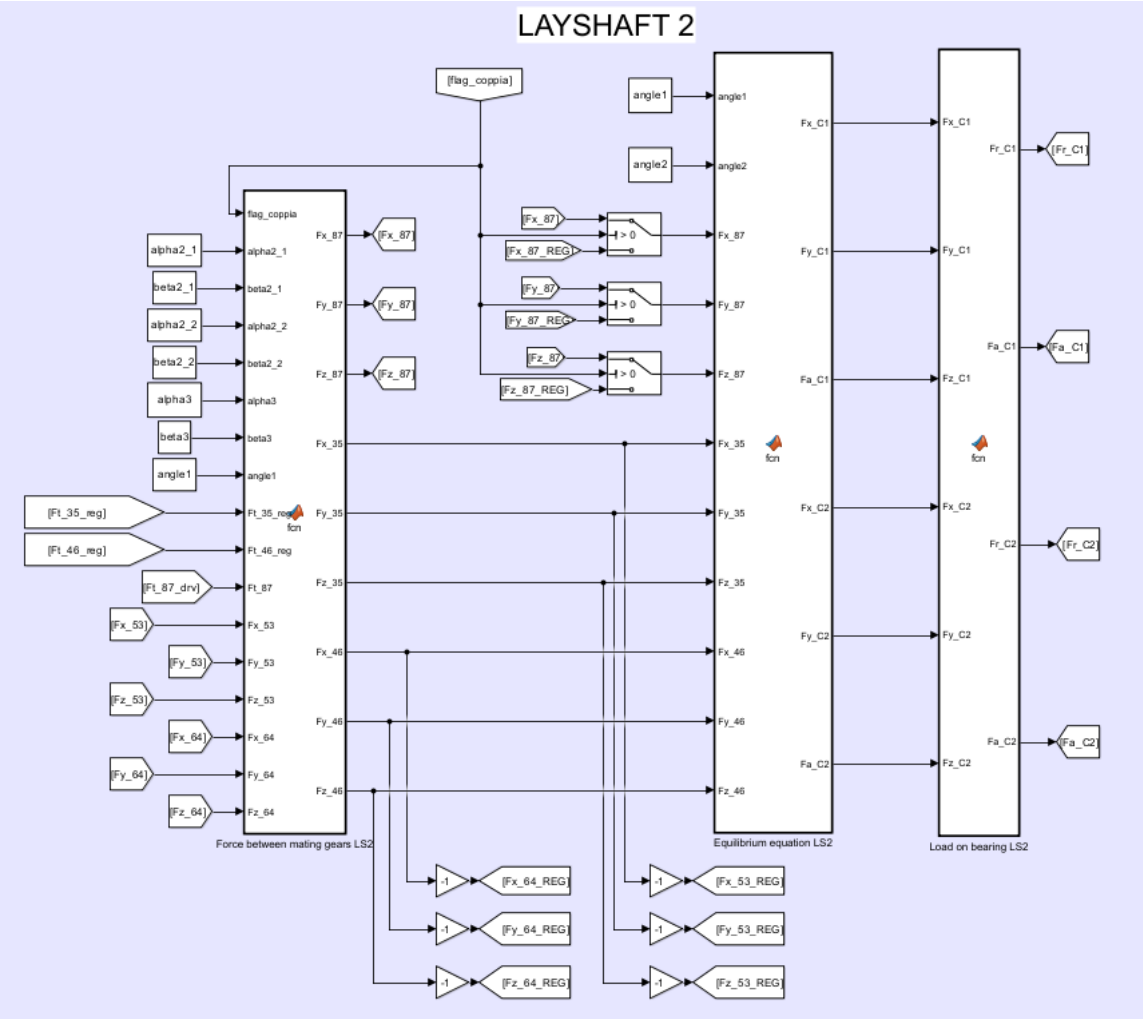

Figure 4.12: Layshaft 2 computation

Differential

As the final step, the differential submodel calculates the output forces of the transmission under drive conditions. If the transmission is operating in regeneration mode, the submodel becomes the first step in calculating the forces, as in this case, the power flows from the wheels to the electric motor. Similar to the previous models, the last block is dedicated to calculating the forces acting on the bearings, specifically those of the differential shaft.

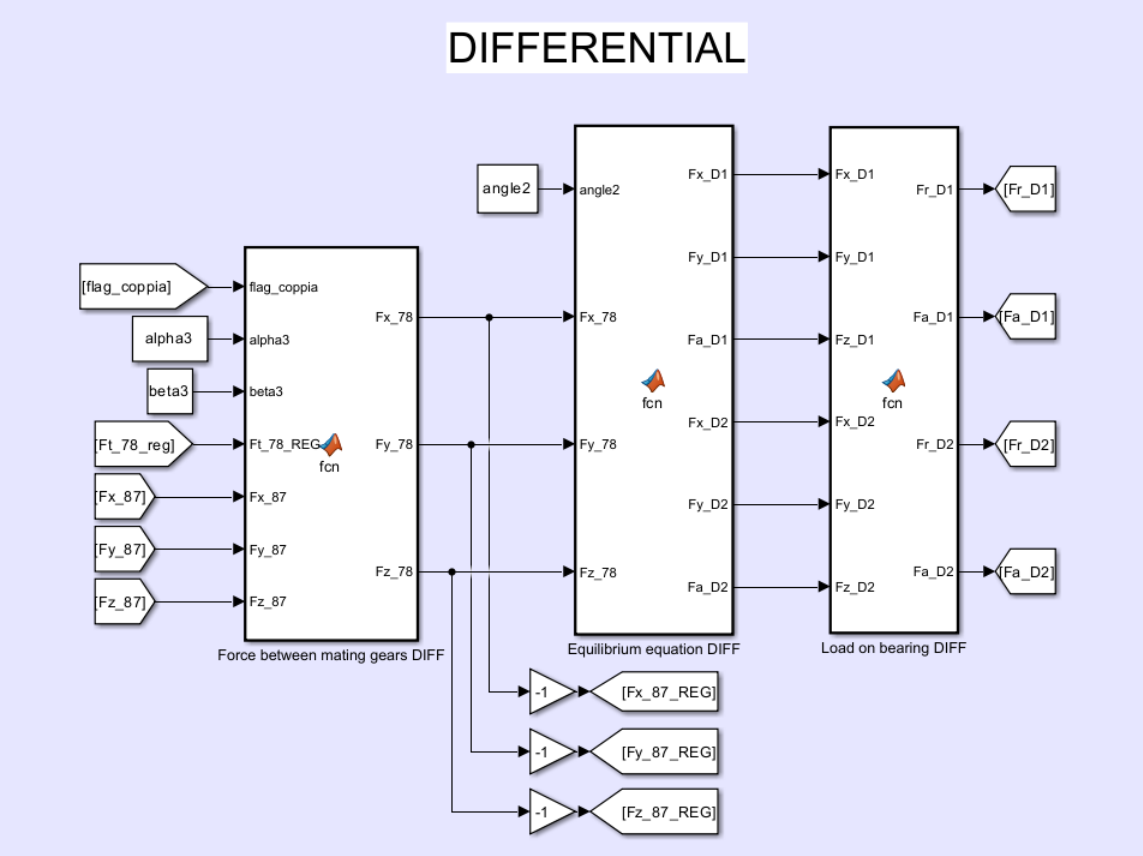

Figure 4.13: Differential computation

4.1.3 Lubricant properties submodel

The submodel "Oil properties" is designed to calculate the properties of the lubricating fluid. This data is subsequently utilized by other submodels to perform various calculations. In particular, the submodel provides the specifications for the oil jet at the first stage, which is the only stage lubricated by an oil jet. Additionally, it determines the oil specifications for lubricating the other stages, crucial for calculating load-independent losses. Furthermore, the submodel supplies the oil specifications necessary for calculating losses in the friction clutch.

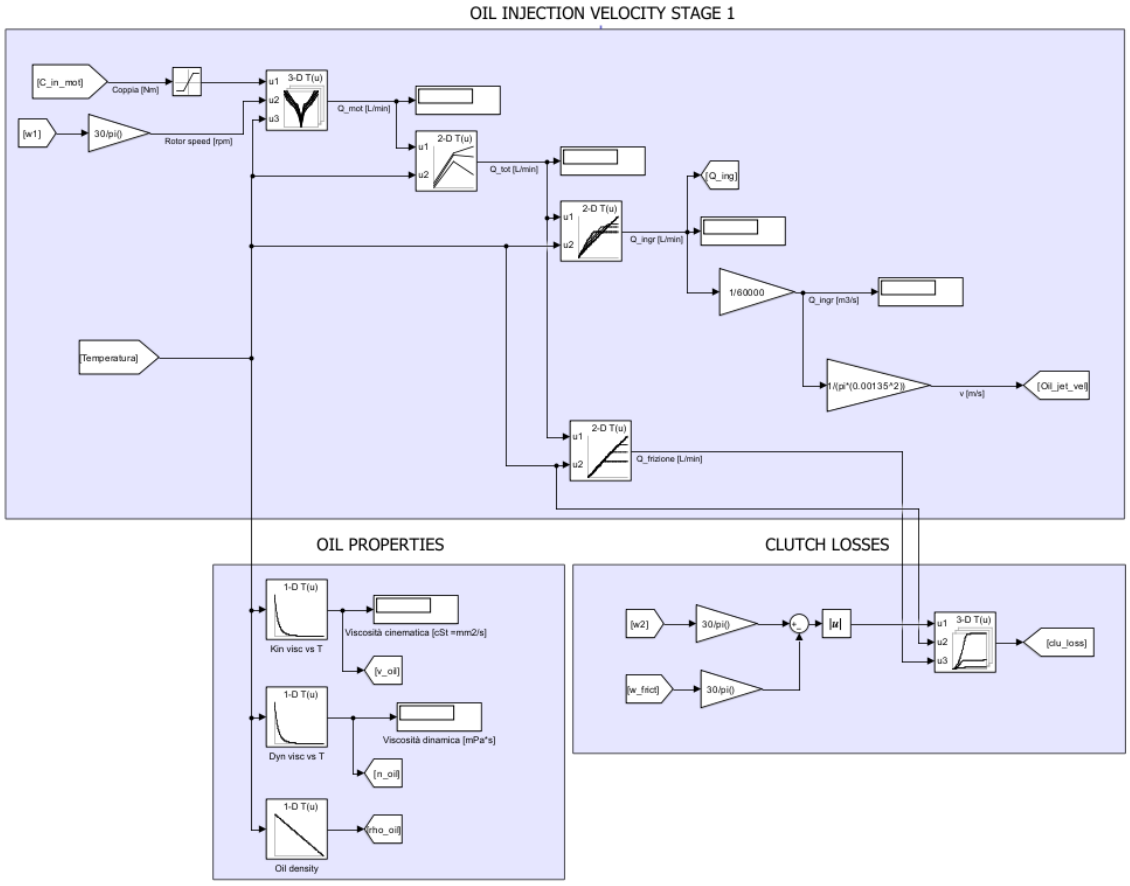

Figure 4.14: Oil properties submodel - blocks

4.1.4 Power losses computation submodel

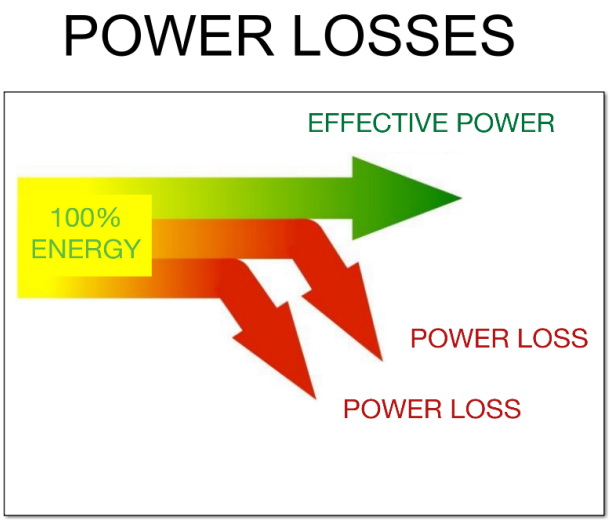

Figure 4.15: Power losses submodel

The "Power losses submodel" represents the final stage of the comprehensive model. Embedded in the submodel, there are various blocks specifically designed to calculate the power losses occurring within the transmission system, quantified in terms of power in Watts. The blocks are crucial for providing a detailed assessment of the transmission's efficiency by breaking down the power losses into specific categories. In particular, the power losses submodel consists of four primary blocks: the "total losses" block, the "losses per component" block, the "seals losses" block, and the "losses per type" block, as illustrated in Figure 4.16.

The "total losses" block aggregates all the power losses within the transmission, providing a complete measure of the overall efficiency.

The "losses per component" block offers a more detailed breakdown, calculating the power losses attributed to individual components of the transmission, such as shafts or bearings. This helps in identifying which parts of the system are the most inefficient and may need further optimization.

The "seals losses" block deals with the power losses due to the seals within the transmission.

Finally, the "losses per type" block categorizes the losses by type, such as load dependent and load independent losses in bearings or gears, providing a deeper insight into the nature of the inefficiencies.

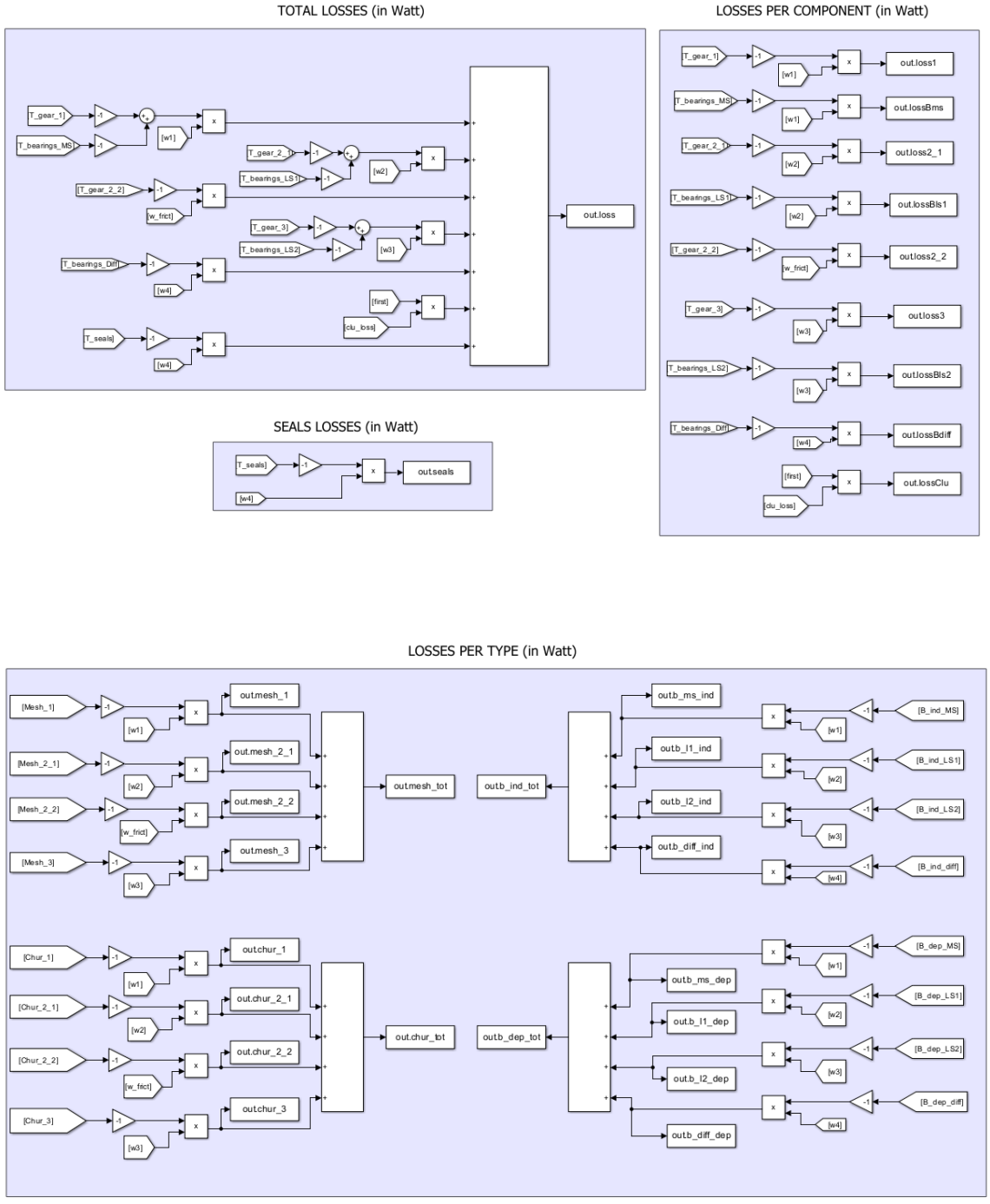

Figure 4.16: Power losses submodel - blocks

4.2 Vehicle model

The second Simulink/Simscape model employed in this thesis is the vehicle model. The main purpose of this model is to obtain efficiency measurements of the transmission over various driving cycles. These driving cycles encompass the range of operational points that a transmission might encounter under real-world driving conditions. As will be discussed in Chapter 5, the specific driving cycles simulated for this study include the *New European Driving Cycle* (NEDC), the *Worldwide Harmonized Light Vehicles Test Procedure* (WLTP), and the *Federal Test Procedure* (FTP-75). Their simulation provides an extensive evaluation of the transmission's performance in terms of efficiency, offering valuable insights into its real-world behavior.

The vehicle model used in this thesis (Figure 4.17) is an advanced evolution of the model presented in [**59**]. It is composed of several interconnected submodels that exchange information with one another to simulate the overall vehicle dynamics. These submodels include the vehicle model, which simulates the physical and mechanical properties of the vehicle; the control model, which manages the control strategies and decision-making processes; and the power loss model, which calculates the power losses occurring within the vehicle's transmission.

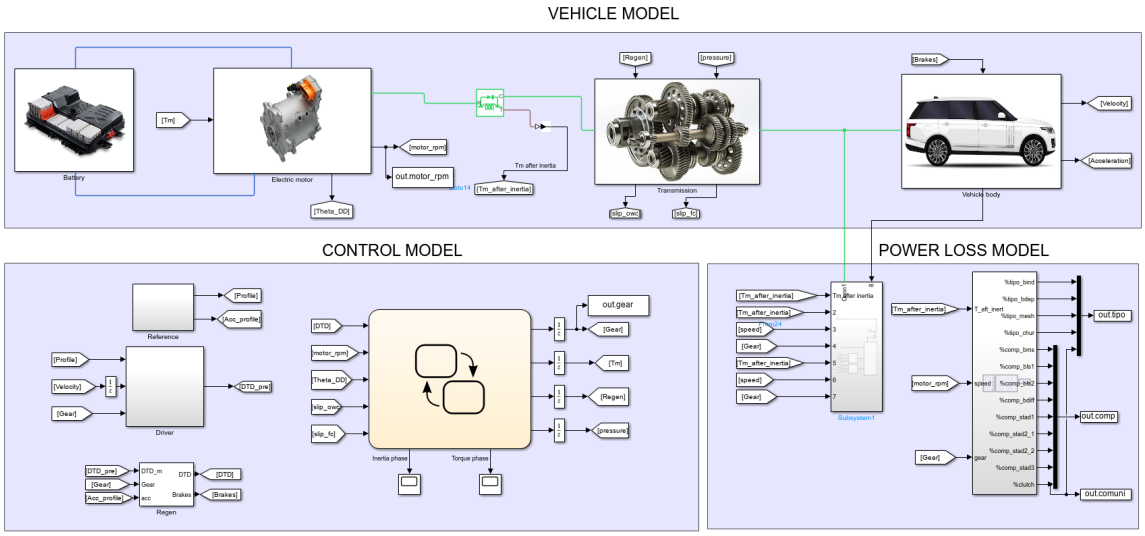

Figure 4.17: Vehicle model

4.2.1 Vehicle submodel

The vehicle submodel comprises several components, that are interconnected to simulate the overall dynamics of the vehicle itself. Each component is represented by specific blocks within the Simulink/Simscape environment: the battery, electric motor, transmission, and vehicle body.

Battery

The battery block is a crucial element that consists of an ideal voltage source, modeled by the "DC Voltage Source" Simulink/Simscape block. This source is designed to maintain a constant voltage across the battery terminals, irrespective of the current being drawn by the battery. In addition to the ideal voltage source, the battery block includes a series resistor. This resistor is essential for modeling the power losses that occur within the battery system, thereby providing a more accurate representation of the battery's behaviour.

Electric motor

Connected to the battery block is the electric motor block. This component features a permanent magnet synchronous motor (PMSM), which is modeled in Simulink using the "Motor and Drive (System Level)" block. This block also integrates the inverter, which is crucial for converting the direct current (DC) from the battery into alternating current (AC) needed to drive the motor. The function of the electric motor block is to transform the electrical energy provided by the battery into mechanical energy, used to move the vehicle.
The efficiency of the motor and inverter unit is a significant factor when dealing with the overall efficiency of the vehicle. To accurately account for this, the block includes an efficiency map. This map provides a representation of the motor's efficiency as a function of motor torque and speed.

Transmission

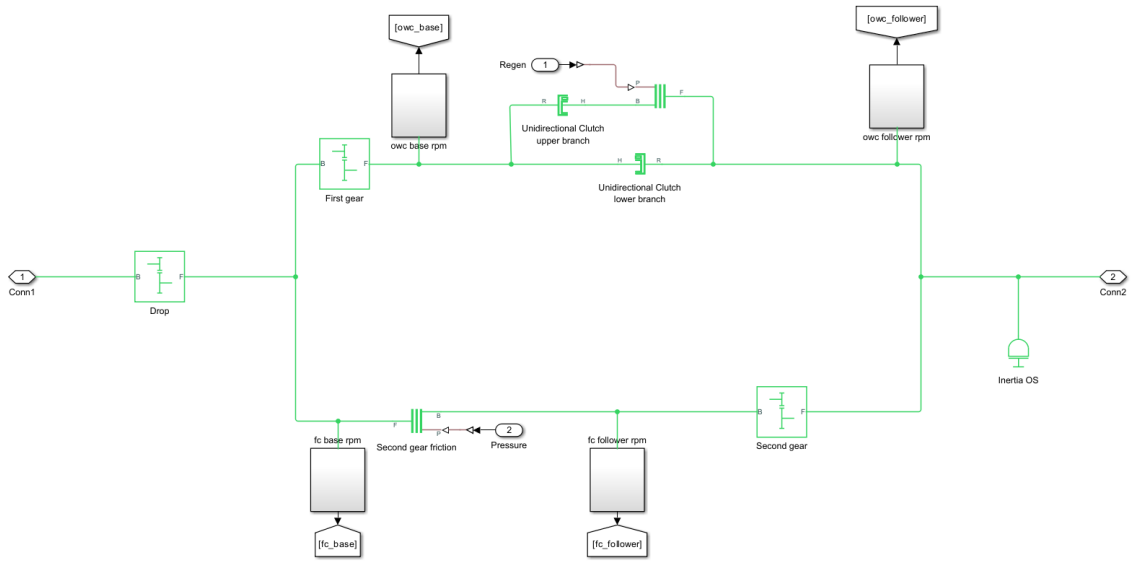

Figure 4.18: Transmission block

The transmission block represents a detailed model of the Dana 2-speed transmission. It is quite similar to the one discussed in the previous section, with the key difference being that the regeneration dynamics are accounted for in greater detail. Specifically, the SOWC (Selectable One Way Clutch) behaviour is modeled using three clutches Simulink/Simscape blocks: two "Unidirectional Clutch" blocks and one "Disc Friction Clutch" block, as shown in Figure 4.19. This setup allows for the control of the bidirectional behavior of the SOWC, in particular, in driving conditions, when the power flows from the motor to the wheels, the "Disc Friction Clutch" block is disengaged, and the power flow occurs solely through the unidirectional clutch (the lower branch of Figure 4.19). Conversely, during regenerative braking, a pressure signal engages the disc friction clutch, enabling the power flow to pass through it. In series with the disc friction clutch is a second unidirectional clutch, but it is oriented in the opposite direction. This specific configuration of two oppositely directed unidirectional clutches placed in parallel function as a sort of rigid body with 1 degree of freedom, allowing motion not only in a unidirectional manner but in both directions. This configuration permits the power flow to travel back up to the motor.

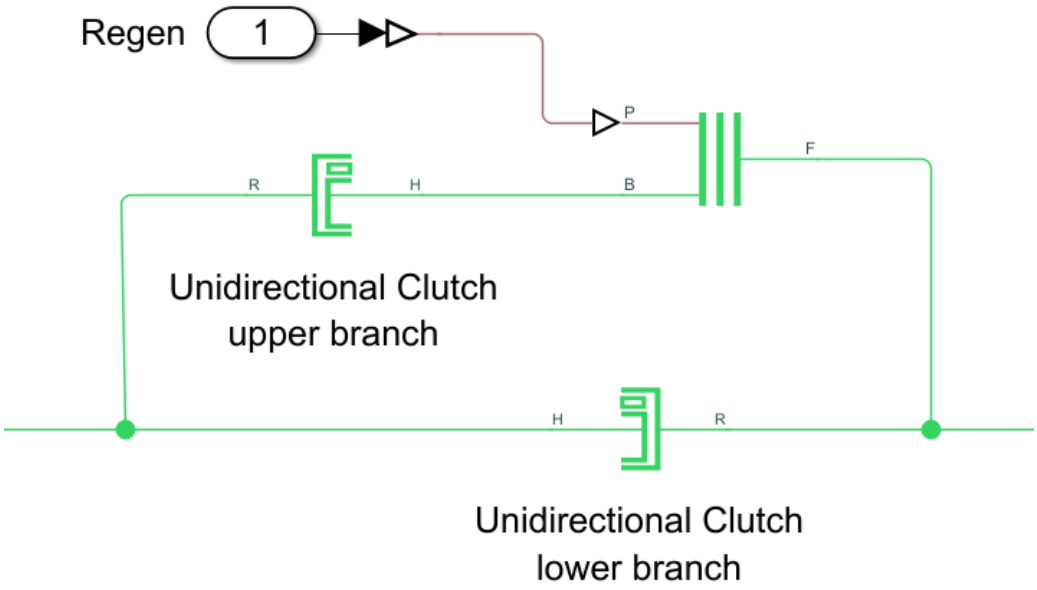

Figure 4.19: Selectable One Way Clutch

Vehicle body

The vehicle dynamics were modeled using the Simulink/Simscape "Vehicle Body" block, which accurately simulates the longitudinal behavior of a two-axle vehicle. This model outputs the vehicle speed used to calculate the velocity error, which is input to the PID block.
The torque generated by the transmission is split through a differential and distributed between the two half-shafts before reaching the drive wheels. The "Vehicle Body" block interfaces with the transmission via the drive wheels, receiving torque from the half-shafts. The brakes were simulated using "Ideal Torque Source" blocks. The braking system is configured with a fixed distribution of 75% front and 25% rear braking torque. At the rear, braking is performed by using dissipative brakes, while at the front, braking is regenerative through the use of the electric machine. Dissipative braking is limited to the rear axle because, in the simulation scenarios, front brakes were unnecessary due to the electric motor's ability to perform regenerative braking effectively even under high torque conditions across the three simulated cy-

cles. Anyway, for a more realistic representation, 100% regenerative braking (solely using the motor without the use of the brakes) is applied to the rear axle for vehicle accelerations up to 0.15g. Beyond this acceleration threshold, braking force distribution is shifted to 75% front (regenerative braking) and 25% rear (dissipative braking).

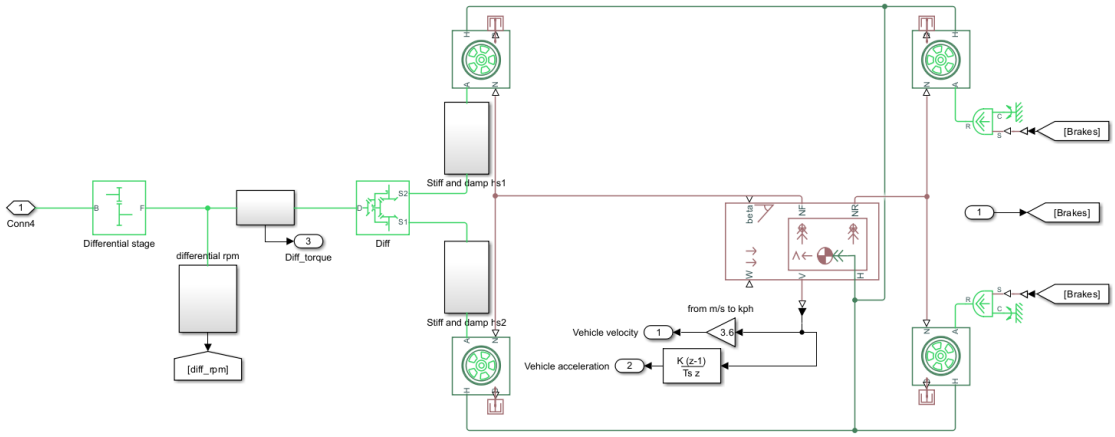

Figure 4.20: Vehicle body block

4.2.2 Control submodel

The control submodel includes the driver block and the block responsible for managing the gear shift logic.
The primary function of the driver block is to ensure that the vehicle follows the driving mission, which is essentially a reference speed signal generated by the Simulink/Simscape "Drive Cycle Source" block. To achieve this, a PID control system is employed. This control system calculates the torque request to be supplied to the motor at each simulation step, based on the difference between the vehicle's speed and the desired speed indicated by the driving cycle.
The block that handles the gear shift logic is designed to optimize driver comfort. The gear shift logic within the model is implemented using the Matlab's Stateflow tool. The Stateflow diagram takes the torque request signal as input from the driver block and manipulates this signal to achieve optimal gear shifting. For more detailed information on the functioning of this gear shift logic, please refer to [**59**].

4.2.3 Power loss submodel

The part of the model responsible for calculating power losses during driving cycles is carried out by the power loss submodel. Within this submodel, there are two main blocks. The first block is tasked with calculating the total transmission losses, and its output is fed back into the vehicle model as a resistive torque to account for the power loss caused by the transmission. The second block's (Figure 4.21) purpose is to break down the total losses into categories. Specifically, the total losses are divided by type, such as losses caused by gears, bearings, or those dependent or not on transmitted load. Additionally, the losses are categorized by component, referring to each component of the transmission, such as the bearings of a particular shaft or a specific gear stage.
To obtain this detailed information, efficiency maps are used, which are functions of motor speed, torque, and the engaged gear. These efficiency maps are the same ones derived from the transmission model described in the previous section. In Simulink, the "3-D Lookup Table" block is utilized to input the efficiency map data in table form. The results generated by these two blocks will be analyzed in the following chapter.

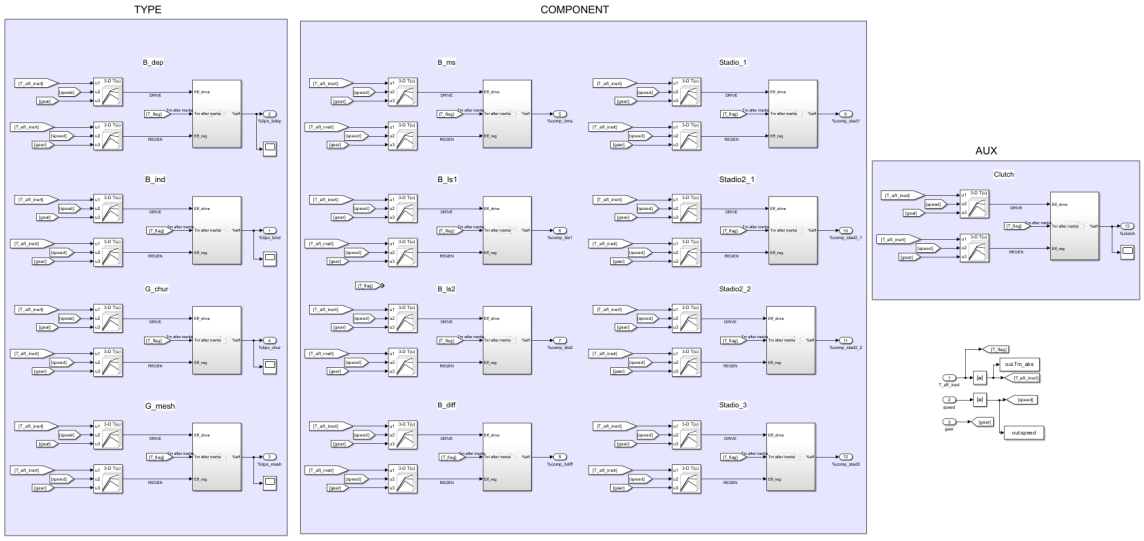

Figure 4.21: Power losses blocks

Chapter 5

Results

5.1 Motor & Inverter efficiency

The efficiency plots of the motor-inverter group are provided directly from the manufacturer. Figures 5.31 and 5.2 show the efficiency plots for positive and negative torques used for the simulations of the driving cycles..

Motoring

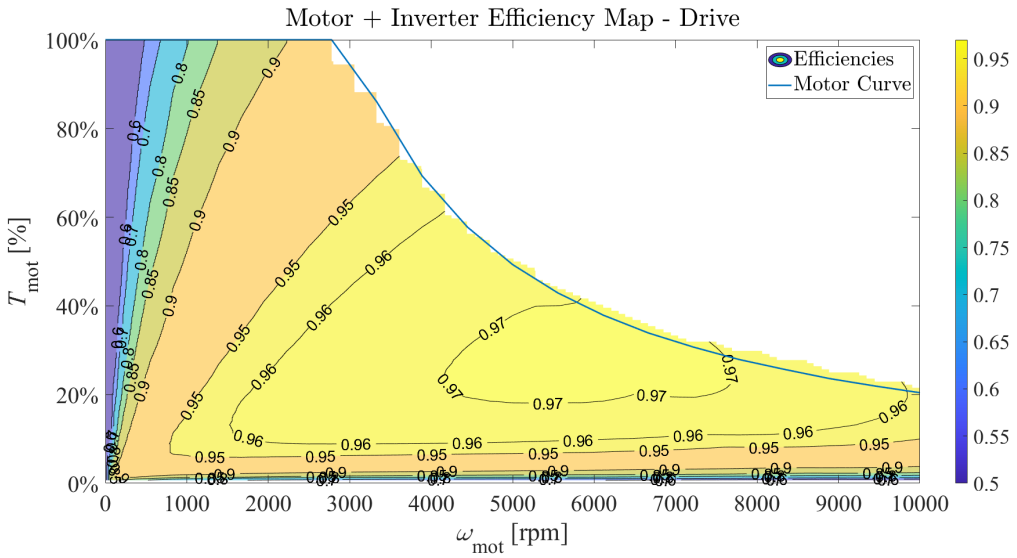

Figure 5.1: Motor + Inverter Efficiency - Drive

Regen

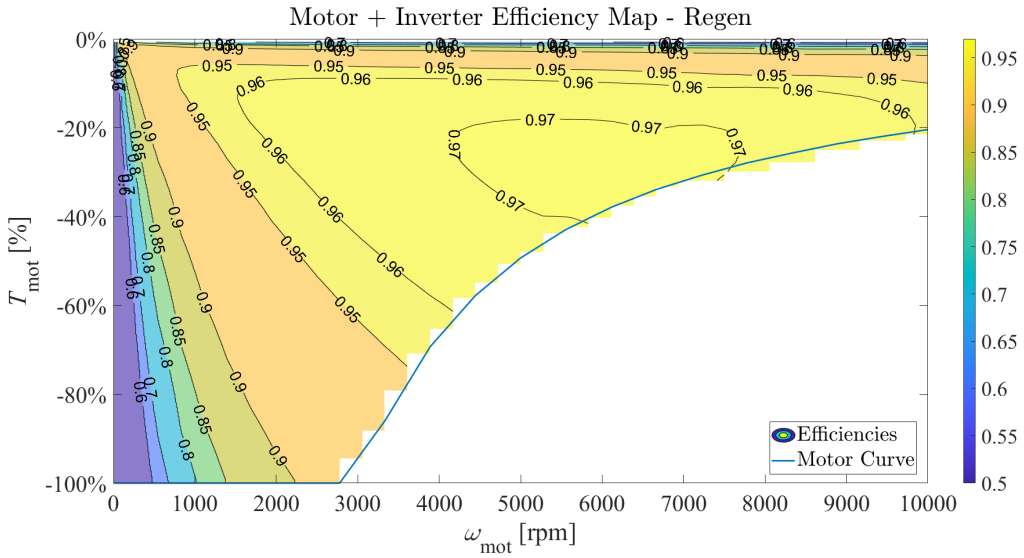

Figure 5.2: Motor + Inverter Efficiency - Regen

5.2 Transmission efficiency

Figure 5.3 and 5.4 show the efficiency maps of the 2-speed transmission obtained by the real-time transmission efficiency calculator model developed in Matlab/Simulink environment, details of which are described in Chapter 4. The overall system efficiency in first and second gear is computed for a lubricant temperature T=40° and for the *drive* condition, when the power transmitted from the motor to the wheels is positive, and the vehicle moves forward.

Motoring

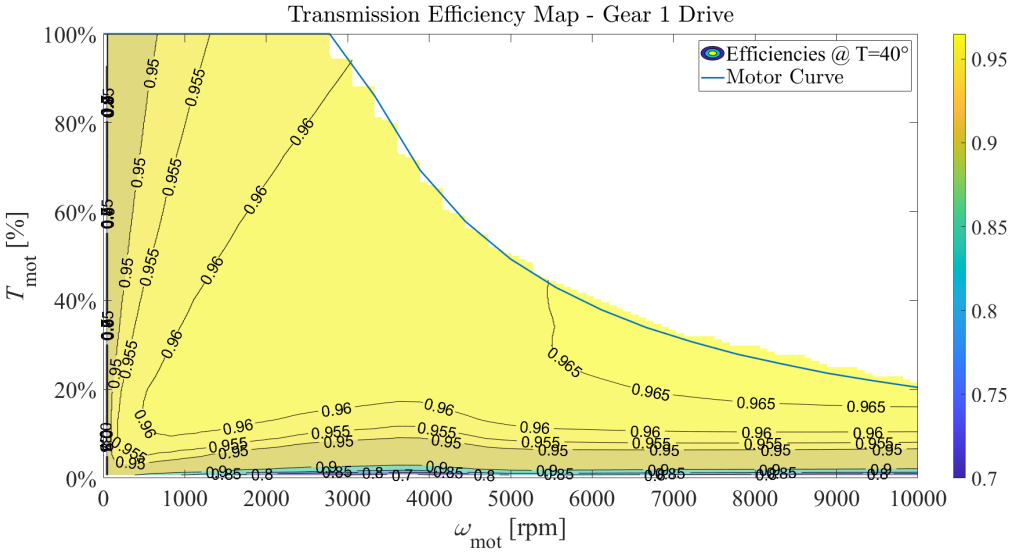

Figure 5.3: Efficiency map 1st gear - Drive

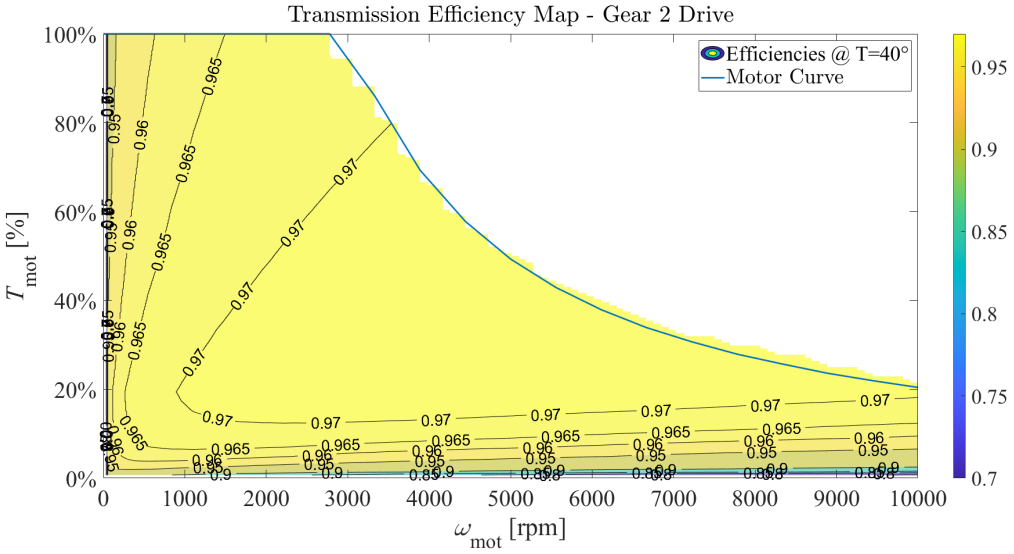

Figure 5.4: Efficiency map 2nd gear - Drive

As the above graphs show, in second gear the transmission efficiency is higher than in first gear. This is mainly due to the fact that, in second gear, the amount of load transmitted between the gears is lower than in first gear, because of the major loss contribution, for the whole transmission loss, is the gear meshing. Below, the following paragraphs and graphs will highlight this concept.
Furthermore, when in first gear, the wet clutch is an additional source of power loss. When disengaged, clutch plates rotate with different velocities, while immersed in a viscous oil. The relative velocity of the immersed friction discs generates a viscous drag between them.
Accordingly, plots shown above highlight how load dependent losses and clutch loss are impactful in the assessment of the total transmission efficiency.

Equivalent maps (Figure 5.5 and 5.6) are obtained for the *Regenerative* case, hereafter shortened as *Regen*, the case in which the power transmitted from the wheels to the motor is positive, and the vehicle moves forward.

Regen

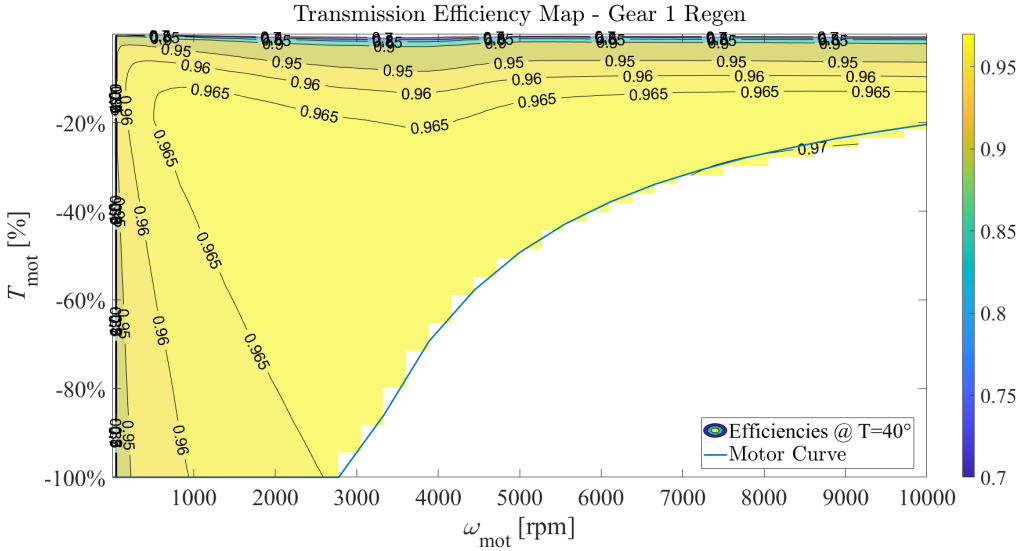

Figure 5.5: Efficiency map 1st gear

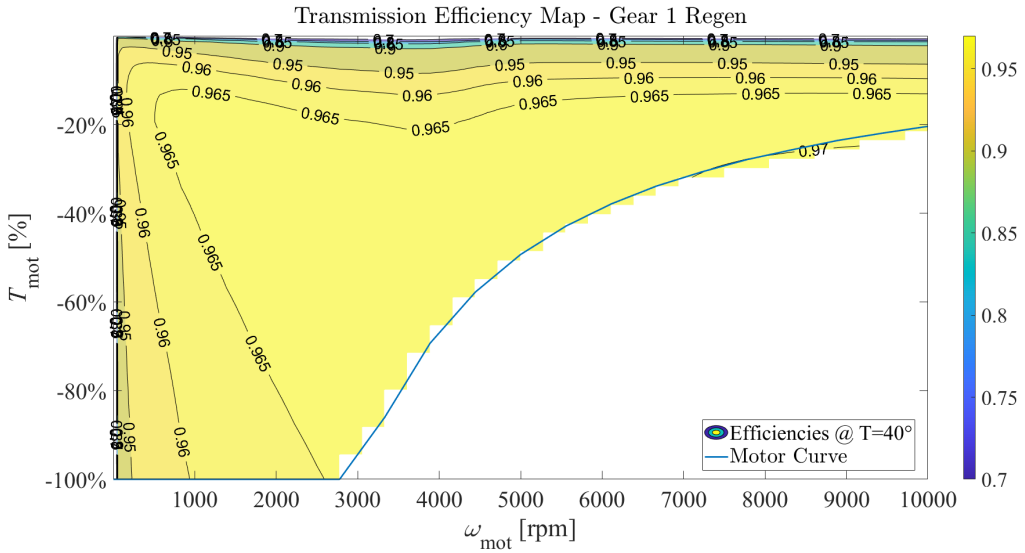

Figure 5.6: Efficiency map 2nd gear

The considerations previously outlined, for the *drive* case, also apply in this instance. Specifically, the wet clutch and load dependent factors, contribute to the raised losses observed in the case of first gear.

5.3 Motor-Inverter vs Transmission efficiency

The following graphs present a comparison between the efficiency of the transmission system and the efficiency of the motor-inverter unit. This comparison seeks to determine whether the efficiency of the transmission can be overlooked or if it holds an importance in the overall system energy evaluation. The graphs show the difference between the value of the motor-inverter group efficiency and that of the transmission. Therefore, regions with negative values on the graphs indicate areas where the motor-inverter efficiency is lower than that of the transmission, whereas, regions with positive values highlight areas where the transmission efficiency is lower to that of the motor-inverter.

Motoring

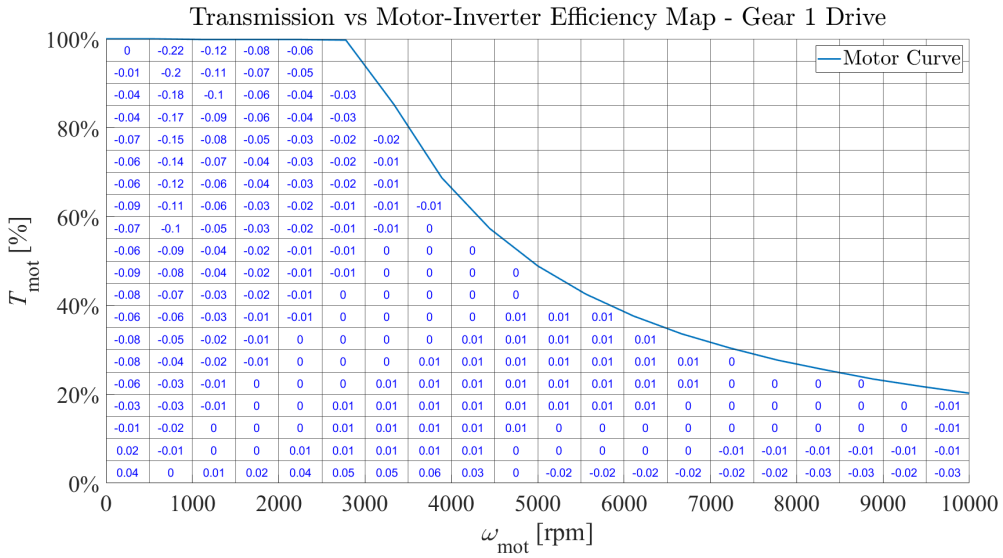

Figure 5.7: Efficiency Comparison Gear 1 Drive

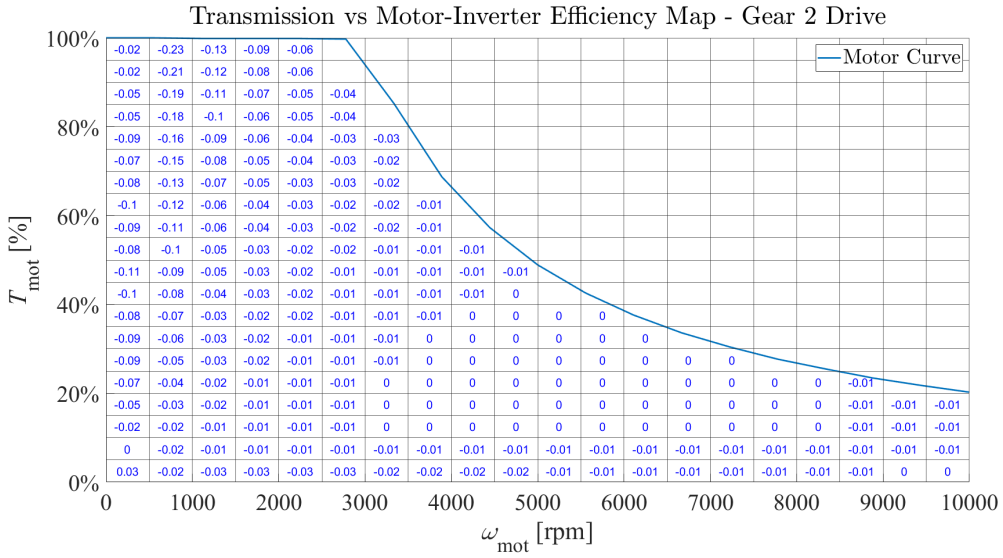

Figure 5.8: Efficiency Comparison Gear 2 Drive

Regen

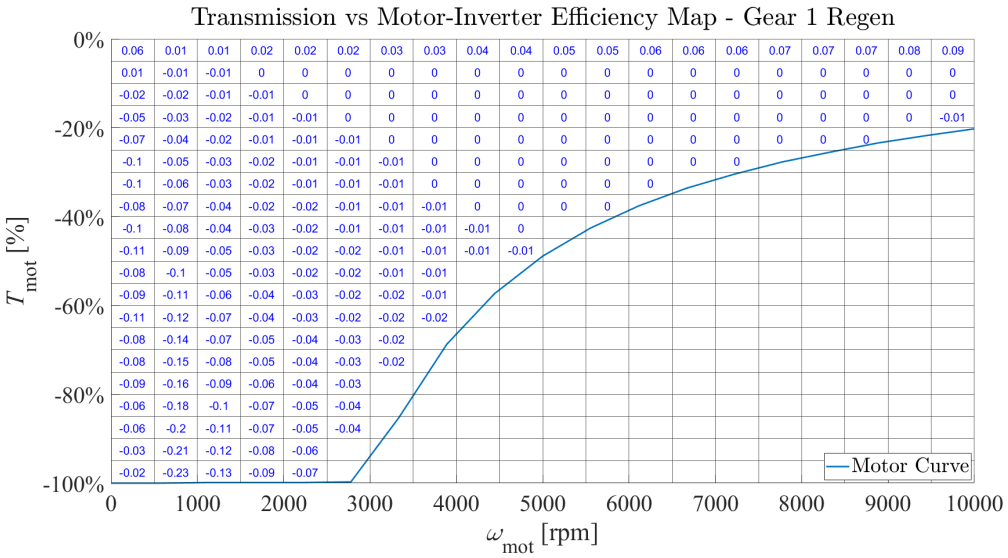

Figure 5.9: Efficiency Comparison Gear 1 Regen

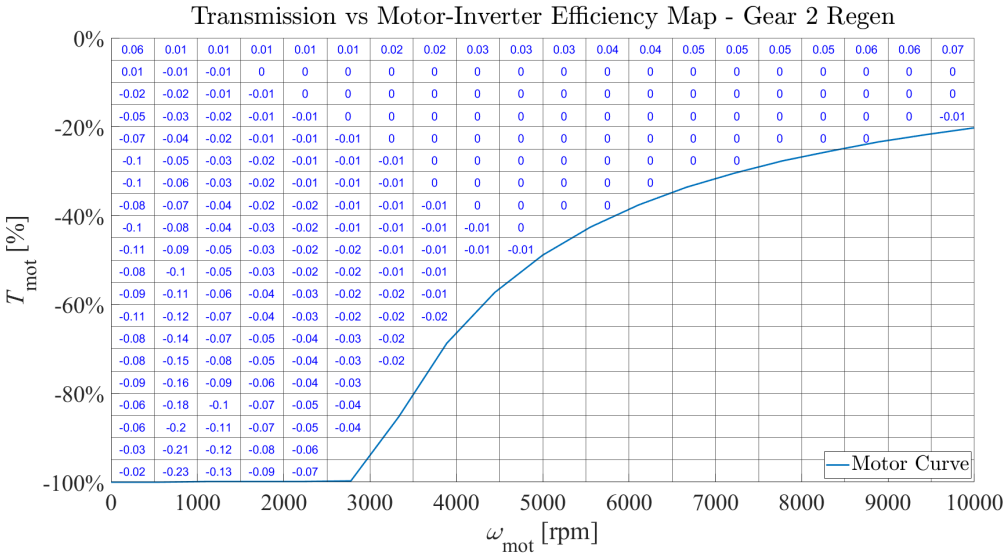

Figure 5.10: Efficiency Comparison Gear 2 Regen

Analysis of the graphs reveals that, in nearly all operational areas, the transmission system demonstrates higher efficiency than the motor-inverter group. However, it is important to note that, despite the motor-inverter efficiency being generally lower, the margin of difference between the two efficiencies is quite small. This observation suggests that the energy losses within the transmission are nearly as significant as those within the motor-inverter assembly. Consequently, this implies that the transmission's efficiency is a critical factor and cannot be neglected in an energy assessment.

5.4 Transmission losses contributions by typology

In order to gain a clearer understanding of the efficiency trend for the total efficiency maps, the contribution that each source of loss gives to the overall transmission power dissipation has to be analyzed. The loss sources that have been investigated in this work result from the gears, the bearings, the wet clutch, and seals. Their contribution is examined and analyzed below as part of the research.
Calculations revealed that shaft seals have an insignificant impact on the total loss, with their contribution amounting to a percentage ranging between 10e-17% and 10e-8% of the total dissipation. Given this minimal effect, further discussion regarding seals is deemed unnecessary and thus omitted.

Bearing load independent loss

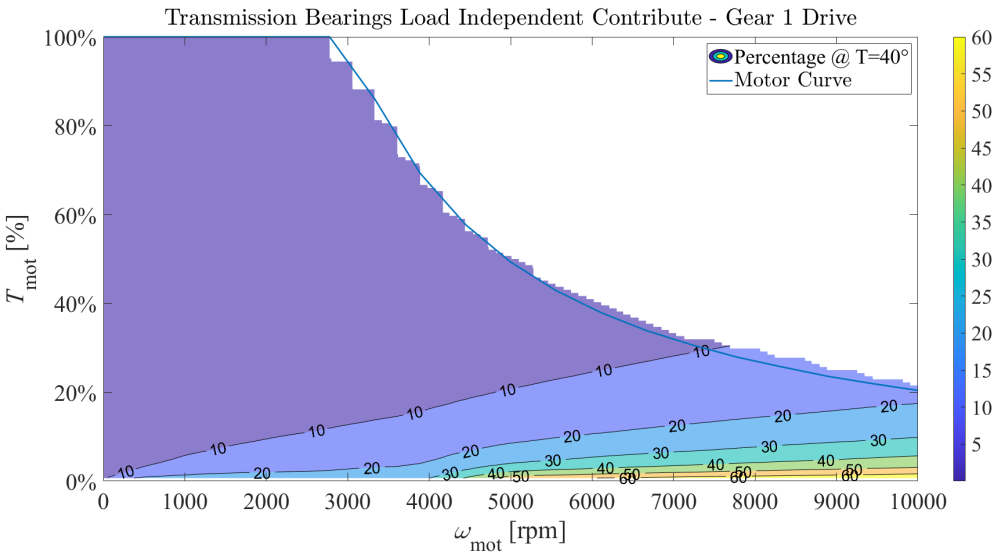

Figure 5.11: Bearing load independent contribute in first gear

The plot showing the bearings independent contribute (Fig. 5.11) points out that, at low torque values, this type of loss becomes more impactful in the overall summation. This occurs because, at low transmitted torques, bearings experience a reduce load, consequently, the percentage contribution attributed to independent loss carries greater significance. Furthermore, this type of loss escalates with increasing shaft angular velocity.
Indeed, at higher speeds, bearings encounter heightened frictional resistance torque, stemming from factors such as greater centrifugal force and temperature elevation. Hence, at low loads and high speeds, this form of loss exerts a more pronounced influence on the total calculation.

Bearing load dependent loss

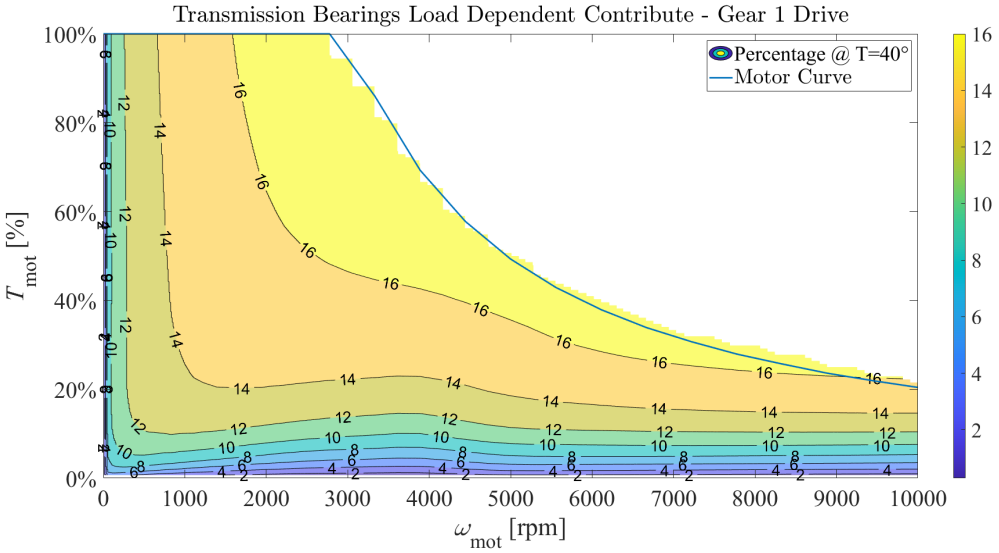

Figure 5.12: Bearing load dependent contribute in first gear

The relevance of bearing load dependent loss, in relation to overall power dissipation, seems to grow as both speed and load increase. This phenomenon is largely due to the inherent characteristics of bearing load dependent loss, which naturally rises with an increase in load, thereby, as the load intensifies, the portion of power dissipation attributable to bearing load also increases.
Moreover, there is an evident dependence on speed as well. It is important to note that the data is presented in percentage terms relative to the total power dissipation. The underlying reason for this observed behavior lies in the diminishing significance of meshing contributions, which are the most substantial factors in power dissipation, as speed increases. Essentially, while the meshing contribution's impact wanes with higher speeds, the bearing load dependent loss becomes more pronounced, highlighting its increasing relevance in the overall power dissipation framework. This interplay between bearing load dependent and gear meshing contributions underscores the complex dynamics involved in power dissipation under different operational conditions.

Gears churning loss

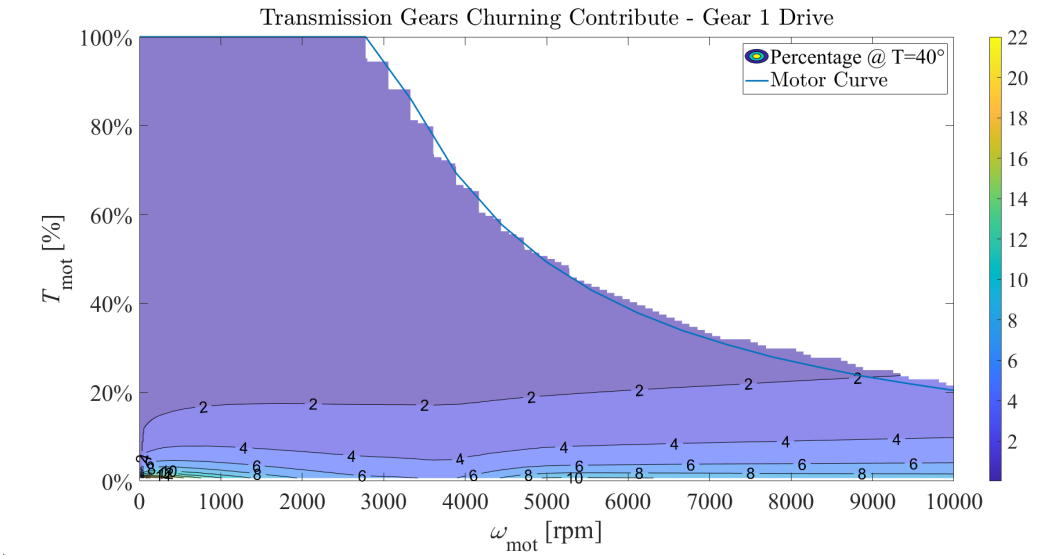

Figure 5.13: Gears churning contribute in first gear

As the graph shows, the churning losses contribution of the whole transmission, in first gear, is below 2% of the total power dissipation, for loads higher than 20% of the maximum available torque. For these type of losses, it is reasonable to expect an increase of power losses when the gears angular rotation increases. Also, churning losses strongly depends on the immersion depth of the gear in the transmission oil. For this particular 2-speed transmission case, the amount of gears immersion depth is sufficient to guarantee a proper lubrication for the components, even if the oil level depth is lower than other oil lubricated transmissions. For this reason, the contribution of the churning losses is not so prominent in the whole system, and therefore, the churning losses increases slightly with the gears velocity.

Gears meshing loss

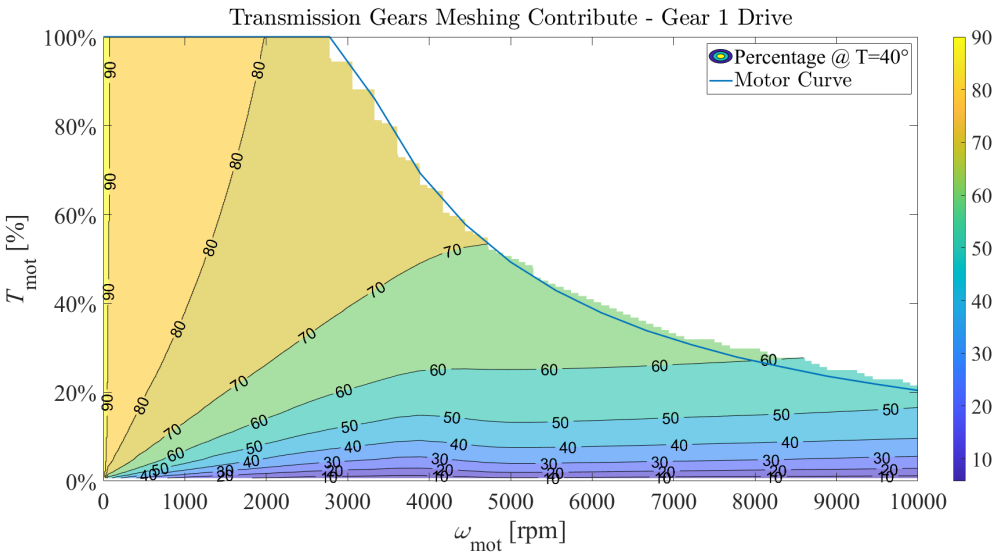

Figure 5.14: Gears meshing contribute in first gear

As expected, the most relevant contribution in transmission losses is the friction generates between the gears of the stages that are transmitting power. In fact the load dependent loss component of the gears is the major source of loss, with percentages that reach even more than 80% of the total, for those operating points that lay on the torque most demanding area. The load dependency is quite evident, especially at low torques, where the bearing independent loss contribution is dominant.

Wet clutch loss

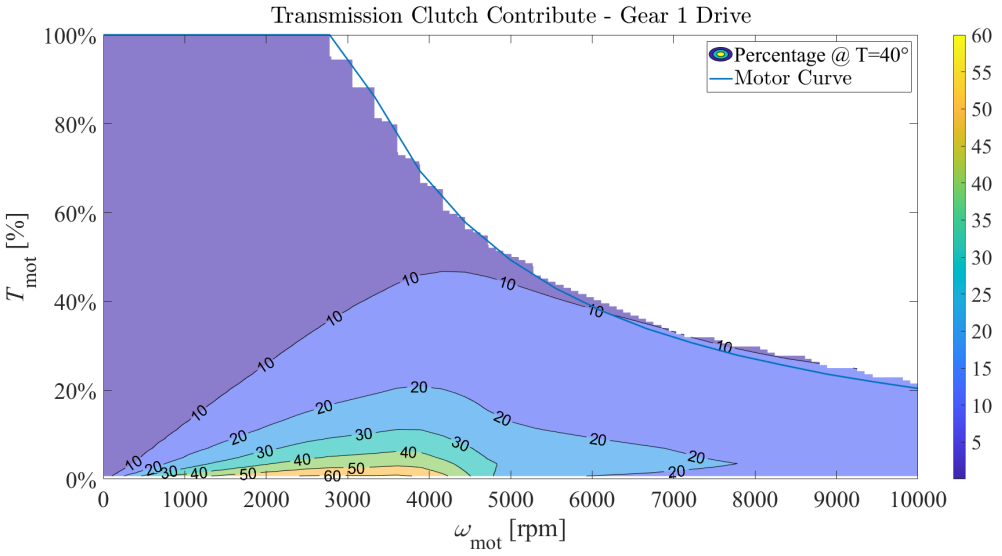

Figure 5.15: Wet clutch contribute in first gear

The figure 5.15 presents the loss contribution of the wet clutch. It is evident that the losses due to the clutch are particularly significant in the region where the torque is low. In this area, the viscous friction losses between the clutch discs, which rotates at different speeds, are considerable, accounting for up to 50% of the total transmission losses in certain operating points.

5.5 Transmission losses contributions by component

In this paragraph, a similar analysis to the previous one has been conducted, attributing the sources of loss to the specific components that generate them, instead of categorizing them by type. Below, efficiency maps of each individual component of the transmission are presented, expressed as a percentage of the total transmission losses. This approach aids in understanding the impact of each component on the overall inefficiency of the system. This information is valuable in the design phase, as it can indicate whether a component should be redesigned to improve system efficiency.

Bearings

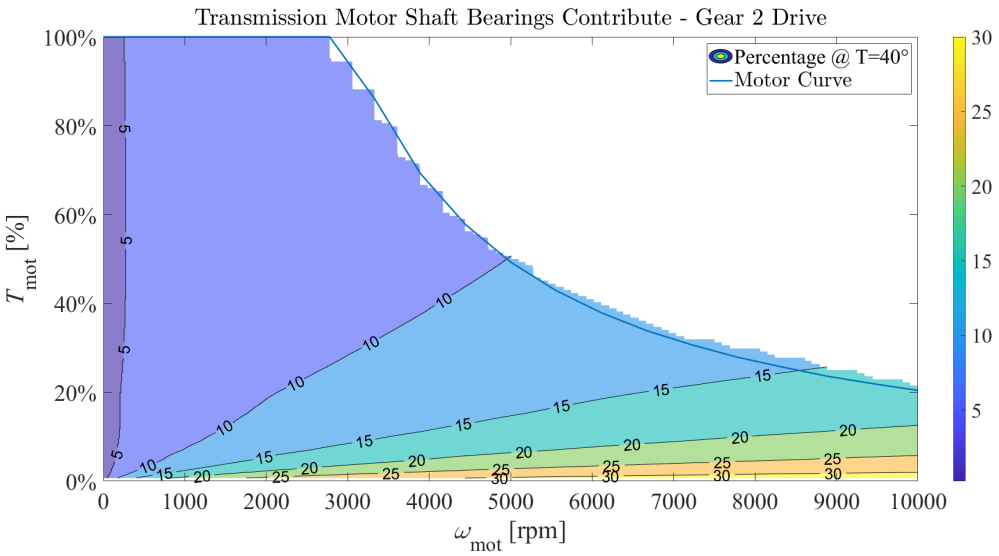

Figure 5.16: Motor shaft bearings contribute in second gear

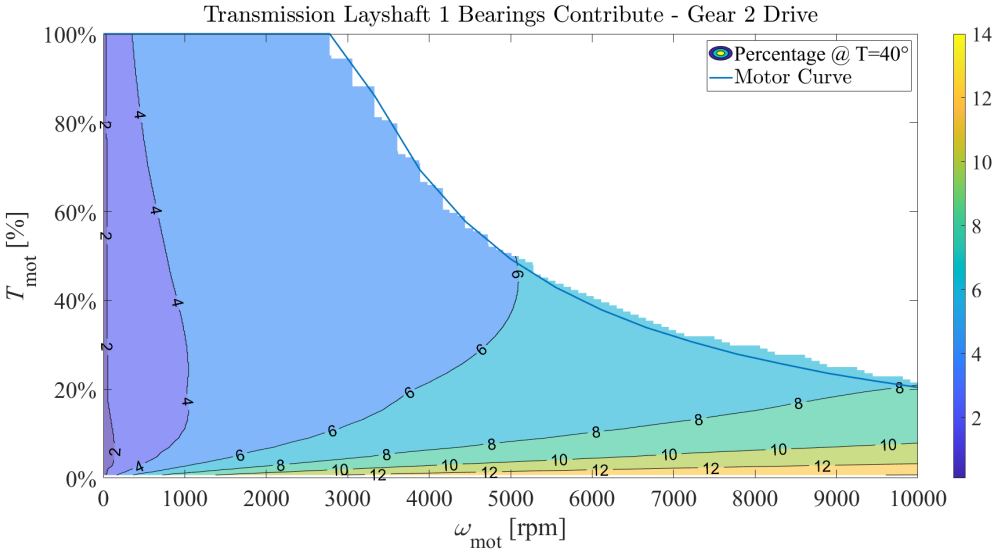

Figure 5.17: Layshaft 1 bearings contribute in second gear

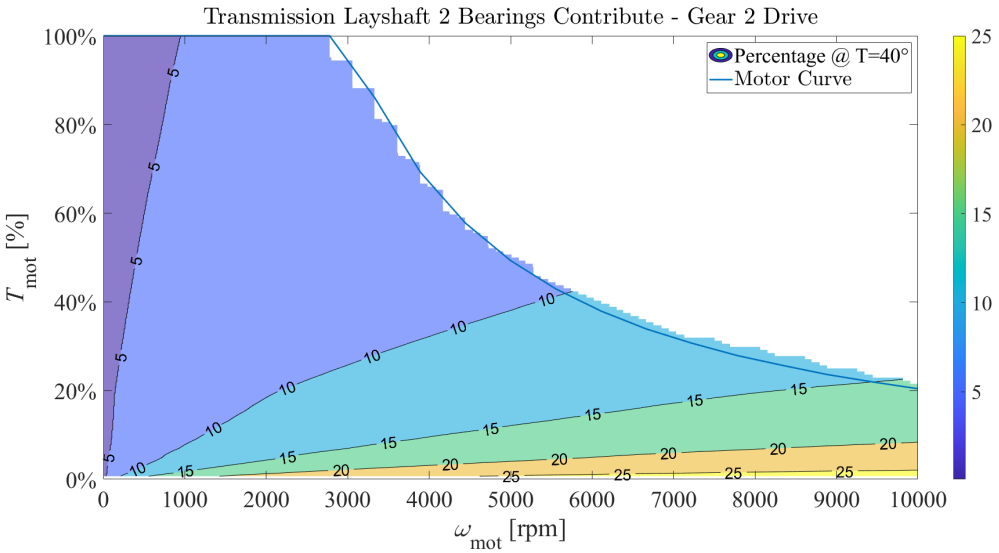

Figure 5.18: Layshaft 2 bearings contribute in second gear

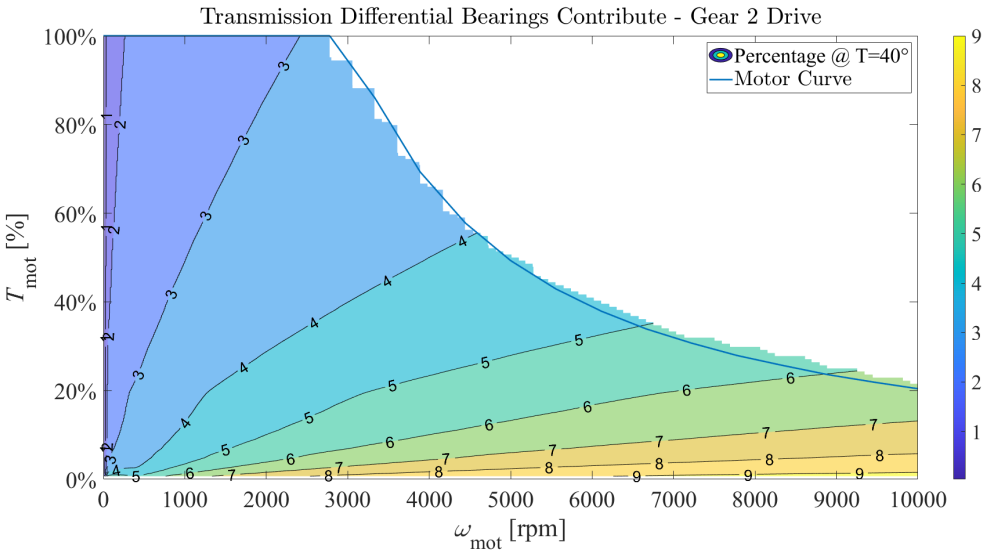

Figure 5.19: Differential bearings contribute in second gear

Gears

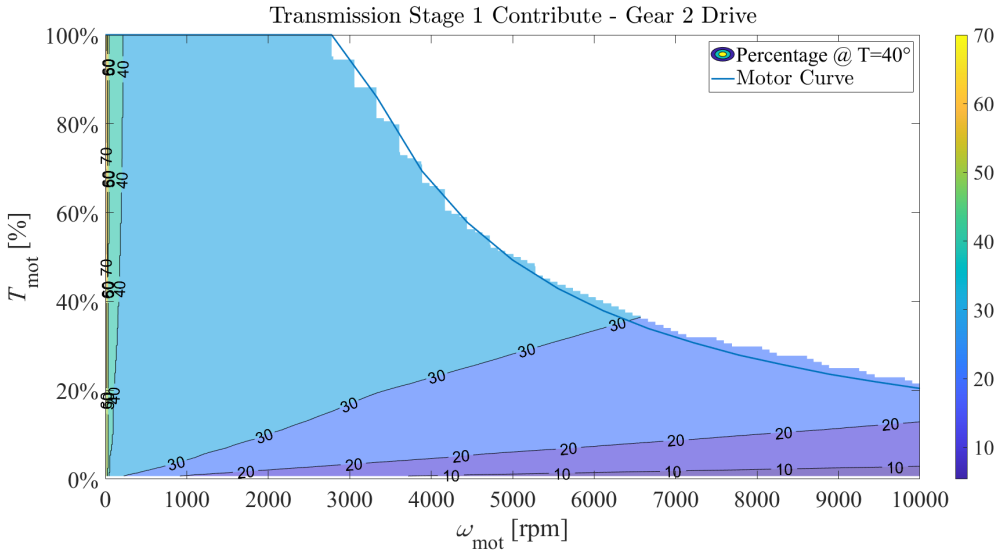

Figure 5.20: Stage 1 contribute in second gear

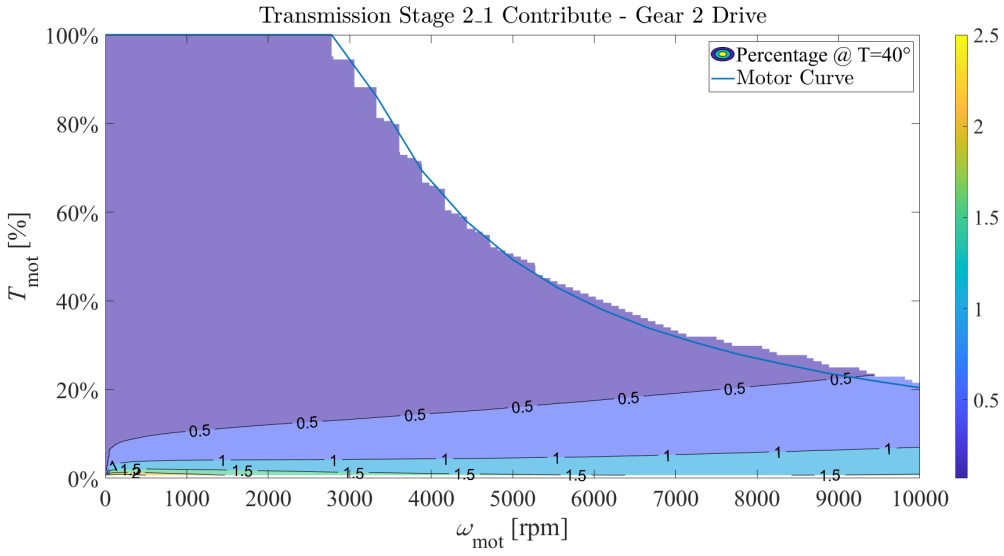

Figure 5.21: Stage 2_1 bearings contribute in second gear

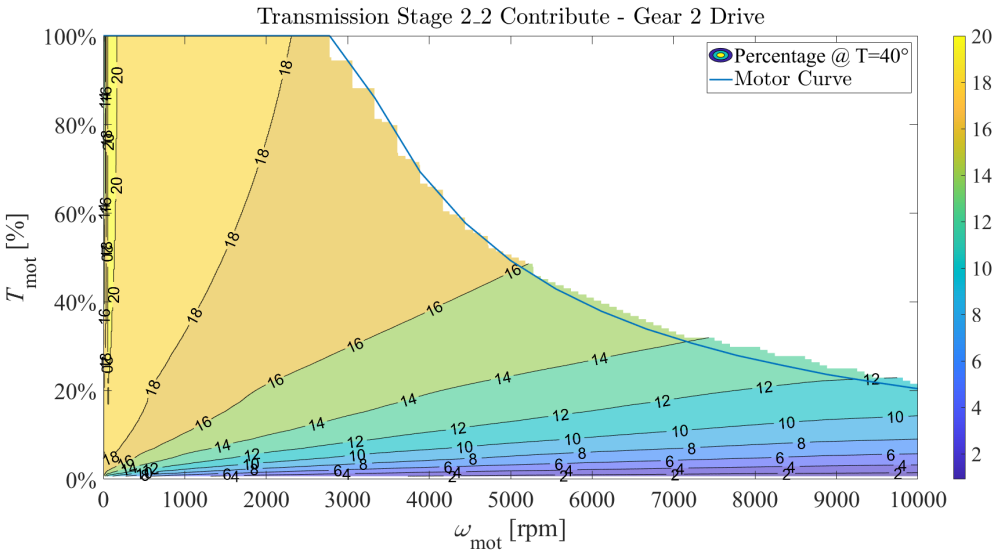

Figure 5.22: Stage 2_2 bearings contribute in second gear

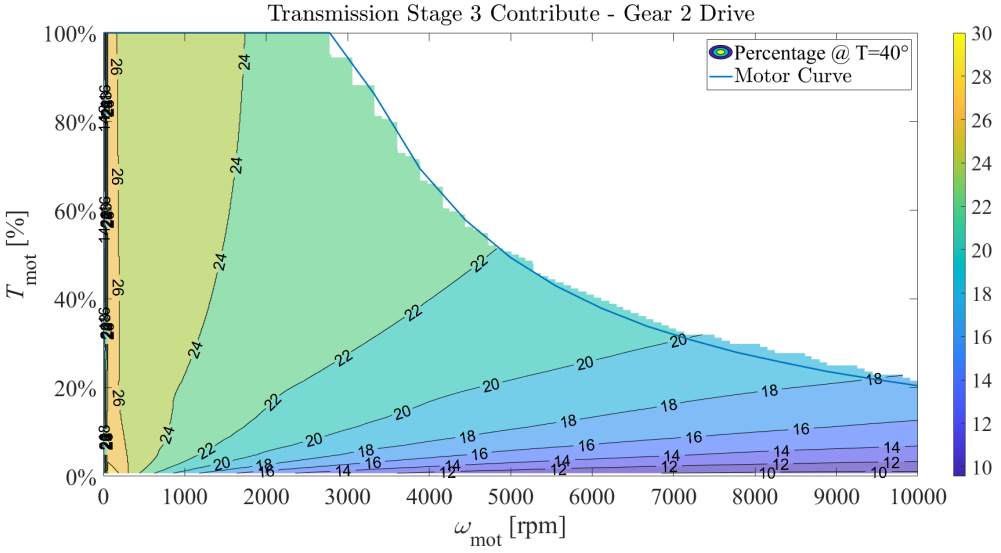

Figure 5.23: Stage 3 contribute in second gear

5.6 Driving cycles

To effectively evaluate the impact of transmission power losses in real driving applications, the Simulink model of a vehicle described in Chapter 4 has been utilized. The key components that this model includes are:

- The vehicle model, composed by:
  - The battery system
  - The electric machine
  - The 2-speed transmission
  - The vehicle body model
- The control systems, composed by:
  - The driver model
  - The gearshift control system

Through this modeling and simulation approach, the study aims to provide a detailed assessment of how transmission losses affect vehicle performance across different standardized driving conditions.

The Simulink model was configured to accurately replicate the speed of three different driving cycles. It has been calibrated, by employing a PID controller, to precisely follow the speed profiles provided by the Simulink "Drive Cycle Source" block. The following figures are derived from a simulation of the model on the NEDC driving cycle, to provide an example of how the model operates. The graphs illustrate several aspects: the accuracy of the control system in following the speed profile (Figure 5.24), the speed and torque of the motor throughout the cycle (Figures 5.25 and 5.26), and the selected gear (Figure 5.27). In particular, gear selection depends on the driving torque demand and the vehicle's speed. When at low torque demands, the gearshift logic already shifts the gear at a defined velocity that is lower than 10 km/h, this explains why the vehicle stays in second gear for the majority of the driving cycle duration.
Figures from 5.28 to 5.32 show the temporal variation of loss contributions throughout the cycle, each contribution is expressed as a percentage of the total loss. They are computed in the vehicle model using the maps described in Section 5.4.

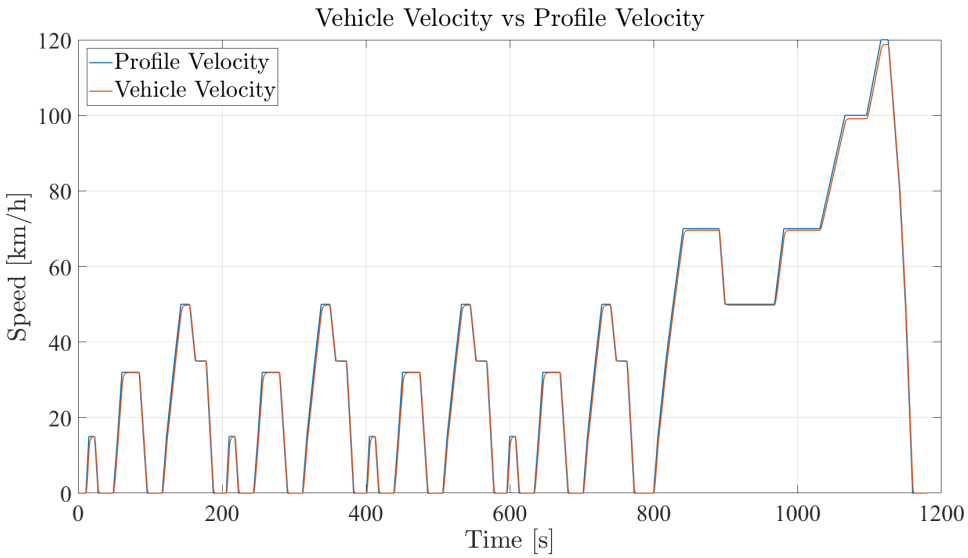

Figure 5.24: Speed profile

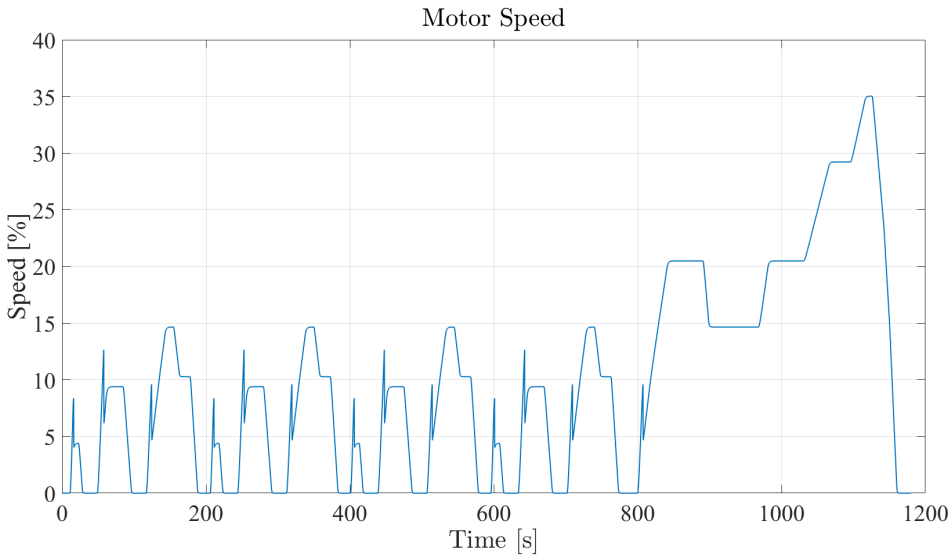

Figure 5.25: Motor speed

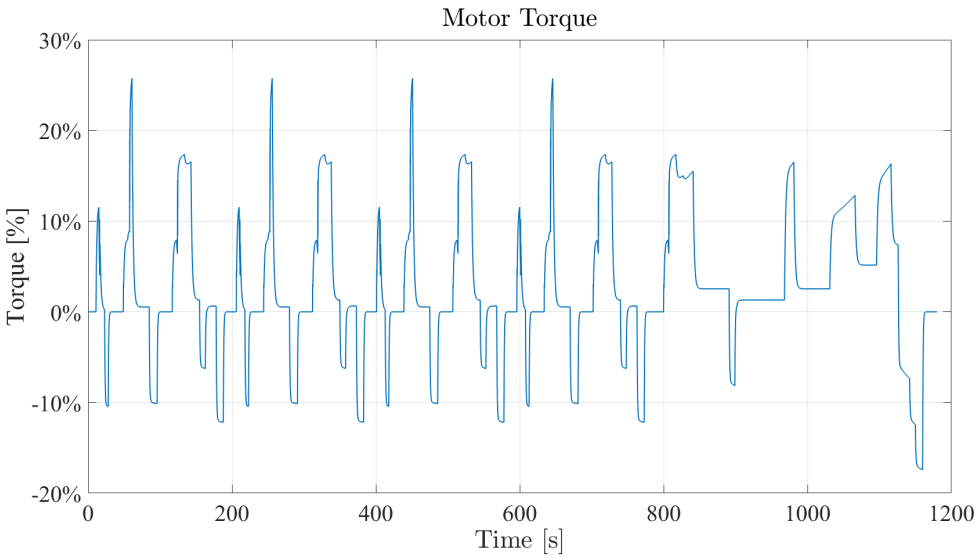

Figure 5.26: Motor torque

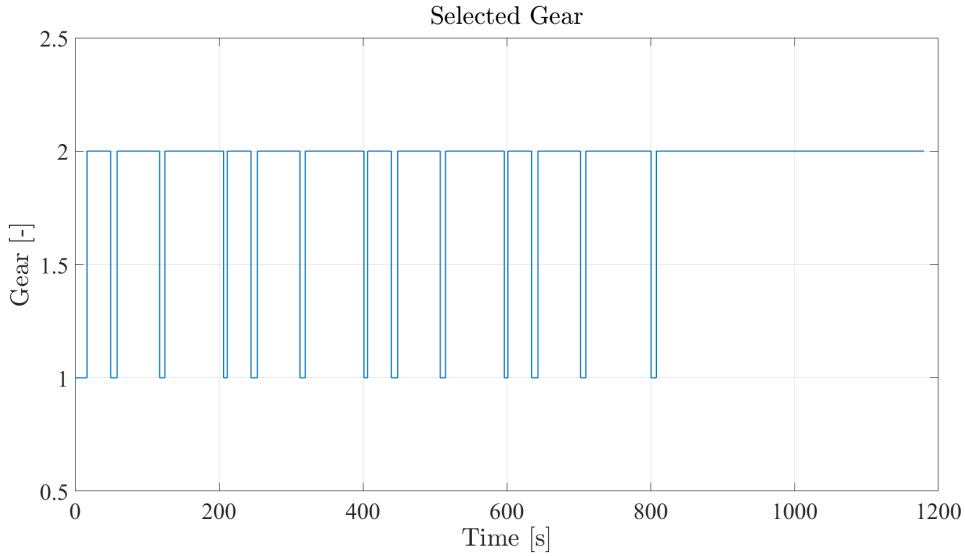

Figure 5.27: Gear selected

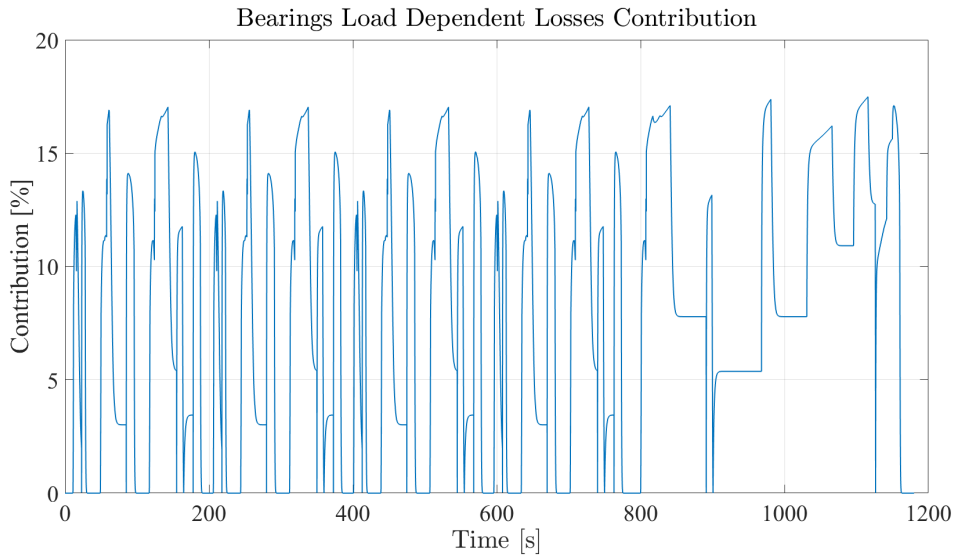

Figure 5.28: Bearings Load Dependent Losses

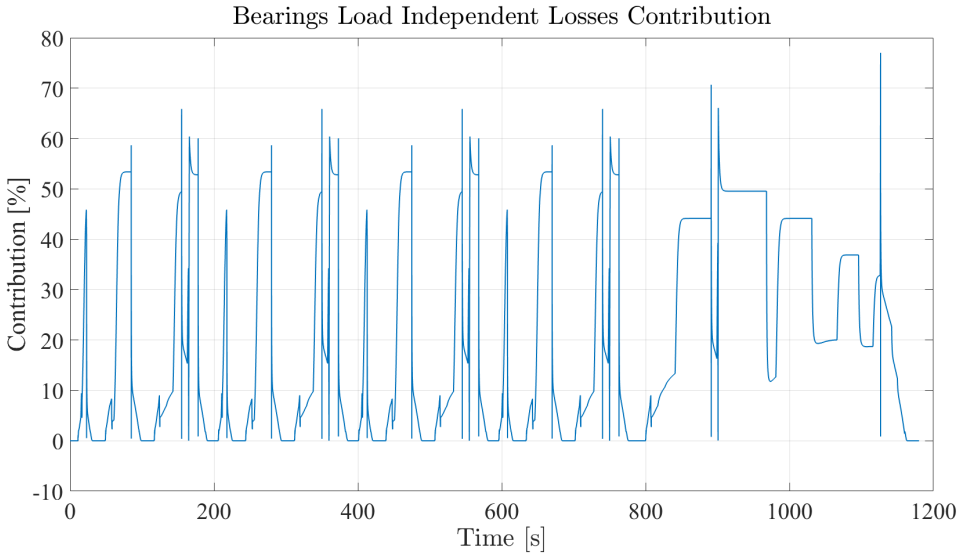

Figure 5.29: Bearings Load Independent Losses

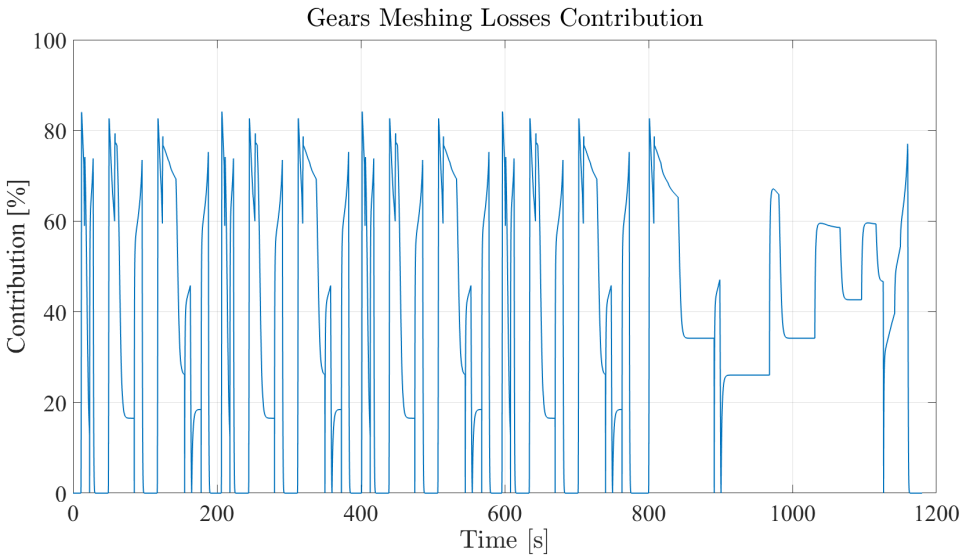

Figure 5.30: Gears Load Dependent Losses

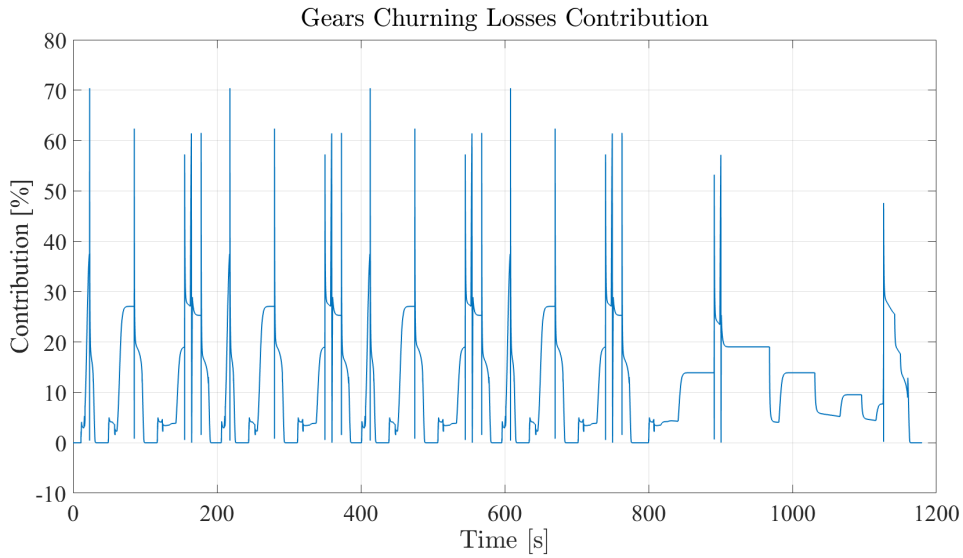

Figure 5.31: Gears Load Independent Losses

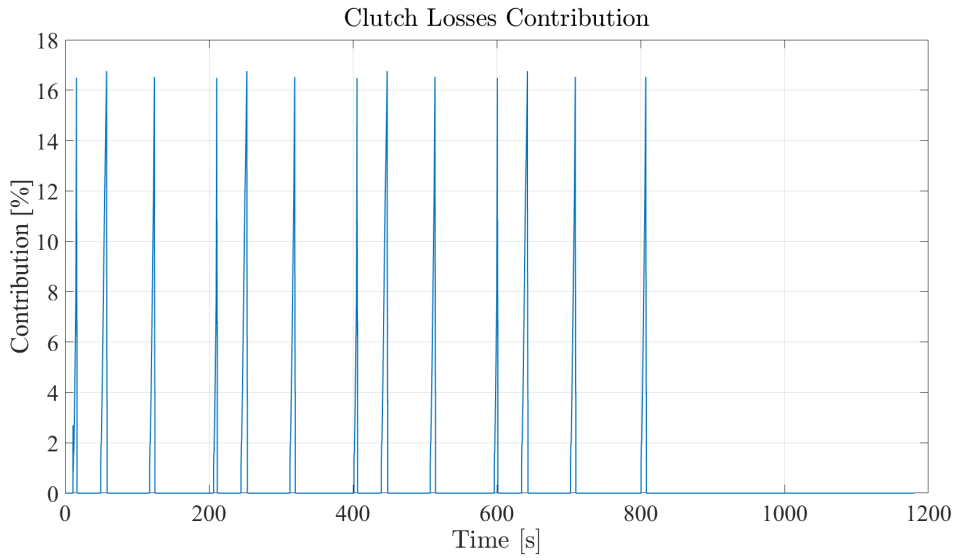

Figure 5.32: Clutch Losses

In order to analyze transmission performance in terms of energy efficiency, simulations of the WLTP, NEDC and FTP75 driving cycles were conducted. The driving cycles used, represent the different possible set of operational conditions that a vehicle might encounter in real world scenarios. This is essential in order to provide a comprehensive assessment of the impact of transmission losses across various driving profiles.
Figures from 5.33 to 5.41 illustrate the duration of time the transmission operates within specific regions of the transmission map, plotted as a function of torque and motor speed. Additionally, the average efficiency for each area of the map where the transmission operates is also displayed. The analysis is conducted for the NEDC, WLTP and FTP75 driving cycles.

NEDC

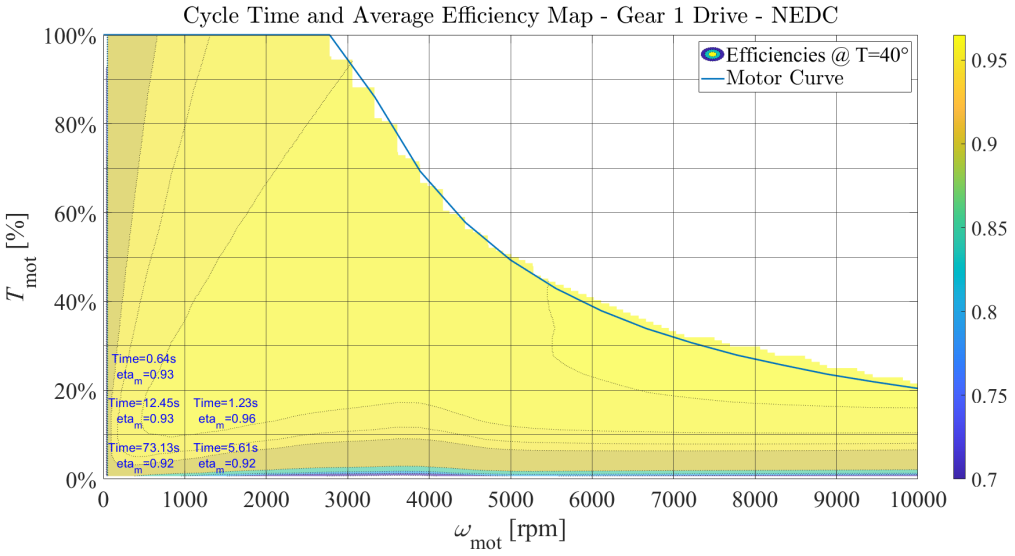

Figure 5.33: Cycle time and average efficiency

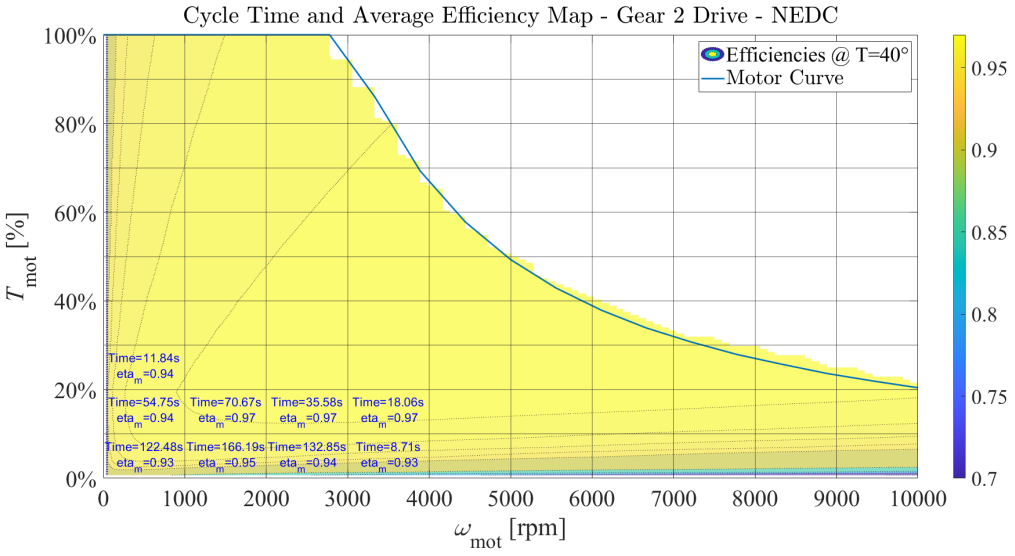

Figure 5.34: Cycle time and average efficiency

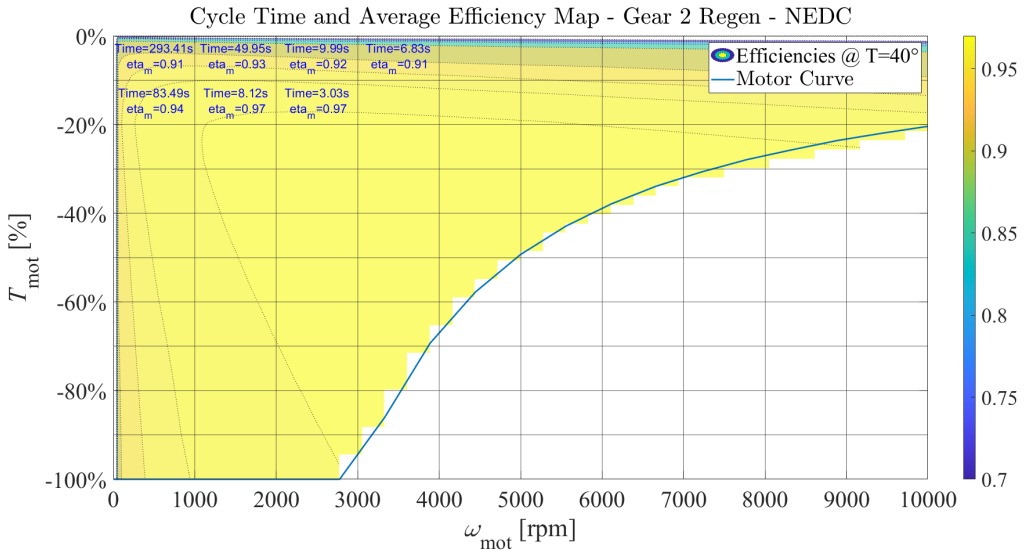

Figure 5.35: Cycle time and average efficiency

WLTP

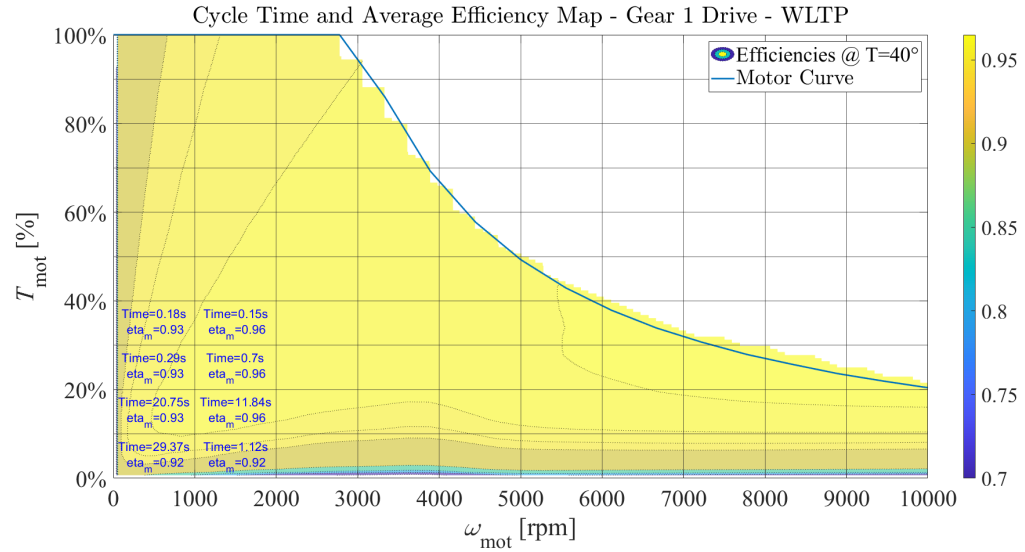

Figure 5.36: Cycle time and average efficiency

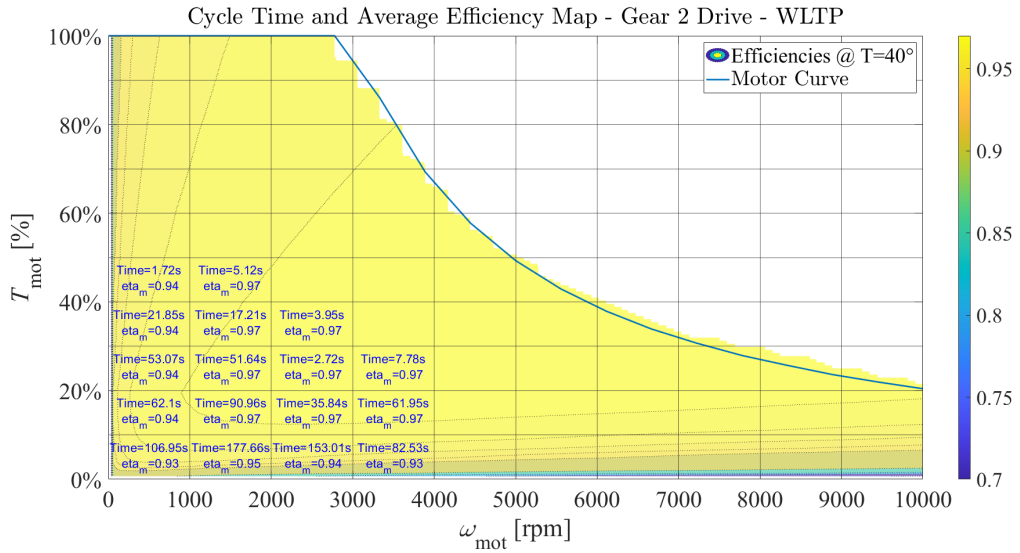

Figure 5.37: Cycle time and average efficiency

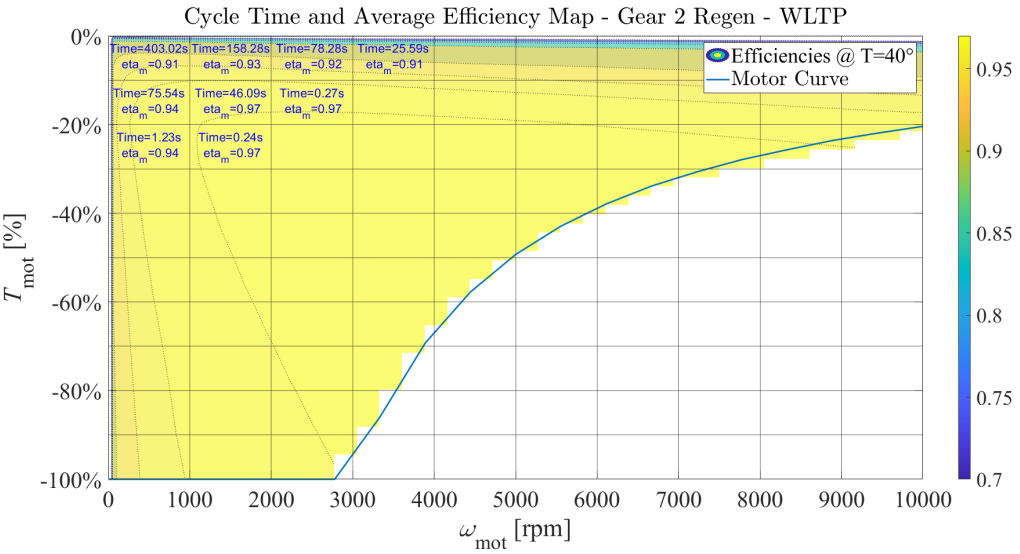

Figure 5.38: Cycle time and average efficiency

FTP75

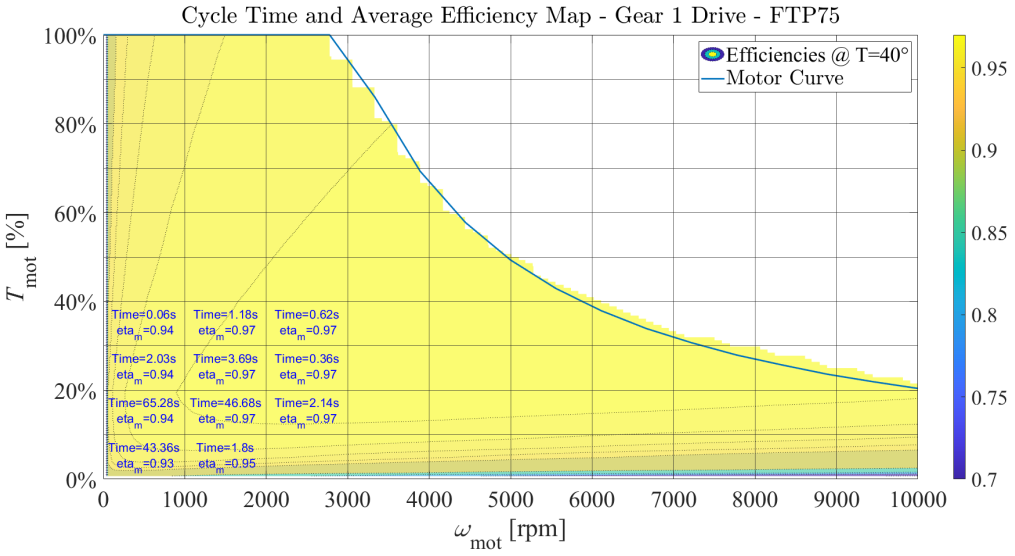

Figure 5.39: Cycle time and average efficiency

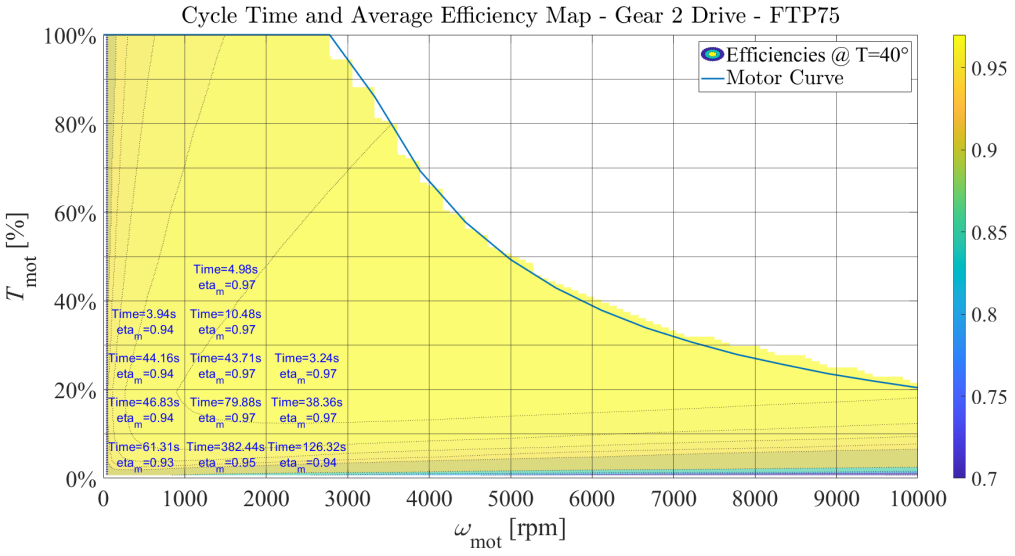

Figure 5.40: Cycle time and average efficiency

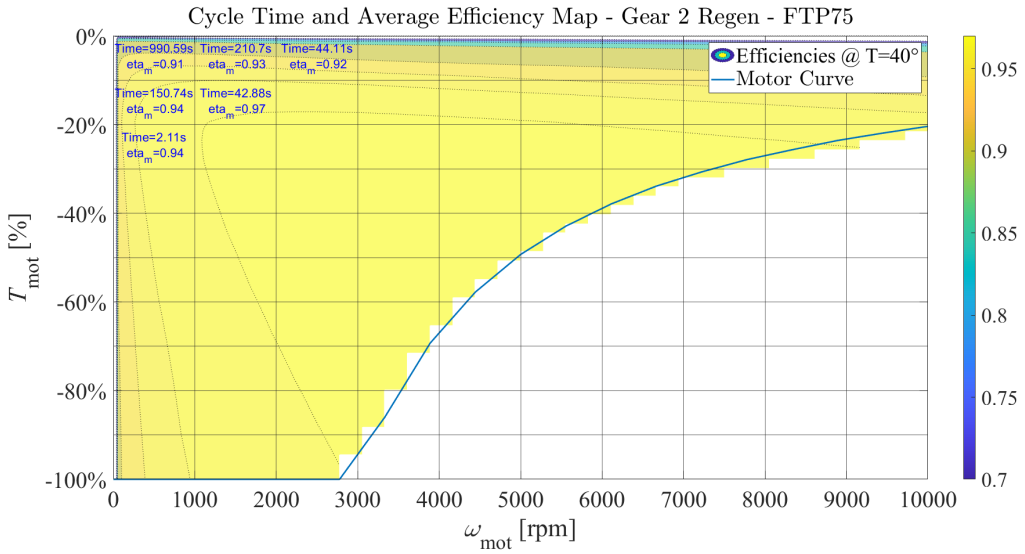

Figure 5.41: Cycle time and average efficiency

The graphs above presented do not include the regenerative braking data for first gear. This is because, throughout all three simulated cycles, the transmission does not engage first gear during regenerative braking. The transmission's design restricts downshifting during regenerative braking, due to its gearshift logic that maintains the gear the vehicle was in at the start of the regenerative braking event throughout its duration. Given the torque demands and speed profiles of each cycle, and the gearshift map used, there is no instance where regenerative braking initiates in first gear, for all three simulated cycles. As a result, there are no graphs reporting regenerative braking case in first gear.

The results in Fig 5.42, 5.43 and 5.44 show the energy losses contribution, expressed as a percentage of the overall transmission energy loss, for the WLTP, NEDC and FTP75 test cycles.

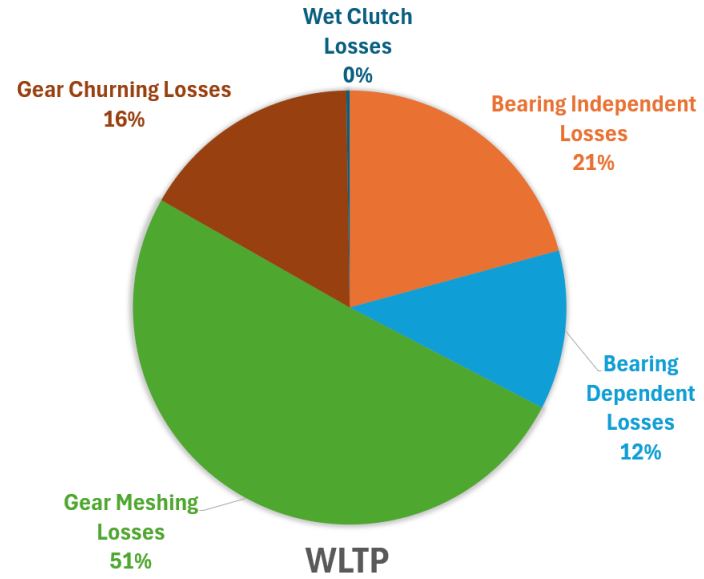

Figure 5.42: Power losses contribution for WLTP

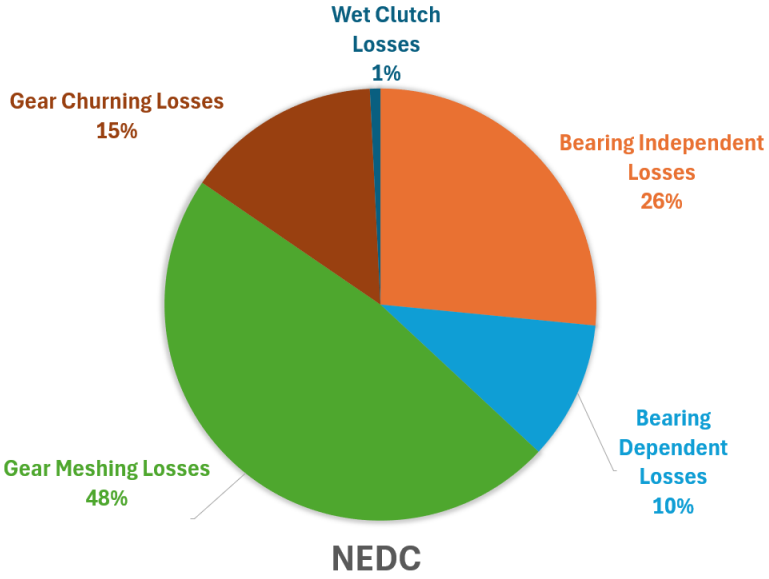

Figure 5.43: Power losses contribution for NEDC

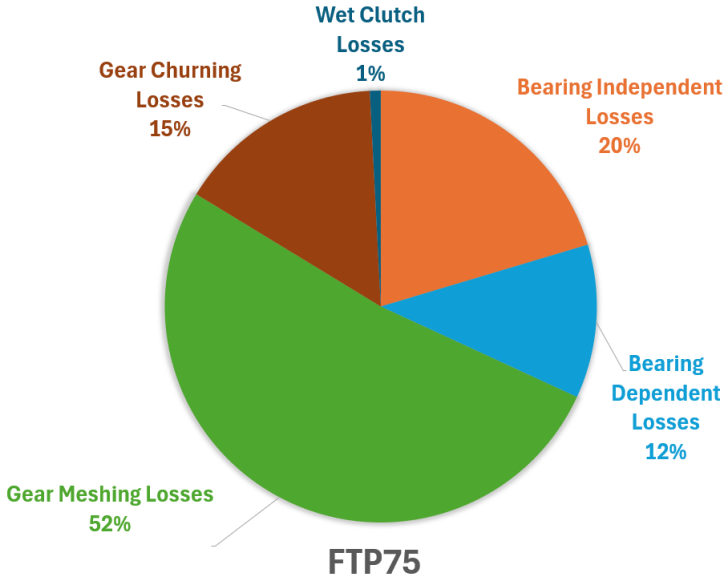

Figure 5.44: Power losses contribution for FTP75

The analysis reveals that the contributions to the transmission losses exhibit a consistent trend across all the driving cycles tested. Specifically, approximately 50% of total transmission losses is attributable to the gear meshing. The remaining 50% of the transmission losses are distributed among the three other sources of loss: bearing losses, both load independent and dependent, and gear churning losses. Among these, load independent bearing losses represents the largest contribution. While, both load dependent bearing losses and gear churning losses account for the remaining portion of the transmission losses, and their contributions are found to be approximately equal.

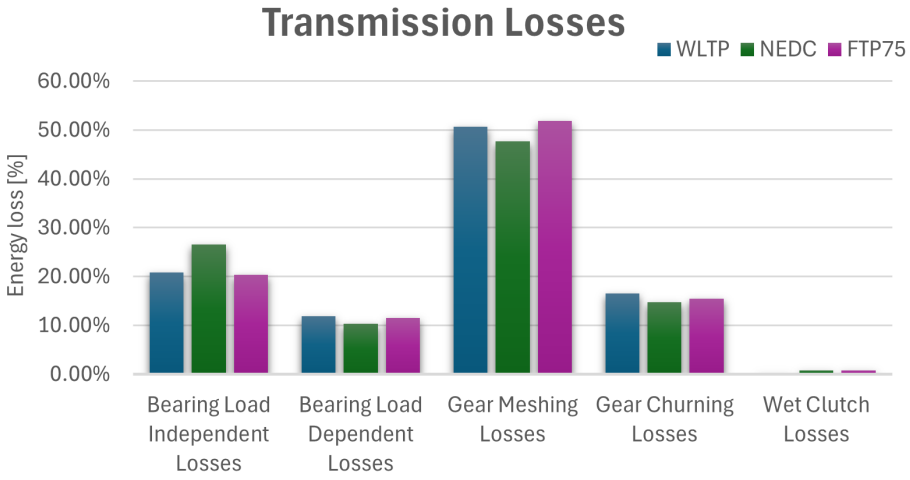

Figure 5.45: Power losses contribution for different driving cycles

A comparison of the power loss contributions across the different driving cycles is shown in Fig 5.45. The primary source of energy loss in a transmission is due to gears. In particular the meshing component of the gear loss is the main cause of energy dissipation within the transmission. Contrary to initial expectations based on the churning losses map, where churning losses appear to have limited significance, simulations of driving cycles reveal that churning losses are far from insignificant.
This notable contribution is attributable to two key reasons:
During the simulation of the driving cycles, the maximum torque request from the motor by the cycles is much lower than the motor's maximum torque capacity. Consequently the motor operates predominantly within a low load range, above 35% of its maximum torque. In this range, as discussed in the preceding paragraph, churning losses become relevant.
Furthermore, the gearshift logic at low loads, requires the transmission to upshift in second gear as soon as the vehicle reaches a speed of approximately 10km/h. As a result, the transmission operates in second gear for the majority of the time of the cycles. Since, as highlighted in the previous section, churning losses in second gear are higher than in first gear, due to the increased rotational speed which agitates more lubricant, this further explain the non negligible impact of the churning losses on the total power losses.
Therefore, despite these losses appearing negligible in efficiency maps, compared to the other sources of losses, their impact becomes significant while simulating real world applications, by means of the driving cycles. In fact, the operational characteristics typical of driving cycles emphasized the importance of considering

churning losses in transmission efficiency assessment, particularly under low load conditions.

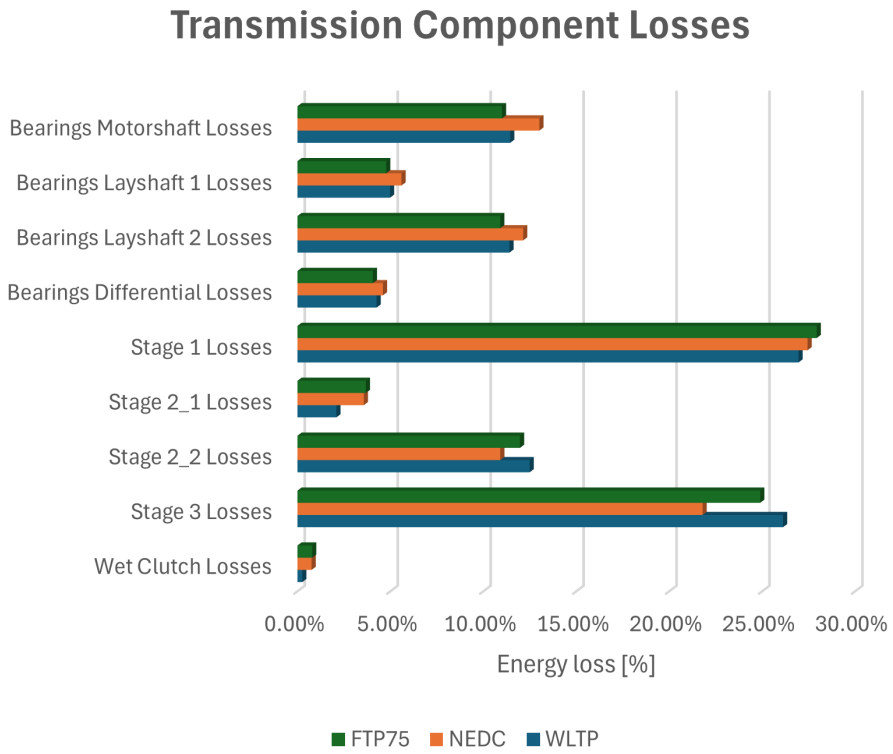

Figure 5.46: Power losses of the transmission component for different driving cycles

The innovative contribution of this study lies in the energy loss analysis and its distribution among the various components that constitute the transmission system. Figure 5.46 illustrates the share that each transmission element contributes to the overall energy dissipation across three different driving cycles (NEDC, WLTP, FTP75). The partition of losses among the transmission components exhibits the same trend across the all driving cycles tested.

The analysis reveals that the first stage is responsible for the highest energy dissipation for all the three driving cycles. Stage 1 is the gear where the highest speeds in the entire transmission are reached, as it is the first reduction gear and so directly connected to the motor's output.
Since the primary source of loss is gear meshing, which is the loss associated with the torque transmission in gears, it is predictable and understandable that the last stage would contribute significantly to the overall energy dissipation within the transmission system.

Stages 2_1 and 2_2 are the gears designated for gear shifting. When the vehicle is in first gear, the Stage 2_1 transmits torque while Stage 2_2 does not. Similarly, in second gear, Stage 2_2 transmits torque while 2_1 does not. This is the reason why, unlike what happens with Stage 1 and 3, which exhibit meshing losses regardless of the engaged gear, Stage 2_1 and 2_2 alternate in terms of meshing contribution depending on the gear selected by the gearshift control. Consequently, the individual contributions of both these stages are less significant compared to stage 1 and 3. Moreover, since the transmission predominantly operates in second gear throughout the driving cycle, the losses in second gear have a more significant impact compared to those of first gear.

Stage 3, despite experiencing lower speed compared to preceding stages, exhibits an important contribution to churning losses. This is due to the significant size of the differential gear, which is the largest gear in the entire system.

Ultimately, the distribution of power losses among the transmission bearings appears to be in accordance with the result shown in figure 5.45, where the biggest contribution of bearing losses in the transmission is attributable to load-independent factors. Based on this, it is anticipated that the differential bearings, which operate at the lowest speeds, would contribute the least to the overall power losses among all the bearings. This expectation is confirmed by the data, as the differential bearings indeed exhibit minimal losses. Conversely, the motor shaft bearings, which operate at higher speeds, are expected to contribute the most to the power losses. This is confirmed by the findings, as the motor shaft bearings do show the highest losses among the bearings in the system.

Understanding which components most significantly impact the overall efficiency of the transmission system is crucial. This knowledge can guide future design improvements and optimizations effectively. By identifying the components that contribute the most to power loss, engineers can focus on modifications that will achieve the greatest efficiency gains. This targeted approach is essential for advancing the performance of multi-speed transmissions in electric vehicles, thereby contributing to the development of more energy-efficient and sustainable automotive technologies.

Conclusions

The literature extensively explores the overall efficiency of automotive transmissions and the factors causing power losses. However, there seems to be a deficit in focusing on the significance of each type of loss and the specific component causing it when considering multi-speed transmissions for electric vehicles (EVs).
This literature gap highlights the need for a detailed analysis of power losses specific to multi-speed transmissions in EVs, considering both the motoring and regenerative conditions.

The primary aims and goals pursued in this study encompass:

- A comprehensive examination of power dissipation associated with a specific 2-speed transmission, incorporating the utilization of a selectable one-way clutch (SOWC), recently developed for electric vehicles.
- An analysis conducted to dissect the distribution of power losses within the transmission, distributing them among its individual components and contributions. This analysis is performed for both motoring and regenerative conditions, providing insights into how the transmission behaves under different operating scenarios.
- An investigation aiming to compare the efficiency of motor and transmission losses, highlighting the importance of transmission losses in relation to those of the motor. This comparison underscores the critical importance of not overlooking gearbox losses when conducting efficiency analyses on 2-speed electric vehicles. It highlights that while motor efficiency often receives significant attention, the efficiency losses within the gearbox can also play a substantial role in the global performance and energy consumption of the vehicle. By carefully considering these transmission losses, a more accurate and comprehensive assessment of the vehicle's efficiency can be achieved, leading to better design decisions and optimizations for electric vehicle performance.

- An evaluation of the power loss weight of each component in relation to the total power dissipation across various drive cycles. This aspect of the study identifies which components contribute most significantly to power losses and how these losses vary under different driving conditions.

Electric vehicles are gaining popularity, and along with this trend, the adoption of multi-speed transmissions for EVs, especially 2-speed systems, is expected to increase. Given that current battery technology does not offer a range comparable to that of internal combustion engine vehicles, it is increasingly important to understand the efficiency implications of all electric drivetrain components in transmitting energy from batteries to wheels.

This thesis aims to provide a foundational analysis of power losses in a 2-speed transmission designed for next-generation electric vehicles. A further critical step towards a comprehensive understanding of these findings is to conduct an experimental bench testing of the examined transmission. This future study could be crucial for validating the accuracy of the efficiency maps derived from theoretical models against real-world data. Should discrepancies arise, such an evaluation would be instrumental in tuning the model parameters for achieving convergence between theoretical and experimental outcomes.

References

[1] Ślaski, G.; Gudra, A.; Borowicz, A.; "Analysis of the influence of additional unsprung mass of in-wheel motors on the comfort and safety of a passenger car" Arch. Automot. Eng. 2014, 3, 51–64.

[2] C. Zhang, S. Zhang, G. Han and H. Liu, "Power management comparison for a dual-motor-propulsion system used in a battery electric bus", IEEE Trans. Ind. Electron., vol. 64, no. 5, pp. 3873-3882, May 2017.

[3] Ehsani, M., Gao, Y., Emadi, A., 'Modern Electric, Hybrid Electric, and Fuel Cell Vehicles', 2nd Edition, Routledge, 2009.

[4] Husani, I., 'Electric and Hybrid Vehicles', CRC Press, 2003.

[5] Miller, J. M., 'Propulsion Systems for Hybrid Vehicles', IEEE, 2004.

[6] M. Ehsani, Yimin Gao and S. Gay, "Characterization of electric motor drives for traction applications," IECON'03. 29th Annual Conference of the IEEE Industrial Electronics Society (IEEE Cat. No.03CH37468), Roanoke, VA, USA, 2003, pp. 891-896 vol.1, doi: 10.1109/IECON.2003.1280101.

[7] A. Sorniotti, M. Boscolo, A. Turner and C. Cavallino, "Optimization of a multi-speed electric axle as a function of the electric motor properties," 2010 IEEE Vehicle Power and Propulsion Conference, Lille, France, 2010, pp. 1-6, doi: 10.1109/VPPC.2010.5729120.

[8] L Mangialardi, G Mantriota, Power flows and efficiency in infinitely variable transmissions, Mechanism and Machine Theory, Volume 34, Issue 7, 1999, Pages 973-994, ISSN 0094-114X.

[9] Tenberge, P., 'Efficiency of Chain-CVTs at Constant and Variable Ratio', SAE 04CVT-35.

[10] Srnik, J., Pfeiffer, F., 'Dynamics of CVT chain drives', International Journal of Vehicle Design, 22(1/2), 1999.

[11] Sun, D.C., 'Performance analysis of a variable speed-ratio metal V-belt drive', Trans. ASME Mech. Transm. Automot. Des., 1988.

[12] Wicke Wicke, V., Brace, C., and Vaughan, N., "The Potential for Simulation of Driveability of CVT Vehicles," SAE Technical Paper 2000-01-0830, 2000, doi: 10.4271/2000-01-0830.

[13] Kulkarni, M.; Shim, T.; Zhang, Y. Shift dynamics and control of dual-clutch transmissions. Mech. Mach. Theory 2007, 42, 168–182.

[14] Bingzhao Gao, Qiong Liang, Yu Xiang, Lulu Guo, Hong Chen, Gear ratio optimization and shift control of 2-speed I-AMT in electric vehicle, Mechanical Systems and Signal Processing, Volumes 50–51, 2015, Pages 615-631, ISSN 0888-3270.

[15] F. A. Machado, P. J. Kollmeyer, D. G. Barroso and A. Emadi, "Multi-Speed Gearboxes for Battery Electric Vehicles: Current Status and Future Trends," in IEEE Open Journal of Vehicular Technology, vol. 2, pp. 419-435, 2021, doi: 10.1109/OJVT.2021.3124411.

[16] Ruan, J., Walker, P. D., Wu, J., Zhang, N., & Zhang, B. (2018). Development of continuously variable transmission and multi-speed dual-clutch transmission for pure electric vehicle. Advances in Mechanical Engineering, 10(2), 1687814018758223.

[17] Fang, Yuhong, et al. "Comparison of effect on motor among 2-, 3-and 4-speed transmission in electric vehicle." 2017 IEEE international conference on mechatronics (ICM). IEEE, 2017.

[18] Sorniotti, A., Subramanyan, S., Turner, A., Cavallino, C. et al., "Selection of the Optimal Gearbox Layout for an Electric Vehicle," SAE Int. J. Engines 4(1):1267-1280, 2011, https://doi.org/10.4271/2011-01-0946.

[19] Sorniotti et al., "Analysis and simulation of the gearshift methodology for a novel two-speed transmission system for electric powertrains with a central motor", IMechE Part D: J. Automobile Eng., vol. 226, no. 7, pp. 915-929, 2012.

[20] Sorniotti, A., Pilone, G. L., Viotto, F., Bertolotto, S., Everitt, M., Barnes, R., & Morrish, I. (2011). A Novel Seamless 2-Speed Transmission System for Electric Vehicles: Principles and Simulation Results. SAE International Journal of Engines, 4(2), 2671–2685. http://www.jstor.org/stable/26278326.

[21] Oerlikon Graziano, S. p. A., Cavallino, C., 'Trasmissione a due marce per veicoli elettrici', Italian Patent TO2009A000750, 2009.

[22] https://en.wikipedia.org/wiki/Freewheel.

[23] K. Holmberg, P. Andersson, A. Erdemir, Global energy consumption due to friction in passenger cars, Tribol. Int. 47 (2012) 221–234.

[24] ISO, B(2001) TR14179-2-2001 Gear-thermal capacity Part2: Thermal load-carrying capacity.

[25] Niemann G, Winter H (2003) Maschinenelemente, 2nd edn. vol. 2. Springer, Berlin Heidelberg.

[26] Ohlendorf, H (1958) Verlustleistung und Erwärmung von Stirnrädern, Dissertation, TU München.

[27] Liu, H.; Jurkschat, T.; Lohner, T.; Stahl, K. Detailed Investigations on the Oil Flow in Dip-Lubricated Gearboxes by the Finite Volume CFD Method. Lubricants 2018, 6, 47. https://doi.org/10.3390/lubricants6020047.

[28] Mauz,Wolfgang(1988) Hydraulische Verluste von Stirnradgetrieben bei umfangsgeschwindigkeiten bis 60m/s. Dissertation, Universität Stuttgart.

[29] Schlegel, Clemens & Hösl, Andreas. (2009). Detailed Loss Modelling of Vehicle Gearboxes. 10.3384/ecp09430059.

[30] Schaeffler Gruppe (2006) INA/FAG Wälzlagerkatalog.

[31] A. Palmgren, Neue Untersuchungen über Energieverluste in Wälzlagern, VDI-Berichte 20, S. 117-121, 1957.

[32] SKF Kugellagerfabriken GmbH, Katalog 2004.

[33] H. Linke, Stirnradverzahnung. Hanser Verlag, 1996.

[34] M. Gronitzki, Untersuchungen zur Funktion und Auslegung von Rechteckdichtringen für Drehdurchführungen, Dissertation Uni Hannover, 2006.

[35] Shen, Y., Rinderknecht, S. & Hoppert, M. General modelling method of power losses in transmission with parameter identification. Forsch Ingenieurwes 81, 117–123 (2017). https://doi.org/10.1007/s10010-017-0241-1.

[36] Shen, Y., Rinderknecht, S. A method on modelling and analyzing the power losses in vehicle transmission. Forsch Ingenieurwes 82, 261–270 (2018). https://doi.org/10.1007/s10010-018-0276-y.

[37] Iso/tr 14179-1:2001. https://www.iso.org, publication date 2001.07.

[38] AGMA 96FTM9, The Development of a Practical Thermal Rating Method for Enclosed Gear Drives.

[39] Seetharaman, S. & Kahraman, A. & Moorhead, M. & Petry-Johnson, T.. (2009). Oil Churning Power Losses of a Gear Pair: Experiments and Model Validation. Journal of Tribology-transactions of The Asme - J TRIBOL-TRANS ASME. 131. 10.1115/1.3085942.

[40] B.-R. Höhn, K. Michaelis, H.-P. Otto, Influence of immersion depth of dip lubricated gears on power loss, bulk temperature and scuffing load carrying capacity, Int. J. Mech. Mater. Des. 4 (2008) 145–156.

[41] E.A. Hartono, A. Pavlenko, V. Chernoray, Stereo-PIV Study of Oil Flow Inside a Model Gearbox, (n.d.).

[42] Otto, H.-P. (2009), "Flank load carrying capacity and power loss reduction by minimised lubrication", Thesis, TU München, München.

[43] Terekhov, A.S.: Hydraulic losses in gearboxes with oil immersion. Vestnic Mashinostroeniya, Vol. 55, Issue 5, 1975, pp. 13-15.

[44] Michaelis, K., Winter, H.: Influence of Lubricants on Power Loss of Cylindrical Gears. 48th Annual Meeting in Calgary, Alberta, Canada, May 17-20, 1993. Tribology Transactions Vol. 37 (1994) p. 161-167. Ohlendorf, H.: Verlustleistung und Erwärmung von Stirnrädern. Diss. TU München, 1958.

[45] C. Changenet, P. Velex, Housing influence on churning losses in geared transmissions, J. Mech. Des. 130 (2008) 62603.

[46] Hoehn, Bernd-Robert & Michaelis, Klaus & Hinterstoißer, Michael. (2009). Optimization of gearbox efficiency. GOMABN. 488330184301821134. 441-480.

[47] Hoehn, Bernd-Robert & Michaelis, K. & Wimmer, A.. (2007). Low loss gears. 24. 28-35.

[48] Magalhaes, Luis & Martins, Ramiro & Locateli, Cristiano & Seabra, Jorge. (2011). Influence of tooth profile on gear power loss. Industrial Lubrication and Tribology. 63. 10.1108/00368791111101812.

[49] Britton, R. & Elcoate, C. & Alanou, M. & Evans, H. & Snidle, R.. (2000). Effect of Surface Finish on Gear Tooth Friction. Journal of Tribology-transactions of The Asme - J TRIBOL-TRANS ASME. 122. 10.1115/1.555367.

[50] S. Sjöberg, On the running-in of gears, Licentiate thesis KTH, (2010).

[51] J. Vetter, G. Barbezat, J. Crummenauer, J. Avissar, Surface treatment selections for automotive applications, Surf. Coatings Technol. 200 (2005) 1962–1968.

[52] Doleschel, A.: Method to Determine the Frictional Behaviour of Gear Lubricants using a FZG Gear Test Rig. FVA Information Sheet No. 345, March 2002.

[53] Doleschel, A.: Wirkungsgradberechnung von Zahnradgetrieben in Abhängigkeit vom Schmierstoff. Diss. TU München, 2003.

[54] Wimmer, A., Salzgeber, K.; Haslinger, R.: WP1 – Analysis of Minimum Oil Requirements Considering Friction in Gears and Engines. Final Report Oil-free Powertrain, EU Project Contract No: IPS-2001-CT-98006, June 2003.

[55] Klaus Michaelis Bernd-Robert Höhn Michael Hinterstoißer, (2011),"Influence factors on gearbox power loss", Industrial Lubrication and Tribology, Vol. 63 Iss 1 pp. 46 – 55.

[56] von Petery, G. Fuel economy by custom-made: Bearings for differentials from BMW. ATZ Worldw 106, 11–12 (2004). https://doi.org/10.1007/BF03224703.

[57] Deepak, K.; Frikha, M.A.; Benômar, Y.; El Baghdadi, M.; Hegazy, O. In-Wheel Motor Drive Systems for Electric Vehicles: State of the Art, Challenges, and Future Trends. Energies 2023, 16, 3121. https://doi.org/10.3390/en16073121.

[58] https://www.osti.gov/servlets/purl/1418158.

[59] Ortuso A., "Modellazione dinamica di una trasmissione a due rapporti per veicoli elettrici", Torino, 2024.

[60] Wu, Guang & Zhang, Xing & Dong, Zuomin. (2013). Impacts of Two-Speed Gearbox on Electric Vehicle's Fuel Economy and Performance. SAE Technical Papers. 2. 10.4271/2013-01-0349.

[61] He, B.; Chen, Y.; Wei, Q.; Wang, C.; Wei, C.; Li, X. Performance Comparison of Pure Electric Vehicles with Two-Speed Transmission and Adaptive Gear Shifting Strategy Design. Energies 2023, 16, 3007. https://doi.org/10.3390/en16073007.

[62] K. Han, Y. Wang, D. Filev, E. Dai, I. Kolmanovsky and A. Girard, "Optimized Design of Multi-Speed Transmissions for Battery Electric Vehicles," 2019 American Control Conference (ACC), Philadelphia, PA, USA, 2019, pp. 816-821, doi: 10.23919/ACC.2019.8815300.

[63] H. Laitinen, A. Lajunen and K. Tammi, "Improving Electric Vehicle Energy Efficiency with Two-Speed Gearbox," 2017 IEEE Vehicle Power and Propulsion Conference (VPPC), Belfort, France, 2017, pp. 1-5, doi: 10.1109/VPPC.2017.8330889.

[64] Jeong, W.; Han, J.; Kim, T.; Lee, J.; Oh, S. Two-Speed Transmission Structure and Optimization Design for Electric Vehicles. Machines 2024, 12, 9. https://doi.org/10.3390/machines12010009.

[65] Xingxing Zhou, Paul Walker, Nong Zhang, Bo Zhu, Jiageng Ruan, Numerical and experimental investigation of drag torque in a two-speed dual clutch transmission, Mechanism and Machine Theory, Volume 79, 2014, Pages 46-63, ISSN 0094-114X, https://doi.org/10.1016/j.mechmachtheory.2014.04.007.

[66] Patel PD and Patel JM. An Experimental Investigation of Power Losses in Manual Transmission Gear Box. International Journal of Applied Research in Mechanical Engineering 2012; 2(1): 1-5.

[67] Iritani M, Aoki H, Suzuki K, and Morita Y. Prediction Technique for the Lubricating Oil Temperature in Manual Transaxle. SAE Technical Paper 1999-01-0747 1999.

[68] Seetharaman S, Kahraman A, Bednarek G, and Rosander P. A Model to Predict Mechanical Power Losses of Manual Transmissions. Automobiltechnische Zeitschrift 2008(4): 346-357.

[69] Per R, Georg B, Satya S, and Ahmet K. Development of an efficiency model for manual transmissions. ATZ worldwide 2008; 110(4): 36-43.

[70] Michlin Y and Myunster V. Determination of power losses in gear transmissions with rolling and sliding friction incorporated. Mechanism and Machine Theory 2002; 37(2): 167-174.